Cape Peninsula
University of Technology

Green synthesis of cobalt oxide nanoparticles from spent coffee

by

Sean William Raymond Drummer

Thesis submitted in fulfilment of the requirements for the degree

Master of Engineering: Chemical Engineering

in the Faculty of Engineering and the Built Environment

at the Cape Peninsula University of Technology

Supervisor: Prof M Chowdhury
Co-supervisor: Prof V Somerset

Bellville Campus
November 2022

CPUT copyright information

DECLARATION

I, Sean William Raymond Drummer, declare that the contents of this thesis represent my own unaided work, and that the thesis has not previously been submitted for academic examination towards any qualification. Furthermore, it represents my own opinions and not necessarily those of the Cape Peninsula University of Technology.

Signed	**Date**

ABSTRACT

Nanomaterials have emerged as a technology with limitless potential in a broad spectrum of fields due to their exceptional magnetic, electrical, optical, mechanical, and catalytic properties compared to their bulk counterparts. This is brought about by their significantly larger surface areas achieved through the rational design of the material, which can be calibrated as desired by precisely controlling the synthesis conditions and appropriate functionalisation. Despite this, conventional techniques do not promote sustainability as they necessitate toxic chemicals and high energy consumption. Recently, green chemistry has been presented as a competent replacement for traditional nanoparticle synthesis methods by using biological precursors such as plants, bacteria, fungi, algae, and yeast. However, this approach faces complications as the physio-chemical properties of the nanoparticles are considerably unpredictable and challenging to control due to the diverse and complex array of biomolecules present in each material.

Clean water has always been essential for social development, and pollution of these systems poses one of the substantial issues in the world today. One of the major contributors to this pollution is dyes, as existing wastewater treatment facilities suffer immense stress due to dye-stained industrial effluents, which inevitably accumulate in large water bodies and damage delicate ecosystems. Several counteracting techniques have been developed, with nanoparticle-induced oxidation processes proving to be an efficient and low-cost path for the degradation of organic pollutants. However, there is much exploration needed for full-scale application.

The successful synthesis of Co_3O_4 nanoparticles using spent coffee extract was demonstrated. The Fourier-Transform Infrared (FTIR) spectrum confirmed the presence of the nanomaterial, while the X-ray Diffraction (XRD) pattern and Transmission Electron Microscopy (TEM) presented the cubic crystal phase of cobalt oxide nanoparticles that possessed spherical and irregular morphologies with average diameters of 29.01 nm. The optical absorption data indicated that the direct band gap energy was 3.09 eV.

Cobalt oxide nanoparticles with these specifications illustrated remarkable catalytic efficiencies, with an 89.27% degradation of Tartrazine dye in 30 minutes. No significant concentration of dissolved cobalt was detected in the system, as an accumulation of only 0.0001% was perceived throughout the entirety of the reaction. Furthermore, the introduction of simulated solar light resulted in a 37.60% increase in catalytic degradation rate, thereby expressing the excellent photoactivity of the nanoparticles. However, to minimise operating costs, the artificial light was replaced with natural sunlight illumination, where dye removal efficiencies were further improved, resulting in an overall Tartrazine degradation of 97.11% and a 45.41% increase in reaction rate compared to the standard oxidation process.

Therefore, spent coffee was presented as an abundant and environmentally-benign raw material for a highly efficient Co_3O_4 nanocatalyst with excellent photocatalytic properties.

ACKNOWLEDGMENTS

First and foremost, I would like to express my sincere gratitude to my supervisor, Prof. Mahabubur Chowdhury, for his patience, motivation, and enthusiasm towards this research. Without his invaluable guidance and caring nature, this thesis would not have come to fruition. Being his student was a great honour, and I could not have asked for a better advisor and mentor. I would like to expand my thanks to Prof. Vernon Somerset for his inspiring advice and generous support.

I owe a deep gratitude to Ms Hannelene Small for her crucial assistance and for ensuring smooth operations throughout all experimentation conducted. The institution is fortunate to have her on the team.

To my brother, Brian Fisher-Holloway, with whom I shared the journey. Thank you for being an irreplaceable aspect of my life. I appreciate you tremendously.

To the love of my life, Michaela: my deepest gratitude. I could not have done this without her. Her monumental support and encouragement kept this research afloat. Thank you for your substantial contribution to this thesis. You truly mean the world to me, and I cannot wait to see what the future holds for us.

I would also like to extend my gratitude to my grandmother for showing me full support when I needed it the most. It has been nothing but a joy to live alongside her. Thank you for the memories I will cherish for the rest of my life.

Last but not least, to my mother. Without her sacrifices and unconditional love, I would not be where I am today. Thank you for giving me the strength to reach for the stars and chase my dreams. For that, I am forever in your debt. I hope this accomplishment makes you proud.

TABLE OF CONTENTS

LIST OF FIGURES

LIST OF TABLES

ABBREVIATIONS

AOC:	Antioxidant Capacity
AOP:	Advanced Oxidation Process
CGA:	Chlorogenic Acid
COD:	Chemical Oxygen Demand
CVD:	Chemical Vapour Deposition
DI:	Deionised
DPPH:	1,1-diphenyl-2-picrylhydrazyl
FCE:	Fresh Coffee Extract
FTIR:	Fourier-Transform Infrared Spectroscopy
GAE:	Gallic Acid Equivalent
IPA:	Isopropyl Alcohol
LED:	Light Emitting Diode
MeOH:	Methanol
NP:	Nanoparticle
PMS:	Peroxymonosulfate
PS:	Persulfate
PVD:	Physical Vapour Deposition
SC:	Spent Coffee
SCE:	Spent Coffee Extract
Tart:	Tartrazine
TEM:	Transmission Electron Microscopy
TPC:	Total Phenolic Content
UV:	Ultraviolet
UV-vis:	Ultraviolet-visible Spectroscopy
XRD:	X-ray Diffraction

Chapter 1

Nanotechnology is a 21st-century frontier that has received tremendous attention in past decades due to its scientific and technological exploitability. Nanotechnologies integrate the creation, control, and manipulation of materials at the nanometer scale, where these new trends welcome vast areas of research in engineering, physics, chemistry, material science, and molecular biology (Benelmekki, 2015). In 1959, Richard Feynman first conceptualised the subject in an academic lecture titled "There's Plenty of Room at the Bottom" (Kornei, 2016). Thereafter, the novel proposal sparked the rapid evolution of developments demonstrating these ideas in molecular manipulation (Hulla et al., 2015). Since then, improvements regarding nanotechnologies have made decisive progress and are now providing the potential to bring benefits in applications as diverse as information and communication technologies, drug development, water decontamination and purification, and the production of more robust and lighter materials (Pushparaj et al., 2022).

Some researchers have gone so far as to suggest that the influence of nanotechnology will be so substantial that the term will be used to describe a new era of world economic growth. With the Global Nanotechnology Market predicted to reach \$70.7 Billion by 2026, it is unambiguous that the scientific knowledge associated with our ability to manipulate matter on the nanoscale is demonstrating drastic technological, economic, and environmental impacts which will only increase (Whatmore, 2006; Anon, 2021).

The manufacturing of nanoparticles is an essential component of nanotechnology due to the distinctive characteristics realised at the nano level, and the assembling of precursor particles and related structures is the most generic route to fabricate nanostructured materials (Roco, 1999). These ultrafine solid particles display unique properties compared to their bulk counterparts due to exponentially high surface areas and increased reactivities (Biswas & Wu, 2005). The exemplary behaviour of the powder gives it a wide range of industrial applications that make it ubiquitous in our daily lives and promising materials for future scientific and technical innovations (Naito et al., 2018). However, the present problem lies with the synthesis of the nanoparticles.

1.1. Background

Nanoparticle synthesis has been around for centuries, and only now have the benefits begun to be reaped as new capabilities are discovered. Modern synthesis techniques have shown a remarkable degree of controllability, where the size and morphologies of the nanostructures can be manipulated to achieve desired physio-chemical properties (Tao et al., 2021). These characteristics are distinguishable between bulk materials as the nanoparticles present exceptional catalytic, optical, electrical, magnetic and mechanical properties (Baig et al., 2021).

Researchers have established various physical and chemical techniques for the fabrication of nanopowders. Nanoparticle synthesis is categorised according to the practices employed, with the two main strategies being top-down and bottom-up approaches (Ettadili et al., 2022). Top-down techniques involve the miniaturisation of larger composites of the substance by deconstruction, while the latter utilises atomic structures as "building blocks" for the formation of clusters and, thereafter, the desired nanoparticles (Drummer et al., 2021). Some examples of the processes include mechanical milling, laser ablation, arc discharge, micro-emulsion, pyrolysis, co-precipitation, sol-gel, spinning, and hydrothermal methods (Heiligtag & Niederberger, 2013). Despite the accuracy and precision of these procedures, several issues have arisen due to their toxic chemical requirements, harmful by-product production, and high energy consumption (Rastogi et al., 2018). Hence, a reliable and environmentally-benign approach to nanoparticle synthesis has been sought.

The discovery of biologically-induced synthesis routes has begun to address the significant complications related to conventional nanoparticle fabrication. The biological or "green" synthesis of nanoparticles employs diverse groups of living organisms or biomolecules to replace the hazardous elements in traditional fabrication techniques (Rana et al., 2020). More specifically, biosynthesis adopts the use of plants (Ryaidh & Al-Qayim, 2017), bacteria (Deljou & Goudarzi, 2016), fungi (Molnár et al., 2018), algae (Kathiraven et al., 2015), and yeast (Niknejad et al., 2015) as they possess reductive capabilities due to the metabolites present in the organic material. Not only are these phytochemicals directly implicated in the formation of nanoparticles, but they are also involved in the stabilisation by enveloping the structures (Iwuozor et al., 2022).

Previous researchers have suggested that plants are superior agents, in contrast to other biological synthesis routes, as they are more stable, have a faster metallic ion reduction rate, and are easier to scale up (Hussain et al., 2016; Kharissova et al., 2013; Singh et al., 2016). Therefore, plants have been the prime precursor for the biosynthesis of nanoparticles.

However, since this area of green nanotechnology is relatively new, the problem lies with controlling the size and morphology of the nanoparticles, as each plant species contains an

array of diverse biomolecules that significantly affect the sensitive physio-chemical properties of the material (Altemimi et al., 2017). Hence, achieving a better understanding of green synthesis is crucial to acquire the desired size, shape, composition, and dispersity with exceptional repeatability. For this to become a reality, the intricacies posed by the complex natural concentrations need to be defined before precise biosynthesis mechanisms can be brought forward.

A promising biological material for the production of nanoparticles is coffee. The beverage is the second most-consumed liquid in the world after water, with it being one of the top global commodities, second in value only to oil (Burger, 2018). It is estimated that South Africa's coffee consumption has increased from 35 340 tonnes in 2017 to 40 500 tonnes in 2020, with a compounded annual growth rate of 4.4% as the demand for premium coffee rises (Biacuana, 2017; Dutta, 2021). A recent survey in the Western Cape, displayed in Appendix A, reveals that each store discards an average of approximately 2.2 tons of spent coffee grounds to landfills per annum. Therefore, this problem must be addressed as coffee waste can be utilised as a cheap and abundant raw material in synthesising nanoparticles. Table 1.1 presents the previous studies that have successfully used coffee extract as a reducing agent for the synthesis of nanoparticles and their applications.

Table 1.1: Coffee-mediated nanoparticles from previous studies

Nanoparticle	Application	Authors
Ag	Antibacterial and Catalytic Activity	Wang et al. (2017)
Ag	Biological Activities	Rónavári et al. (2017)
Fe	Removing volatile chlorinated organic compounds from groundwater samples	Kozma et al. (2016)
Ag, Pd	Demonstrates that organic constituents of coffee were present as adlayers on the metal nanoparticle surface.	Metz et al. (2015)
Ag, Pd	Human welfare, biological and medical applications	Hussain et al. (2016)
Ag, Pd	Medicinal and Technological Applications	Nadagouda & Varma (2008)
Ag	Antibacterial activity	Dhand et al. (2016)
Ag	Antibacterial Activity	Calle & López (2017)
CuO	Antibacterial Activity	Sutradhar et al. (2014)
ZnO	Solar Cell	Sutradhar et al. (2016)
Al_2O_3	Biomedical Applications	Sutradhar et al. (2013)
ZnO	Photocatalyst	Fatimah et al. (2016)
Ag	Markers, Sensors, and Antimicrobials	Zuorro et al. (2017)
Au	Catalytic Activity & Environmental Remediation	Bogireddy et al. (2017)
Cu	Wastewater Treatment	Gerits (2016)
Au	Solution for controlling the size distribution of the Au nanoparticles	Bogireddy et al. (2018)
Au, Ag & Se	Antioxidant and Antibacterial Activity	Abbasian & Jafarizadeh-Malmiri (2020)
Ag	Antibacterial Activity	Chien et al. (2019)
Ag	Antibacterial Activity	Panzella et al. (2020)

C	Sensor Applications	Crista et al. (2020)
Ag	Antibacterial activity	Baghaienezhad et al. (2020)
Cu	Catalytic Activity	Wang et al. (2021)
ZnO	Environmental Toxicity Reduction	Abel et al. (2021)
CuO	Antibacterial Activity	Mary et al. (2021)

The nanoparticle under investigation in this study is cobalt oxide, as the literature surrounding the plant-mediated nanoparticle is inadequate, and the transition metal possesses interesting characteristics that need exploration. Cobalt, in its oxide form, being an antiferromagnetic material, retains several possible oxidation combinations due to its multi-electronic valence (Banerjee & Chattopadhyay, 2019). This unique aspect of the transition metal, coupled with the distinct properties of nanoparticles, allows for a broad spectrum of applications in energy systems (Mei et al., 2019), wastewater treatment (Adekunle et al., 2019), biomedical sensors (Karuppiah et al., 2014), and even anticancer therapeutics (Huang et al., 2021).

Rapid industrialisation and economic expansion have stressed existing wastewater treatment facilities, and the removal of dyes from industrial effluents has been a persistent problem. Therefore, there is an urgency to adopt innovative ways to overcome this issue. Traditional treatment methods, such as adsorption on activated carbon, chemical precipitation and separation, and coagulation, are non-destructive and only transfer dyes from one phase to another, causing secondary pollution and requiring further treatment (Saratale et al., 2011; Yaseen & Scholz, 2019). On the other hand, green nanostructures present a more sustainable and environmentally-benign practice for the catalytic degradation of toxins, as they destroy the undesired molecules through decomposition (Dihom et al., 2022). Depicted in Figure 1.1 are some studies that have demonstrated the successful use of metallic nanoparticles as effective catalysts for the removal of pollutants. However, the catalytic activity of nanomaterials is highly dependent on the particles' size, shape, structure, and composition (Nagar, 2018). Therefore, due to the unpredictability of the synthesis, an in-depth study is in need before the speculation of industrial use, as it is essential for the nanocatalyst to be efficient and cost-effective for it to be feasible in real-world applications.
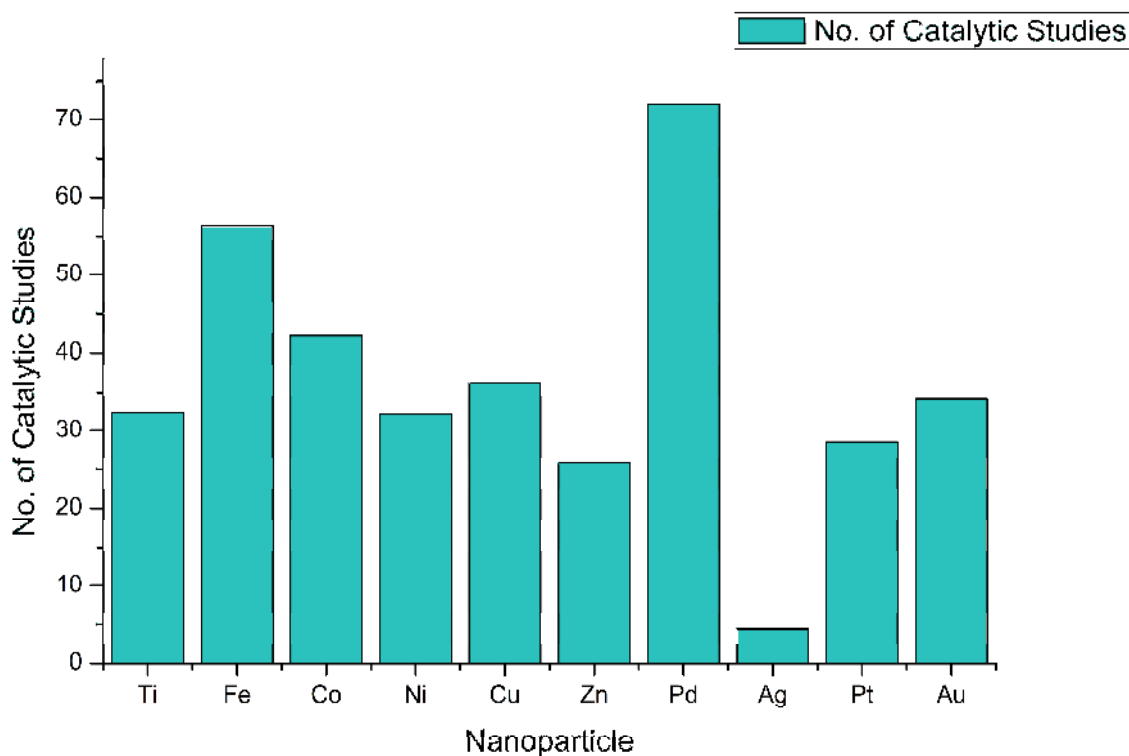
Figure 1.1: The catalytic studies of metallic nanoparticles (2007 – 2021)

1.2. Problem Statement

Current chemical synthesis techniques rely on expensive, toxic, and hazardous chemicals; hence, environmentally-benign processes are required. However, green synthesis routes retain a degree of unpredictability due to diverse and complex biomolecules, which directly affect the catalytic performance of these materials. Therefore, it is of utmost importance to evaluate their catalytic properties. In addition, since spent coffee is being discarded in landfills, it does not contribute to a circular economy.

1.3. Research Questions

1. Can spent coffee be used as an effective reducing agent for synthesising nanomaterials?

2. Can the developed nanoparticles be used as an efficient catalyst/photocatalyst for azo dyes?

1.4.   Aim and Objectives

This dissertation aims to extract the valuable metabolites from spent coffee and, in turn, demonstrate the biosynthesis of cobalt oxide catalyst/photocatalyst nanoparticles.

The objectives of this study are:

- To determine the optimal extraction parameters for total phenolic compounds and antioxidant capacity.
- To utilise the spent coffee extract in the biosynthesis of cobalt oxide nanoparticles.
- To optimise the Co_3O_4 nanoparticle synthesis process (i.e. precursor concentration, reaction temperature, reaction time, pH, and calcination temperature).
- To thoroughly characterise the nanoparticles obtained within this study.
- To evaluate the catalytic and photocatalytic performance of the Co_3O_4 nanoparticles in Tartrazine dye degradation via peroxymonosulfate activation.

1.5.   Scope of Study

The scope of this study will cover spent coffee-mediated cobalt oxide nanoparticles and their catalytic/photocatalytic degradation of an azo dye.

1.6.   Delineation

This study focuses on the synthesis of Co_3O_4 nanoparticles through the reaction between spent coffee extract and cobalt nitrate hexahydrate. All other cobalt-based precursors are delineated. In addition, the nanoparticles will be combined with peroxymonosulfate to initiate an advanced oxidation process against Tartrazine dye in a batch reaction. Continuous flow systems are delineated, along with other radical-producing reactants. With regards to light, white LED light, simulated solar, and sunlight were individually coupled with the Co_3O_4 nanoparticle and peroxymonosulfate system. Other sources of light are delineated. This research did not consider a sulphur leaching study due to time constraints.

1.7. Structure of Dissertation

Chapter 1: Introduction

Chapter 2: Literature Review

Chapter 3: Research Methodology

Chapter 4: Results & Discussion

Chapter 5: Conclusion

Chapter 2

Literature Review

2.1. Introduction

This chapter presents a detailed review of nanoparticles, various synthesis routes, and their advantages and disadvantages. Furthermore, the valuable antioxidants in coffee were investigated, along with the effect of roasting on the biomolecules. Cobalt oxide nanoparticles and their unique properties are highlighted herein. Lastly, an in-depth study of azo dyes and their catalytic/photocatalytic degradation via advanced oxidation processes are included.

2.2. Nanoparticles

Nanoparticles are seen as either agents of change in various phenomena and processes or as building blocks of materials and devices with tailored characteristics. The recent invention of various tools for studying systems at the atomic level, coupled with the development of techniques for producing nanoparticles, has led to the emergence of nanoscience as a new field of study. These nanoscale materials frequently demonstrate a behaviour which is intermediate between that of a macroscopic solid and that of an atomic or molecular system (Torres-Martínez et al., 2019). In general, nanoscience can be defined as the art and science of manipulating matter at the nanoscale to create new and unique materials. The emergence of nanomaterials has provided promising results in recent years by intersecting with various other branches of science and forming an impact on all forms of life (Vijayaraghavan & Ashokkumar, 2017).

Nanoparticle applications aim to take advantage of specific characteristics that are determined by the size and morphology of the solid particles. As they are micronised, the behaviour of the colloids tends to be affected as a more significant fraction of the relative atoms or molecules are located at the surface of the particle, leading to a higher reactivity due to the ease of bonding with the contacting material (Naito et al., 2018). The manufacturing processes of nanoparticles have been based on several other kinds of effects that occur:

8

a) Smaller particle sizes create larger surface areas, increased surface tension, quantum electromagnetic interactions, and size confinement effects, where the electrons within the particles display wavelike properties that are affected by varying the size and shape of the structures (Pal et al., 2011).

b) Due to the particles being on the nanoscale, new phenomena occur as interactions between physical, chemical, and biological materials become proportionate to the size of the particle (Jamkhande et al., 2019).

c) Different synthesis techniques allow for the generation of new atomic, molecular, and macromolecular structures of materials. Therefore, discovering unique characteristics of various substances (Parveen et al., 2016).

d) In particulate systems, time scales are altered due to the smaller distances and increased spectrum of forces between particles, thus, significantly increasing the degree of complexity and speed of processes (Roco, 1999).

2.3. Nanoparticle Synthesis Techniques

Nanoparticle synthesis is essential to understand the particle formation process, fine-tune the physiochemical properties of the material, and enable specific functionalities and applications. There are two general techniques for the fabrication of nanostructures, namely, bottom-up and top-down approaches (Figure 2.1). Top-down methods involve the miniaturisation of the larger substitutes by deconstruction, while the latter utilises atomic structures to synthesise the nanostructures of the material (Choi et al., 2008).
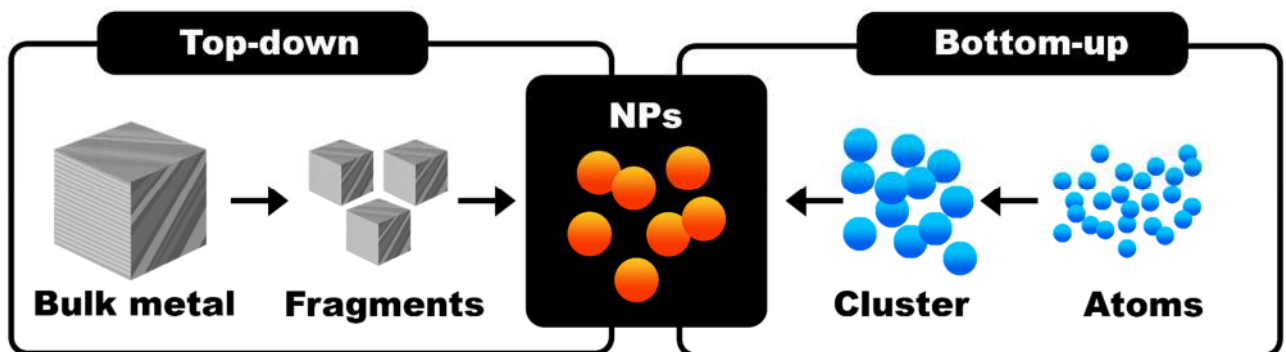
Figure 2.1: The top-down and bottom-up approach for nanoparticle synthesis

2.3.1. Top-down Techniques

2.3.1.1. Mechanical Milling

The objective is to reduce the particle size of a suitable powder by placing it in a high-energy mill. This process encourages the deformation and fracture of particles due to the continuous collision between ball and powder (Shi et al., 2000). In addition to the size reduction, a mechanochemical effect may be brought upon the ground particles due to the energy transferred within the duration of milling (Prasad Yadav et al., 2012; Damonte et al., 2004).

Drawbacks:

- The structures may experience structural dislocations and defects, resulting in reduced crystallinity (Zhang et al., 2007).
- The mechanical behaviour, phase equilibria, and stress state of the powder components during milling could complicate the outcome of the processes (Chin et al., 2005; Arbain et al., 2011).

2.3.1.2. Laser Ablation

Another common method for the retrieval of a desired colloidal material is laser ablation. The process requires the condensation of a laser-induced plasma plume, which, in turn, produces metallic nanoparticles from the surface of a bulk metal plate (Mafuné et al., 2000; Geohegan et al., 1998). In addition, this method may be utilised to alter the morphology of nanoparticles synthesised using chemical or electrochemical routes. This simple, one-step technique has been previously carried out in various solvents such as liquid, gas, or vacuum. (Amoruso et al., 2004; Mafuné et al., 2001; Mafuné et al., 2003; Amendola & Meneghetti, 2009; Becker et al., 1998; Dolgaev et al., 2002).

Drawbacks:

- Laser ablation has the ability to produce high yields of nanoparticles; however, the procedure requires dangerous and expensive equipment with high energy consumption.

2.3.1.3. Nanolithography

Within this synthesis technique, various nanolithographic paths may be taken; these include photolithography, electron-beam lithography, micro-contact printing, nano-imprint lithography, and X-ray lithography (Pimpin & Srituravanich, 2012). Generally, the process involves the "printing" of a required shape or structure on sheets of light-sensitive material by removing portions of the surrounding area. The procedure is usually carried out using a focused beam of high-intensity light or electrons that allow for accurate control (Ealia & Saravanakumar, 2017; Baig et al., 2021).

Drawbacks:

- Despite nanolithography's ability to generate complex and high-resolution structures, the disadvantages lie with the costly equipment and complex process that is easily contaminated by its environment (Ruchita et al., 2016; Venugopal & Kim, 2013).

2.3.1.4. Arc Discharge

This method was initially utilised for synthesising carbon nanotubes through two graphite electrodes immersed in an inert gas, where a direct-current arc voltage is allowed across the system. The arc discharge occurs when a high-density current between two electrodes forms a plasma that ionises and dissociates the gas atoms (Arora & Sharma, 2014). In a liquid, gas bubbles are formed through the vaporisation or decomposition of the anode plasma material and water. These escaping gas bubbles act as condensing media and carriers of the final product to the surface of the water. Cooling the metal vapour in the liquid leads to the formation of primary particles through nucleation mechanisms. Subsequently, nanoparticles are produced on the surface of the designated electrode (Kassaee et al., 2011; Yao et al., 2005; Fang et al., 2012).

Drawbacks:

- Research suggests that arc discharge may be considered a simple, cost-efficient technique that can be easily implemented for the mass production of nanomaterials. However, this method has its drawbacks as the process can produce nanostructures with a broad size range due to the melting of the electrodes (top-down synthesis) and the reduction of the metal salt solution (bottom-up synthesis) (Ashkarran, 2010; Bera et al., 2004; Lung et al., 2007; Ashkarran et al., 2009).

2.3.1.5. Ion Sputtering

This nanoparticle synthesis technique involves bombarding a solid area with energetic gaseous or plasma ions, where microscopic particles are simultaneously ejected and condensed to form a thin layer of the nanomaterial on the surface (Baptista et al., 2018). Therefore, sputtering, or physical vapour deposition (PVD), is considered an effective method for producing thin films of nanoparticles. This process can be performed in different ways by utilising a DC diode, radio-frequency diode, and magnetron sputtering (Boone, 1986).

Drawbacks:

- This procedure has a significant advantage as it is able to produce nanoparticles on an industrial scale in an environmentally benign manor. However, sputtering technologies must be maintained at high temperatures and vacuums, increasing operating costs and requiring skilled operators (Aliofkhazraei & Ali, 2014).

2.3.2. Bottom-up Techniques

2.3.2.1. *Sol-gel*

The sol-gel method involves converting a homogeneous solution into colloidal particles through polymerisation reactions catalysed by water. This technique is usually carried out in two steps, namely, hydrolysis ("sol" formation) and condensation ("gel" formation) when inorganic metal salts or metal-organic species like alkoxides or acetylacetonate are used. Metal alkoxides are favourable in this technique as they readily react with water through the nucleophilic attack of the oxygen atom possessed by the solvent. Hence, this inherently results in the release of alcohol and the formation of metal hydroxide (Jagadale et al., 2008; Vafaee & Ghamsari, 2007; Mittal et al., 2013; Hench & West, 1990). After the colloidal solution has aged, the condensation reaction occurs between two metal hydroxyl/alkoxy species and leads to M-O-M bonds (ref). This reaction then induces the formation of an interconnected, semirigid colloidal dispersion of a solid within a liquid phase, in other words, the gel. Thereafter, the gel is dried, and the desired nanomaterials are obtained (Lu et al., 2002).

Drawbacks:

- Despite the nanoparticle's controllability of size and morphology, this synthesis route requires toxic chemicals. In addition, separating the nanostructures from the gel requires a considerable amount of energy if a high production rate is obligatory (Niederberger, 2007; Gu et al., 2004; Trewyn et al., 2007).

2.3.2.2. *Hydrothermal*

This fabrication path entails dissolving and recrystallising otherwise insoluble materials under normal conditions by increasing the temperature and pressure of the solution. However, according to previous research, there have been instances where these conditions were undermined, and it was concluded that there is no lower limit to the temperature and pressure of the reaction (Hayashi et al., 2010). Therefore, the method is more accurately defined as a heterogeneous chemical reaction, with water as a catalyst, above room temperature and atmospheric temperature in a closed vessel (Köseoğlu et al., 2012; Chiu & Yeh, 2007).

Drawbacks:

- This process generates highly crystalline nanostructures with substantial control over their content and composition. However, agglomeration is the primary concern in the hydrothermal synthesis of nanoparticles (Baruwati et al., 2006; Daou et al., 2006; Lu et al., 2011).

2.3.2.3. Microemulsions

Emulsions are isotropic, macroscopically homogeneous, and thermodynamically stable synthesis mediums that consist of a polar phase, a non-polar phase, and a surfactant. On a macroscopic level, the introduction of the surfactant forms an interfacial film that separates the polar and non-polar substances and allows the occurrence of microemulsions due to the establishment of nanodroplets in the aqueous phase. These microstructures range from water droplets dispersed in a continuous oil phase (water-in-oil) to droplets of oil dispersed in a continuous water phase (oil-in-water) (Vidal-Vidal et al., 2006; Chhabra et al., 1995; Zhang & Chan, 2003). More specifically, two identical microemulsions are prepared in the water-in-oil process: one is comprised of the soluble metallic salt, and the other contains the precipitation agent dissolved in water. These microdroplets constantly collide, coalesce, and break again. During the process, inter-droplet exchange and nuclei aggregation occur, which initiates the formation of nanoparticles in the aqueous core of the microemulsion.

Drawbacks:

- The restricted reaction media provides a degree of controllability over the size of the nanoparticles by precipitating the metallic salt. However, the procedure is susceptible to change, requires labour-intensive work, and produces a low yield of nanoparticles (Hingorani et al., 1993; Malik et al., 2012; Ohde et al., 2001; Singhai et al., 1997).

2.3.2.4. Chemical Reduction

This approach is deemed one of the most prevalent methods for synthesising colloidal metal particles. The reaction traditionally involves a precursor and a reducing agent. The precursor for this reaction consists of a metallic salt, and the reducing compound is used to generate electrons for the metal ions to initiate nanoparticle nucleation (Pulit et al., 2013; Khandelwal et al., 2019). According to Martínez-Abad (2011), potent reducing agents yield smaller nanoparticles; however, due to excess surface energy and high thermodynamic instability, smaller particles rapidly undergo alternating nucleation leading to agglomeration. Therefore, the reduced nanoparticles need to be stabilised through the use of appropriate agents such as ligands, polymers, or surfactants (Zhao et al., 2019; Nam & Luong, 2019).

Drawbacks:

- Chemical reduction methods are relatively rapid and straightforward. However, the reagents possess various negative aspects, such as high costs and elevated toxicities (Jamkhande et al., 2019).

2.3.2.5. Laser Pyrolysis

Laser pyrolysis is a vapour-phase synthesis technique based on the resonance between the emission of a CO_2 laser beam and the absorption of a gaseous or liquid precursor (Figgemeier et al., 2007). The absorption of the laser's infrared photons increases the overall temperature of the gas due to the materialisation of a flame in the reaction media. If the precursor molecules are excited above the dissociation threshold, molecular decomposition, followed by collision-assisted energy pooling, occurs with the formation of volatile products (Spreafico et al., 2022). Nucleation is initiated when the condensable products reach a sufficient degree of supersaturation. Thereafter, particle growth commences at a high rate through coalescence or coagulation rather than further nucleation. The nucleation and growth of the nanoparticles are instantaneous and immediately terminated when the particles exit the irradiation region (Galvez et al., 2002; Lacour et al., 2007).

Drawbacks:

- The laser's intense nature poses a significant disadvantage as temperatures may exceed 4000°C. Therefore, this stipulates tremendous energy usage for the minimal production of nanoparticles (Ghaem et al., 2020; Bomatí-Miguel et al., 2008).

2.3.2.6. Co-precipitation

Co-precipitation is the simultaneous precipitation of an ordinarily soluble component with a macro-component by forming mixed crystals through adsorption, occlusion, or mechanical entrapment (Petcharoen & Sirivat, 2012). The procedure generally involves mixing the desired metal salt solution and a base under inert atmospheric conditions (Kim et al., 2003). The synthesis is initiated by partially oxidising the metal hydroxide suspensions with various oxidising agents, followed by the ageing of stoichiometric mixtures of the metal and metal hydroxides in the aqueous media, therefore, yielding nanoparticles as the precipitate (Sharifi et al., 2013; Mascolo et al., 2013; Kolthoff, 1932; Rajaeiyan & Bagheri-Mohagheghi, 2013).

Drawbacks:

- This technique is the most widely used method for nanoparticle synthesis due to its simplicity and lack of hazardous materials and equipment. In addition, it is possible for large quantities of magnetic nanoparticles to be produced; however, the size distribution of the structures is vast as they are unstable and succumb to aggregation easily. This being said, the procedures that follow may become quite costly and require a substantial amount of maintenance (Wadekar et al., 2017; Kandpal et al., 2014; Sari et al., 2017).

2.3.2.7. *Chemical Vapour Deposition*

Chemical vapour deposition (CVD), similar to physical vapour deposition, is a method for depositing non-volatile films on substrates by incorporating chemical reactions between an organometallic or halide compound and other gases. The process is typically initiated when the substrate is exposed to one or more gaseous precursors, which then decompose on the surface of the substrate to produce the desired nanolayer (Martin, 2010). Since the reactions possess high activation energies, the substrate is heated in a vacuum chamber to aid the dissociation of the vapours (Madhuri, 2020; Tahir et al., 2020). CVD differentiates from PVD in that it uses a multidirectional deposition method to deposit material onto the substrate, whereas PVD employs a line-of-site impingement approach. Furthermore, PVD does not exploit the use of chemical interactions between the gases and the bulk surface of the material, resulting in no chemical decomposition on the surface of the base material (Behera et al., 2020; Senapati & Maiti, 2020).

Drawbacks:

- The CVD process is capable of producing high-purity nanoparticles with fine structural regularity. However, operating costs are substantial due to the extreme heat required, and a potentially toxic gas is released through the exhaust of the chamber (Barua et al., 2020).

2.4. Biological Synthesis Techniques

Despite most chemical and physical synthesis routes able to fabricate nanoparticles with precise physio-chemical properties and a high degree of repeatability, they possess an array of devastating faults linked to the procedures employed. To summarise section 2.3, conventional methods use aggressive reagents, necessitate high energy input, and pose potential environmental and biological risks as by-products or waste streams retain toxic qualities (Genuino et al., 2012).

Rapid industrialisation, urbanisation, and population growth have exponentially increased modern society's environmental and energy demands; therefore, the nano-industry should not have to contribute to this. Fortunately, solutions to negate the drawbacks of traditional synthesis techniques have been sought, striving for a more sustainable approach and a reduction in the environmental footprint. Recent developments have advertised a revolutionary technique that has merged nanotechnology and green chemistry by utilising biological systems as an alternative nanoparticle fabrication method (Hussain et al., 2016; Malik et al., 2014).

For a truly "green" synthesis, three conditions are essential: an environmentally-benign solvent, a renewable reducing agent, and an innocuous material for stabilisation (Jadoun et al., 2021). The ecological assemblage of nanoparticles is a simple and cost-effective technique that effortlessly combines these principles by replacing toxic reagents with biological components such as bacteria (Lee et al., 2004), fungi (Mustapha et al., 2022), yeast (Fernández et al., 2016), algae (Singaravelu et al., 2007), and plants (Moghadam et al., 2022). This is possible due to the reductive capabilities held by the biomatter to enable the formation of the desired nanoparticle (Figure 2.2). Besides nullifying the toxicity of conventional synthesis methods, the procedure maintains a fast production rate under ambient conditions, thereby eliminating additional energy requirements (Gardea-Torresdey et al., 2002; Kowshik et al., 2002; Lee et al., 2004; Mukherjee et al., 2002).

The stability of the nanocolloids produced through physical and chemical paths remains an issue due to the requisite of synthetic additives. However, the organic compounds provided by biological reactants double as both reducing and stabilising agents as they encase the surface of the nanostructures (Singh et al., 2016). Therefore, the risk of particle agglomeration is dramatically reduced while still preserving the fundamental characteristics of the nanopowder (Li et al., 2011).
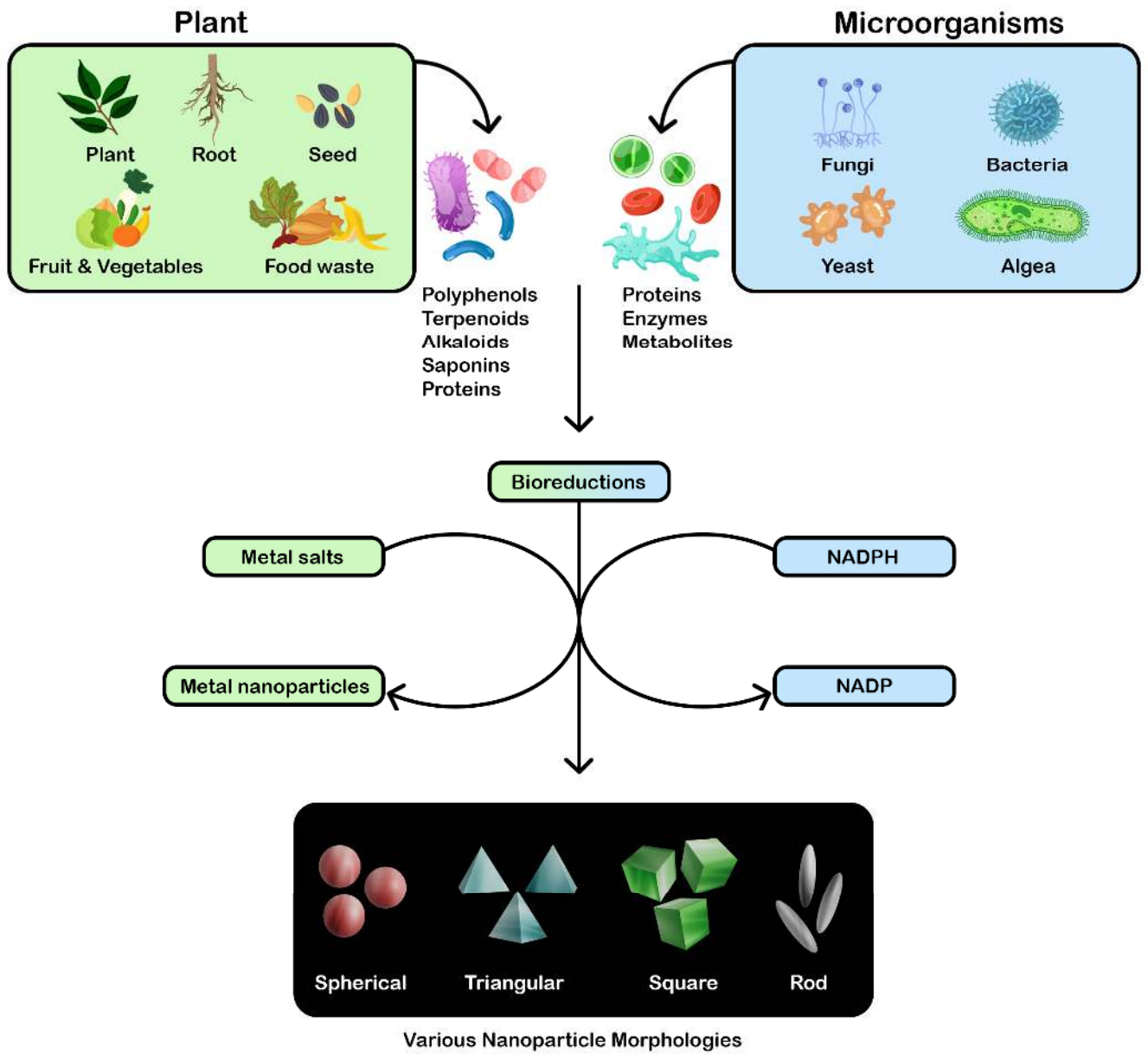
Figure 2.2: The biological synthesis routes of nanoparticles

2.4.1. Bacterial Synthesis

Numerous studies have successfully demonstrated the synthesis of nanoparticles through various bacterial species (Table 2.1). Different bacteria follow diverging mechanisms for nanoparticle synthesis; however, it has been deduced that the generation of the nanoarchitectures is initiated through the entrapment of metallic ions on the surface (extracellular) or within (intracellular) the microbe (Pandit et al., 2022). Typically, electrons possess the quality to shift from reduced organic to oxidised inorganic compounds through microbial dissimilatory anaerobic respiration, thus promoting the formation of the nanomaterial (Ghosh et al., 2021). In addition, some bacteria have developed the ability to resort to specific defence mechanisms to quell stresses like the toxicity of metals and heavy metal ions, where it has been observed that specific strains could survive and grow even at high metal ion concentrations (Iravani, 2014).

Table 2.1: Examples of bacteria-mediated nanoparticles

Bacterial Species	Nanoparticle	Particle Size (nm)	Morphology	Reference
Acinetobacter sp. SW30	Se	79	Spherical	Wadhwani et al. (2017)
Bacillus subtilis	Ag	3-20	Spherical	Alsamhary (2020)
Escherichia coli	Ag	50	Spherical	Aryal et al. (2019)
Klebsiella pneumoniae	Au	35-65	Spherical	Malarkodi et al. (2013)
Lactobacillus	Ag	31	-	Garmasheva et al. (2016)
Lysinibacillus xylanilyticus	Ag	8-30	Spherical	Huq (2020)
Staphylococcus aureus	Ag	160-180	Irregular	Nanda & Saravanan (2009)

Researchers have investigated the bacteria-mediated reduction of metals and reported that the enzymes and other interactive pathways are responsible for the reduction of the metal ions, while the proteins within the cell stabilise the nanostructures through encapsulation (Ghashghaei & Emtiazi, 2015). The core benefit of employing bacteria cells for the development of nanoparticles is the facilitation of large-scale synthesis with minimal use of hazardous and expensive chemicals. However, bacterial culture techniques are quite time-consuming and problematic when controlling the size, shape, and crystallinity of the particles (Lahiri et al., 2021).

2.4.2. Fungal Synthesis

Similar to bacteria, fungal cultures possess the ability to synthesise metallic nanoparticles as they exhibit intracellular absorption capabilities, metal bioaccumulation characteristics, and high binding properties (Guilger-Casagrande & Lima, 2019). Previous studies, displayed in Table 2.2, have demonstrated both extracellular and intracellular reduction locations. The extracellular mechanism utilises microbial enzymes, cell wall components, and organic molecules present in the fungal strain (Alavi, 2022). On the other hand, the intracellular process engages the initial electrostatic attraction of metallic ions to the carboxyl groups of the cell wall, thereby creating a passage for the ions and allowing reduction to commence through intracellular proteins and other co-factors (Sastry et al., 2003).

Table 2.2: Examples of fungi-mediated nanoparticles

Fungal Species	Nanoparticle	Particle Size (nm)	Morphology	Reference
Aspergillus niger	Ag	4-28	Spherical	Farrag et al. (2020)
Candida albicans	Ag	20-80	-	Rahimi et al. (2016)
Fusarium oxysporum	Pt	70-180	Rectangular, Triangular, Spherical	Govender-Ragubeer et al. (2008)
Neurospora crassa	Ag/Au	11	Spherical	Castro-Longoria et al. (2011)
Penicillium chrysogenum	MgO	10	Spherical	El-Sayyad et al. (2018)
Pleurotus florida	Au	20	Spherical	Gurunathan et al. (2014)
Rhodotorula mucilaginosa	Ag	14	Spherical	Cunha et al. (2018)

Fungi, unlike bacteria, preserve the ability to withstand significant flow and agitation in large-scale bioreactors due to the high resistance of fungal mycelial mesh (Chauhan et al., 2022). Furthermore, the fastidious nature of growth enables a high enzymatic production and allows for a larger metallic uptake capacity, resulting in an increased NP fabrication rate and yield (Pal et al., 2019).

Despite these advantageous characteristics, the yield of the nanoparticles may be compromised, considering the necessary downstream extraction procedures. In addition, the fabrication of fungi-mediated nanoparticles requires 24 hours or more, which could be a substantial hindrance to further application (Sadowski et al., 2008; Vigneshwaran et al., 2007; Mishra et al., 2010). Therefore, regardless of fungal synthesis being superior to bacterial routes, the deficiencies of the procedure defeat the purpose of developing a cheap and straightforward process (Jeevanandam et al., 2016; Sharma & Tripathi, 2022).

2.4.3. Plant Synthesis

By virtue of their renewability and wide availability, plants have been utilised as highly sustainable biological factories for the synthesis of nanostructures (Vanlalveni et al., 2021). Previous researchers have exploited their outstanding potential in heavy metal detoxification and accumulation through various species (Table 2.3) (Makarov et al., 2014). The preparation of the nanoarchitectures can be divided into three phases: reduction, growth, and termination. Initially, metal ions are reduced to atoms through phytoactive compounds, which are then self-assembled to form nuclei and, subsequently, nanoparticles (Figure 2.3) (Khan et al., 2022). Finally, the phytochemicals are enriched around the nanostructures through electronic interactions to maintain stability, thereby simultaneously acting as a capping agent (Bao et al., 2021; Parveen et al., 2016).

Table 2.3: Examples of plant-mediated nanoparticles

Plant Species	Nanoparticle	Particle Size (nm)	Morphology	Reference
Azadirachta indica	TiO_2	15-50	Spherical	Thakur et al. (2019)
Capparis spinosa	Cu	17-41	Spherical	Ebrahimi et al. (2017)
Lawsonia inermis	Au	5-10	Spherical	Abd El-Aziz et al. (2018)
Moringa oleifera	Co_3O_4	20-50	Spinel cubic	N Matinise et al. (2018)
Pistacia atlantica	Ag	50	Spherical	Golabiazar et al. (2019)
Salvia officinalis	Fe	5-25	Spherical	Z. Wang et al. (2015)
Xanthium strumarium	Pt	22	Cubic & Rectangular	Kumar et al. (2019)

In comparison to microorganisms, the phytosynthesis of nanoparticles is a genuinely green route that is vacant of complex and multistep processes such as microbial cultivation and maintenance (Akhtar et al., 2013). Another advantage of plant-assisted synthesis is the considerably higher kinetics, which induces a fabrication rate almost equivalent to conventional nanoparticle preparation (Jadoun et al., 2021; Venkat Kumar & Rajeshkumar, 2018). Furthermore, plants provide low-cost cultivation with better control and stability of the nanomaterial that can be effortlessly scaled up for bulk production (Hussain et al., 2016; Ahmed et al., 2022). However, all plant species are known to harbour multitudinous metabolites, which are crucial factors to consider during synthesis as they can drastically alter the physio-chemical properties of the nanoparticle (J. Singh et al., 2018). Therefore, it is essential to determine the composition of the plant material.

It was found that all plant species contain biomolecules categorised as primary and secondary metabolites, which are responsible for the reduction of metallic ions during nanoparticle synthesis (Rastogi et al., 2018). The corresponding phytochemicals also have a direct impact on the size and morphology of the nanostructure (Alharbi et al., 2022). Consequently, the

composition and concentration of these active compounds, and their reactivity towards the metallic precursor, are believed to be the major contributing factors to the diverse aspects of the nanomaterial due to variations in their electron-donating capacities (Jeevanandam et al., 2022; Das et al., 2017). Hence, achieving complete controllability of these characteristics is of the utmost importance for further development in the field.
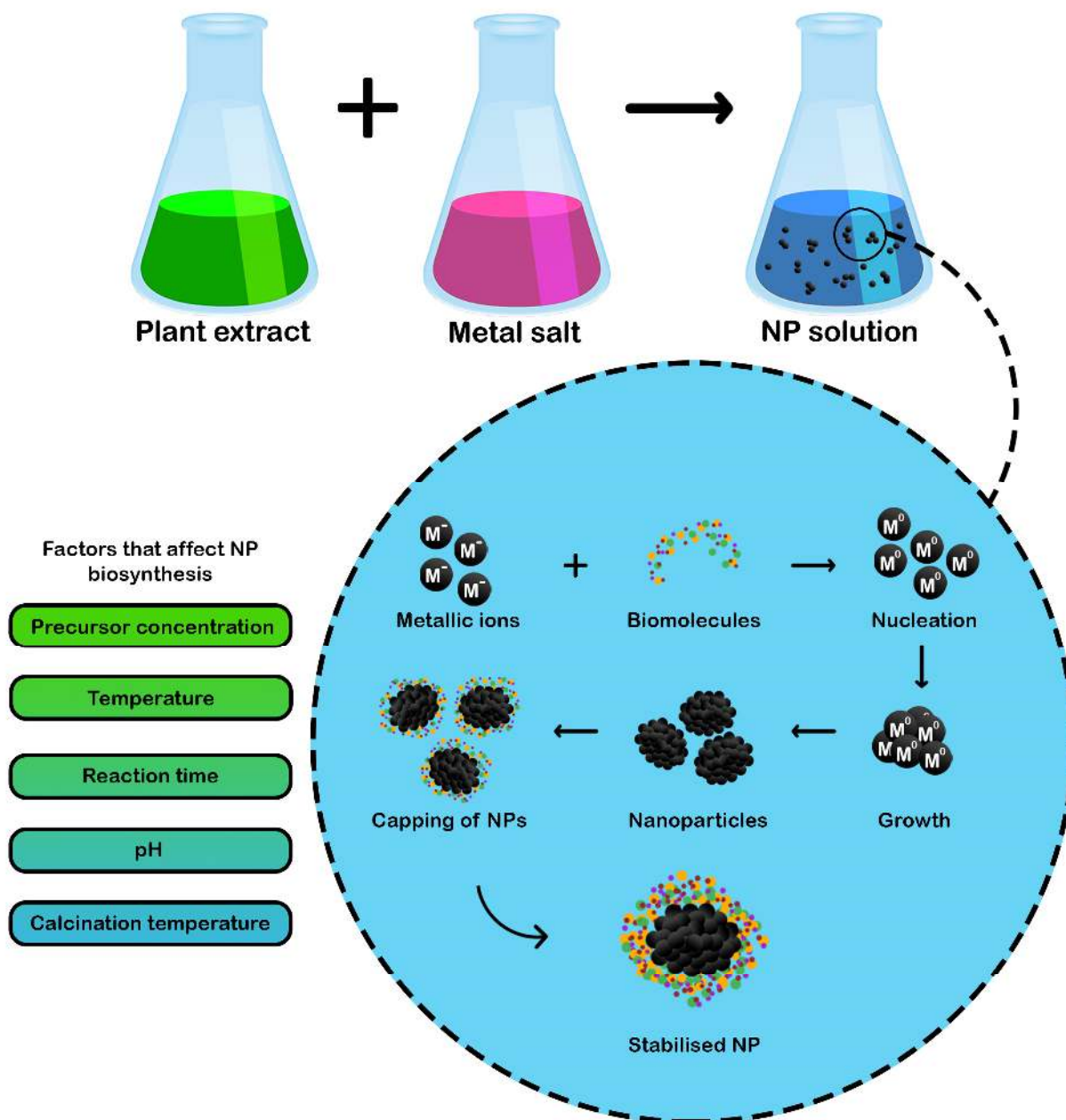
Figure 2.3: The plant-mediated synthesis of metallic nanoparticles

2.5. Plant Metabolites

The crude extracts of plants have been known to harbour a wide range of metabolites. Within a plant cell, two types are produced: primary metabolites, which consist of carbohydrates, organic and amino acids, proteins, nucleic acids, polysaccharides, and glucosinolates, and secondary metabolites, comprising phenolics, alkaloids, saponins, terpenoids, and lipids (Mittal *et al*., 2013; Jeevanandam *et al*., 2016).

Primary metabolites are the phytochemicals associated with essential life functions such as cell division, growth, and development (Hussein & El-Anssary, 2019). Contrarily, secondary metabolites are derived from primary metabolic pathways. In plants, the main purpose of secondary metabolites is to assist in the abiotic stress caused by the environment (Akula & Ravishankar, 2011). In addition, they are utilised in the signalling and regulation of primary metabolic pathways (Pichersky & Gang, 2000). Ultimately, secondary metabolites help the plant maintain an intricate balance with its environment through adaptation (Divekar et al., 2022). However, derivative routes linked to secondary metabolite production are essential for plant development as they constitute hormones or are necessary for photosynthesis (Twaij & Hasan, 2022). Therefore, it becomes difficult to distinguish between primary and secondary metabolites. Nonetheless, secondary metabolites possess specified functions and often depend on the plants that house them, with concentrations varying enormously between different species (Böttger et al., 2018).

Other than the secondary metabolites' purpose in the natural environment, they play a substantial role in the synthesis of nanoparticles due to the amalgamation of their reducing and stabilising properties (Fierascu et al., 2022). It is, therefore, crucial to investigate the major compounds within the plant material responsible for NP synthesis as they may affect morphologies and, thus, alter the core properties. Due to their vast abundance in plants, determining these specific compounds is a tedious effort; however, they have been narrowed down to several classes of metabolites in particular: polyphenols (phenolic acids and flavonoids), terpenoids, alkaloids, saponins, and proteins (Ovais et al., 2018).

Table 2.4: Plant metabolites involved in nanoparticle synthesis

Plant Species	Nanoparticle	Metabolites Identified	Reference
Andrographis paniculata	ZnO	Terpenoids	Kavitha et al. (2017)
Bidens tripartitus	Pt	Flavonoids	Dobrucka (2016)
Desmodium gangeticum	Ni	Flavonoids, alkaloids & phenolics	Sudhasree et al. (2015)
Euphorbia granulate	Pd	Terpenoids	Nasrollahzadeh & Mohammad Sajadi (2016)
Fumariae herba	Pt	Alkaloids & phenolics	Dobrucka (2019)
Hibiscus rosa-sinesis	CuO	Phenolics & tannins	Rajendran et al. (2018)
Lawsonia innermis	MnO2	Flavonoids	Bhatnagar et al. (2014)

Memecylon edule	Au	Saponins	Elavazhagan & Arunachalam (2011)
Peganum harmala	Ag	Alkaloids	Almadiy et al. (2018)
Pulicaria glutinosa	Pd	Phenolics & flavonoids	Khan et al. (2014)
Punica granatum	TiO2	Phenolics	Dubey & Singh (2019)
Satureja intermedia	Ag	Phenolics	Firoozi et al. (2016)
Trifolium pratense	ZnO	Phenolics & tannins	Dobrucka & Długaszewska (2016)
Yucca gloriosa	MnO2	Phenolics	Hoseinpour et al. (2017)

In a study conducted by Roy and Bharadvaja (2017), silver nanostructures were fabricated using the aqueous extract of *Centella asiatica*. Amongst the several active constituents, terpenoids and proteins were the bioactive compounds that participated in the synthesis. According to the FTIR vibrational peaks, the silver nanoarchitectures were encapsulated by a thin layer of phytochemicals with various functional groups, including alcohols, amines, and aldehydes. Furthermore, *Peganum harmala* was successfully utilised to generate platinum and palladium nanoparticles with spherical morphologies and diameters of approximately 21 nm (Fahmy et al., 2021). Therapeutically active alkaloids, including β-carboline and quinazoline, were detected in the extract in addition to oxygenated monoterpenes (eugenol), flavonoids, and polysaccharides. These phytochemicals were responsible for the bio-reduction of the metallic ions.

As seen in Table 2.4, phenolic compounds have been the predominant phytoactive compounds involved in the synthesis of metallic nanoparticles. Salgado and co-authors (2019) have investigated the effect of these components during the synthesis of iron oxide nanoparticles. Several plant species, such as *Luma apiculate*, *Phragmites australis*, and *Eucalyptus globulus,* were employed as precursors for the reaction, resulting in spherical nanoparticles ranging from 5.4 to 36.5 nm. Using the Ferric-Reducing Antioxidant Power (FRAP), Folin-Ciocalteu (FC), and FTIR analyses, it was possible to establish a direct relationship between the concentration of the phenolic compounds and the reducing capacity of the extracts, and the study concluded that the phenolic content was inversely correlated to the hydrodynamic size of the obtained nanoparticles.

Polyphenols' effective radical-scavenging, concerning oxygen-free radicals, is determined by their reactivity as hydrogen- or electron-donating agents, the stability of the resulting anti-oxidant-derived radical, and their metal-chelating properties by virtue of both the electron richness of their phenyl ring and the relative weakness of their -OH bond (Soobrattee *et al.*, 2005). Hence, these compounds can act as a reducing and capping agent via either single-electron or hydrogen-atom transfer mechanisms (Zapesochnaya & Ban'kovskii, 2004).

Equation 1 and 2 demonstrates the two main mechanisms through which polyphenols can express their radical scavenging-based antioxidant action.

$$R^\bullet + ArOH \rightarrow RH + ArO^\bullet \tag{1}$$

$$R^\bullet + ArOH \rightarrow R^- + ArOH^{\bullet+} \tag{2}$$

2.6. Coffee

The coffee commonly consumed derives from the seed of the coffee tree, where there are currently two superior species, namely, *coffea Robusta* and *coffea Arabica* (Martín *et al.*, 1999). The concentrations of phenolic compounds and other secondary metabolites in plants are influenced by several factors, including soil, irrigation, and climatic conditions (Yang *et al.*, 2014). A study by Hečimović and co-authors (2011) showed that *C. Robusta* exhibited a higher total phenolic content when compared to its counterpart. In general, the coffee beverage is rich in volatile (esters, alcohols, aldehydes, ketones, alcohols, and hydrocarbons) and non-volatile substances: carbohydrates, proteins, fibre, amino acids, lipids, minerals, chlorogenic acids, trigonelline, and caffeine (Jeszka-Skowron et al., 2015). Of these compounds found in coffee, chlorogenic acids, trigonelline, caffeine, and diterpenes from the lipid fraction are most likely to be bioactive (Myo & Khat-udomkiri, 2022).

Among the rich moieties, fresh coffee beans provide a high content of phenolic acids of the hydroxycinnamic acids derivatives, comprising caffeic, chlorogenic, coumaric, ferulic, and sinapic acids (Upadhyay & Mohan Rao, 2013). The majority of these compounds can only be found in trace amounts; however, chlorogenic acids (CGA) are considered to be the main components of the phenolic fraction in coffee, reaching levels up to 14% (dry matter basis) (Farah & Donangelo, 2006). Chlorogenic acids include different compounds and related isomers formed by the esterification of one molecule of quinic acid and one to three molecules of a specific *trans*-hydroxycinnamic acid (Mills et al., 2013). The main groups of CGA found in coffee beans are caffeoylquinic acids (CQA), di-caffeoylquinic acids (di-CQA), feruloylquinic acids (FQA), *p*-coumaroylquinic acids (*p*CoQA), and six mixed diesters of caffeoyl-feruloyl-quinic acids (Figure 2.4) (Fujioka & Shibamoto, 2008).

a

Quinic acid Hydroxycinnamic acids

R_1 = OH	Caffeic Acid (CA)
R_1 = OCH$_3$	Ferulic Acid (FA)
R_1 = H	p-Coumaric Acid

b

R_1 = OH	5-CQA
R_1 = OCH$_3$	5-FQA
R_1 = H	5-pCoQA

c

R_1 = CA, R_2 = CA, R_3 = H	5-CQA
R_1 = CA, R_2 = H, R_3 = CA	5-FQA
R_1 = H, R_2 = CA, R_3 = CA	5-pCoQA
R_1 = FA, R_2 = CA, R_3 = H	3F,4CQA
R_1 = CA, R_2 = FA, R_3 = H	3C,4FQA
R_1 = FA, R_2 = H, R_3 = CA	3F,5CQA
R_1 = CA, R_2 = H, R_3 = FA	3C,5FQA
R_1 = H, R_2 = FA, R_3 = CA	4F,5CQA
R_1 = H, R_2 = CA, R_3 = FA	4C,5FQA
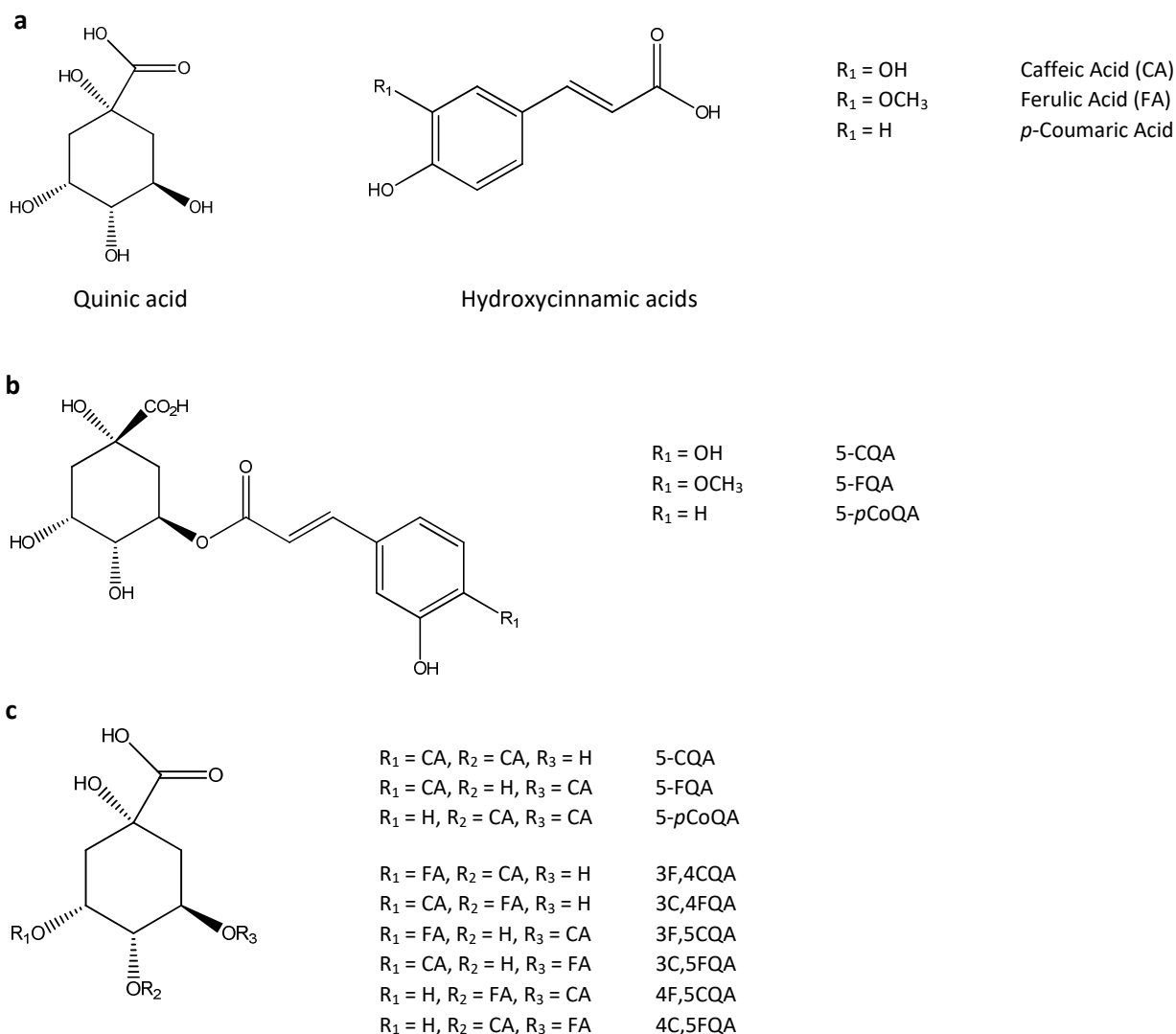
Figure 2.4: Chlorogenic acids and related compounds. (a) Basic compounds, (b) monoesters of quinic acid and hydroxycinnamic acids (example of 5-isomers), (c) di-esters of quinic acid with caffeic acid, and mixed esters

During roasting, several complex reactions are initiated, including the Maillard reactions, lipid oxidations, sugar decompositions, and pyrolysis (Wu et al., 2022). Some compounds are destroyed, and others are formed, along with various bioactive moieties. More specifically, a portion of the protein is dilapidated while free amino acids and reducing sugars are consumed as reactants to form melanoidins and other low-molecular-weight compounds (Van Boekel, 2006). These biochemicals incorporate into their structures' components, such as galactomannans, arabinogalactan-proteins, and chlorogenic acids (Trugo & Macrae, 1984). Experimentation carried out by Tarigan and co-workers (2022) confirmed the gradual degradation of alkaloids with the addition of diverse polyphenolic compounds. On the other hand, the study presented a consistent concentration of caffeine throughout the roasting process (Tarigan et al., 2022).

Despite the substantial quantity of chlorogenic acids in fresh coffee beans, this bioactive substance experiences the most drastic degradation during roasting due to its thermal instability (Izawa *et al.,* 2010). The degradation of this compound is initiated through isomerisation, followed by epimerisation, lactonisation, and deterioration to formulate other constituents (Figure 2.5) (Moon & Shibamoto, 2010). The outcome of these mechanisms is highly dependent on the time and temperature of the roast, where variations in these conditions directly affect the moisture, protein, carbohydrate, and phenolic acid contents (Grzelczyk et al., 2022). With shorter roasting times and lower temperatures, chlorogenic acid can be hydrolysed and temporarily increase caffeic acid concentrations. In contrast, longer roasts at higher temperatures may result in the degradation of caffeic acid released from CGA (Diviš et al., 2019).

According to Diviš and co-workers (2019), CGA concentrations declined by 67% in a "medium" roast (210°C for 14 min), while an 85% decrease was witnessed after an increase in roast intensity (225°C for 19 min). Although the substantial diminution of chlorogenic acids, the presence of phenolic compounds was still evident. Several reasons can reaffirm the statement above. Firstly, CGA is known to break down into its various components, thereby increasing the concentrations of quinic and caffeic acids (de Rigal et al., 2000). Phenolic acids, including gallic, ferulic, and *p*-coumaric, have been proven to increase during heat treatment (Beyene & Sabally, 2013). Also, compounds such as *p*-coumaric acid and cinnamic acid retain higher thermal stability, resulting in minimal degradation (Herawati et al., 2022). In addition to the aforementioned phenolic substances, pyrocatechol, although absent in the analysis of fresh coffee beans, was discovered in roasted coffee samples as a decomposition product derived from CGA (Wianowska & Gil, 2019).

Regardless of the physical and chemical changes occurring during the roasting process, the antioxidant capacity of the extract remains promising. Alterations in the oxidative properties of the coffee beans are associated with the degradation of chlorogenic acid and the formation of Maillard reaction products, such as melanoidins (Budryn et al., 2015; Vignoli et al., 2011). These newly formed compounds exhibit optimistic antioxidant activities due to their metal-chelating properties and free radical scavenging abilities; therefore, they may be considered bioactive substances (Nebesny & Budryn, 2003). Furthermore, caffeine is a significant contributor to the antioxidant capacity by virtue of their $^{\bullet}$OH radical scavenging characteristics (Vieira et al., 2020). Despite the impact of these biochemicals, the oxidative strength of coffee continues to depend on the balance of the compounds formed during this process.

Positional Isomerisation:
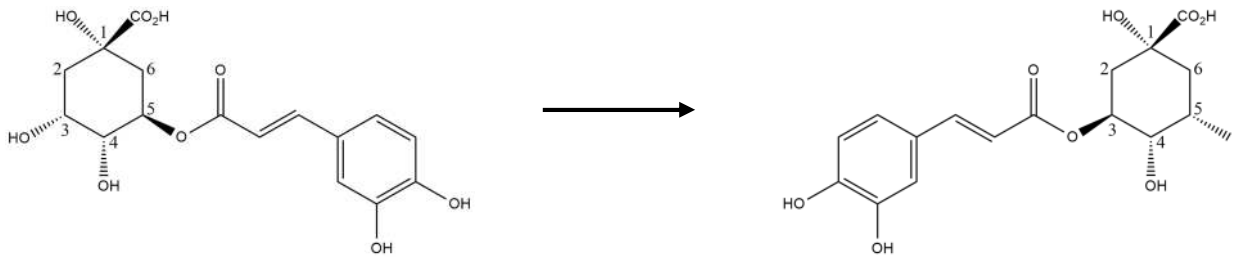
Epimerisation:
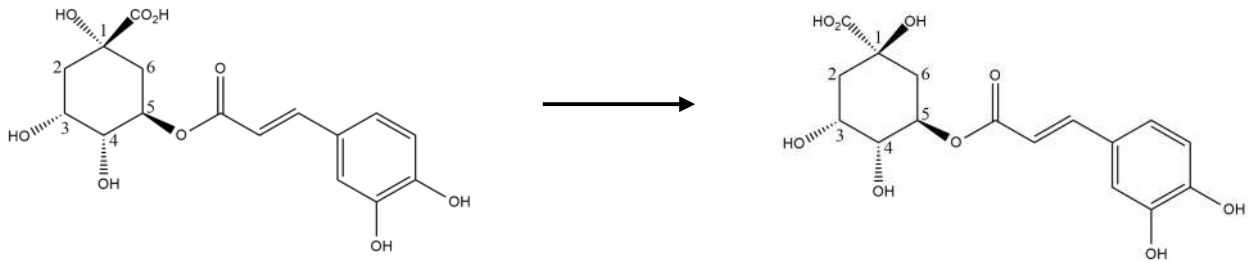
Lactonisation:
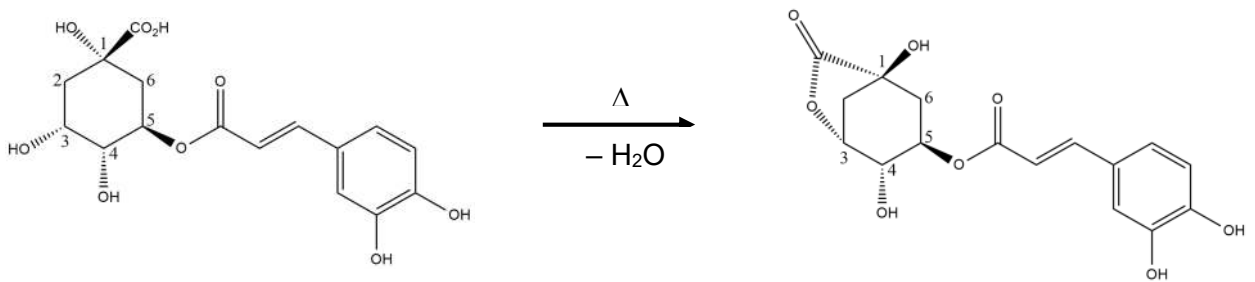
Hydrolysis:
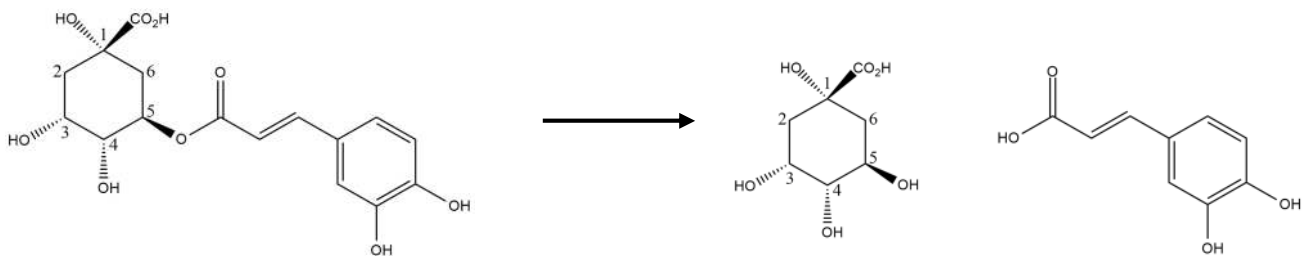
Degradation into lower molecular weight compounds:
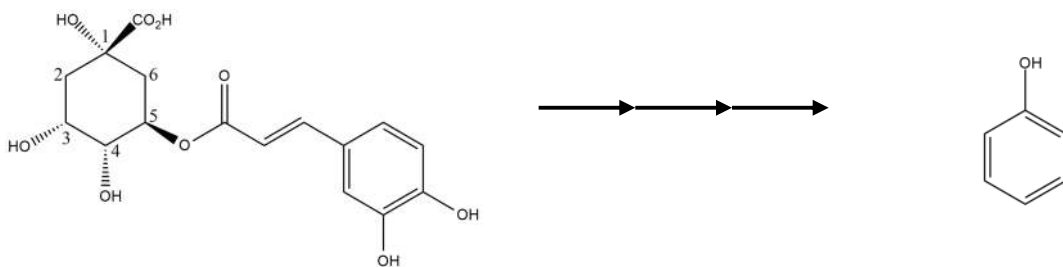
Figure 2.5: Examples of changes in chlorogenic acids during thermal treatment

Previous researchers have proven the participation of the aforementioned compounds in nanoparticle synthesis. Mahmoud and co-authors (2021) successfully fabricated iron nanoparticles through the use of coffee extract. The FTIR spectrum, depicted in Figure 2.6, displayed a dominant peak at 3397 cm^{-1} due to the hydroxyl (-OH) stretching vibration groups caused by the presence of phenols or water. The sharp band at 2930 cm^{-1} indicated the symmetric and asymmetric stretching of =CH bonds in caffeine molecules, and the peak at 1614 cm^{-1} was detected due to the stretching vibrations of carbonyl (C=O) groups located in caffeine and chlorogenic acids. In addition, the characteristic bands at 1393, 1272, 1124, and 1054 cm^{-1} emerged by cause of lesser polyphenols. Looking at the FTIR data obtained from the synthesised Fe-NPs, the shifting of numerous peaks and the disappearance of others confirmed the crucial interactions between the coffee extract and the nanoparticles. The study also revealed the bonding of various phenolic substances to the surface of the nanoarchitectures, thereby increasing their stability (Mahmoud et al., 2021). Other authors obtained similar results when synthesising silver (El-Desouky et al., 2022), gold, and selenium (Abbasian & Jafarizadeh-Malmiri, 2020) nanoparticles through coffee extract.
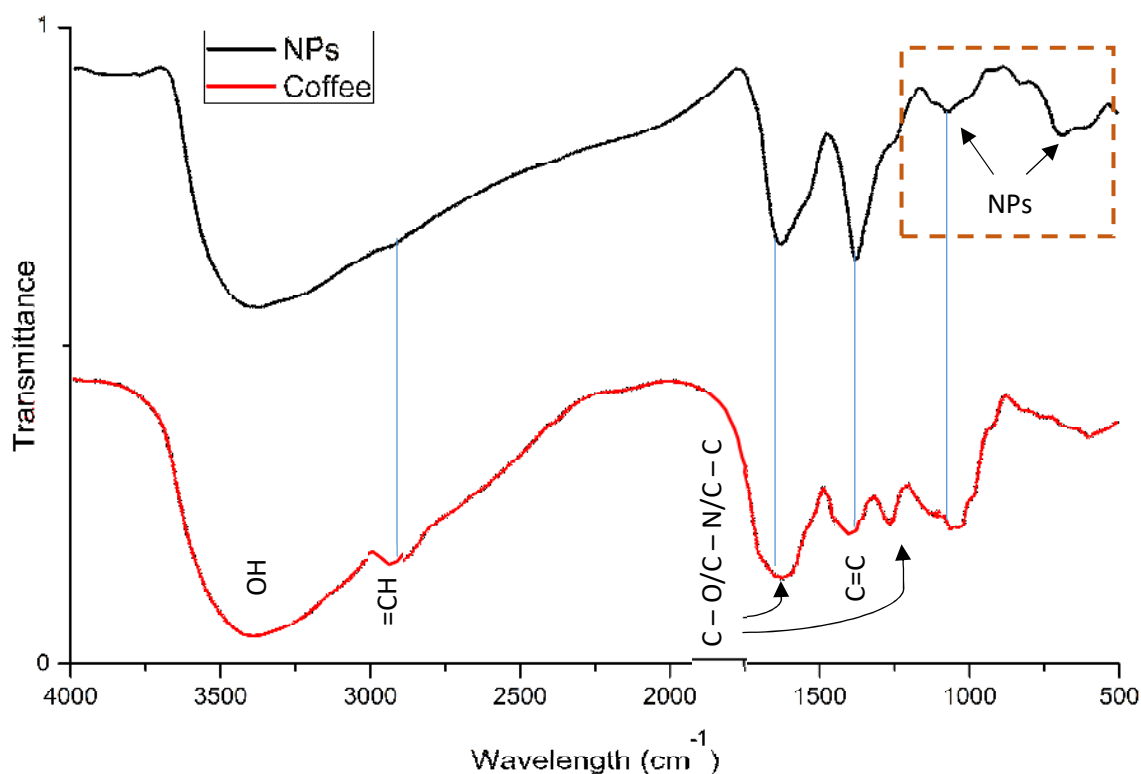
Figure 2.6: The redrawn FTIR spectra of iron nanoparticles synthesised using coffee extract (Mahmoud et al., 2021)

2.7. Cobalt Oxide Nanoparticles

Cobalt, a ferromagnetic transition metal, has unique electrical, optical, magnetic, and catalytic properties that make it suitable for broad-ranging applications. Cobalt and its metastable phases with various crystallographic structures, including face-centred cubic, hexagonal closed packed, and epsilon phases, have been considered one of the most important ferromagnetic metals as it possesses several possible oxidation states, with the most common being Co(II) and Co(III) (Iravani & Varma, 2020; Brown, 2018). Therefore, cobalt's multi-electronic valence allows the substance to be present in various spin states in its oxide forms (Raveau & Seikh, 2012). For example, the presence of Co(III) introduces an additional degree of freedom associated with the nature of their spin states. More specifically, in an octahedral environment, the competition between low-spin (LS), intermediate-spin (IS) and high-spin (HS) states is particularly subtle, leading to a situation prone to the development of spin state transitions (SST) (Guillou et $al.$, 2013). In a dilute and isolated solution, a general equilibrium exists between the LS and HS states which are characterised as follows:

$$LS \leftrightarrow HS$$
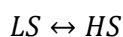
These transitions mainly occur for metal ions characterised by the electronic configurations $3d^4$, $3d^5$, $3d^6$, and $3d^7$ if the cubic crystal-field splitting of the 3d energy level and the Hund's rule exchange energy is comparable in magnitude (Konig et al., 1985). Furthermore, cobalt oxide is a recognised antiferromagnetic p-type semiconductor with both positive and negative polar termination (Tian et $al.$, 2018). The metallic compound with a valence of more than three has an unstable nature; however, cobalt oxide forms such as CoO and Co_3O_4 are considerably more reliable (Makhlouf et $al.$, 2013). This allows for cobalt oxide nanoparticles to have a wide range of applications comprising the removal of dyes from wastewater, catalysts for fuel cells, lithium-ion battery enhancement, electrochemical sensors, and treatment of diseases (Shi et al., 2012; Hussain et al., 2016; Choi et al., 2019; Khalil et al., 2017; Benchettara & Benchettara, 2015).

Previous researchers have demonstrated the successful synthesis of cobalt-based nanoparticles using plant extracts such as *Moringa oleifera* (N. Matinise et al., 2018), *Citrus medica* (Siddique et al., 2021), *Populus ciliate* (Muhammad et al., 2020), *Piper nigrum* (Haq et al., 2021), and *Trigonella foenumgraceum* (Akhlaghi et al., 2020). The proposed mechanism for the green synthesis of cobalt oxide nanostructures involving phenols is displayed in Figure 2.7.
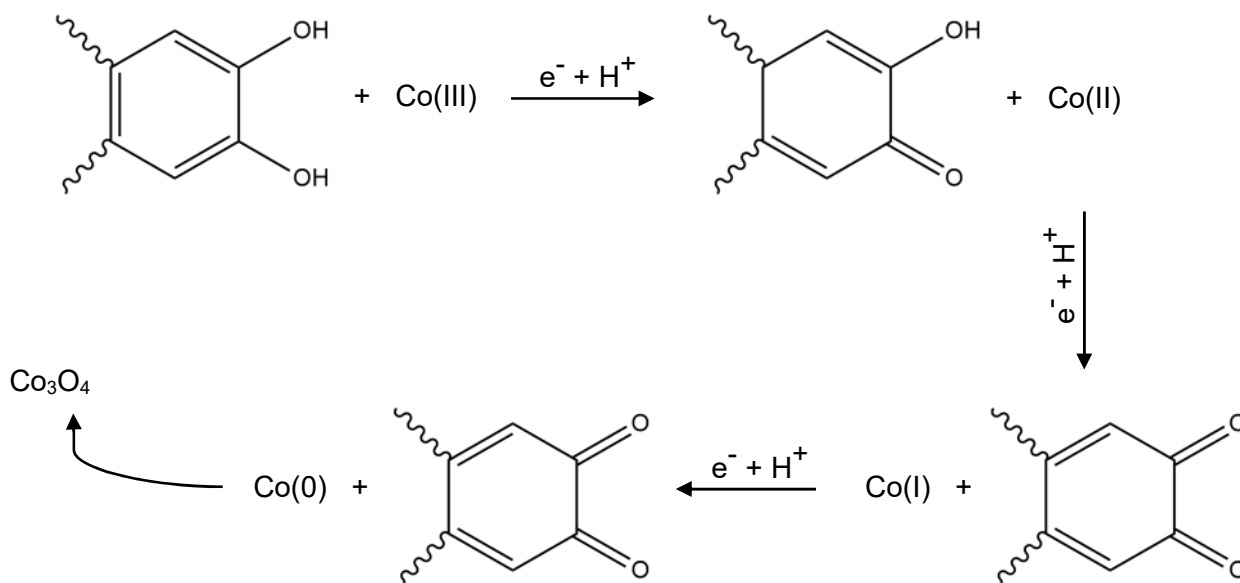
Figure 2.7: The proposed mechanism for the green synthesis of Co₃O₄ NPs

2.8. Nanocatalysis

Catalysis is a procedure known across numerous scientific and technological fields involving the acceleration of a chemical reaction through the addition of foreign material (Chorkendorff & Niemantsverdriet, 2005). This foreign substance is defined as a catalyst. The catalyst accomplishes the increased reaction rate by reducing the required activation energy for the reaction to commence without affecting any resulting products (Schlögl, 2015).

Nanomaterials have become an emerging technology that has produced outstanding results with an array of advantages in nanocatalysis (Figure 2.8). For these catalysts, the reactants are generally adsorbed onto the surface of the dedicated nanoparticle, where they exhibit unique electron transfer capabilities (Ratautas & Dagys, 2020). Therefore, the large surface area of the nanostructures provides more active sites for reactions to take place, and controlling the morphology, size, and composition of these catalytically active particles may catapult efficiencies (van Santen, 2012). More specifically, the catalytic activity of the nanoparticles depends on the quantity, strength, and spatial arrangement of the chemical bonds that are momentarily created between the reactants and the surface, which relies on the unique characteristics of the nanomaterial (Roque-Malherbe, 2019). In addition, Roduner (2014) also stated that rough surfaces with defects in the crystal facets, corners, and edges had been proven to possess considerably higher catalytic activities than perfect single-crystal surfaces. Therefore, this could give an advantage to biologically synthesised nanoparticles due to the imperfections present in the structures.

Nanocatalysts may be classified as either homogeneous or heterogeneous types. Regarding homogeneous systems, the nanoparticles are suspended in a solvent where the reaction occurs, while heterogeneous nanocatalysts tend to be a solid or immobilised on a solid inert matrix (Somwanshi et al., 2020; Schlögl & Abd Hamid, 2004). Despite the reusability and ease of recovery of heterogeneous catalysts, they often display poor catalytic activity and selectivity compared to the latter (Nasrollahzadeh et al., 2014). On the other hand, homogenous catalysts tend to agglomerate and cluster together to form larger particles if not prevented appropriately; thus, the nanoparticles experience a decrease in their surface area, catalytic activity, and other significant features (Narayanan et al., 2008). However, nanoparticles mediated through green methods negate these aspects due to the biomolecule-induced capping. In spite of this, it remains crucial for research to be furthered in nanocatalysts for the economic development and growth of the chemical industry.
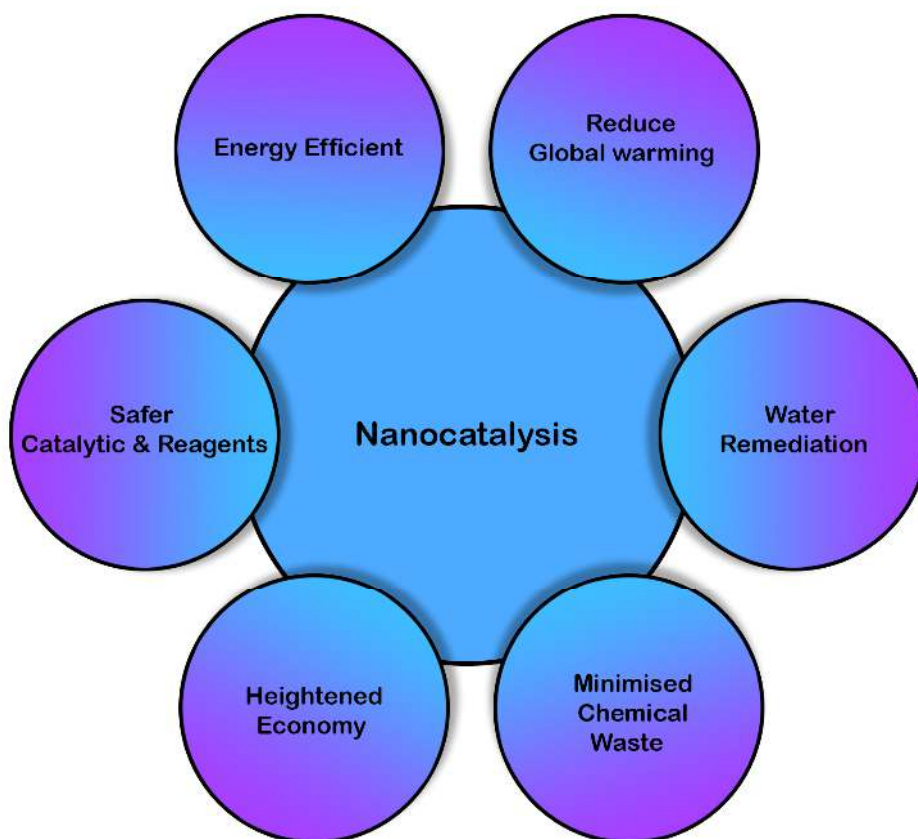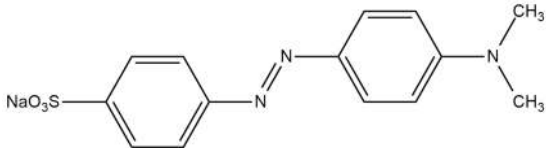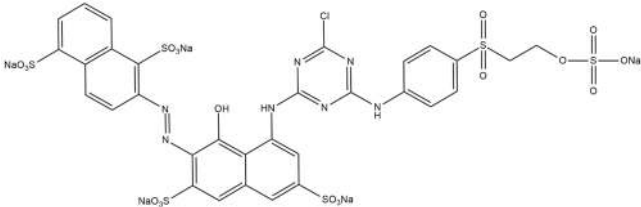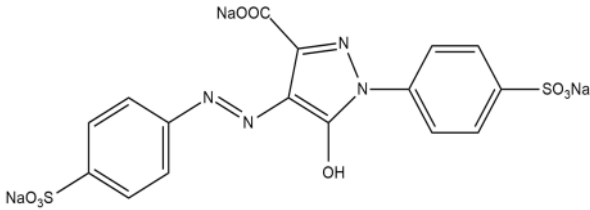
Figure 2.8: The advantages of nanocatalysis

2.8.1. Azo Dyes

Industries that produce textiles, tanneries, dyes, paint, and paper necessitate an important class of pollutants, in other words, dyes (Anastopoulos *et al.*, 2018). During these processes, inefficiencies in the colouring generate substantial amounts of dye residues, where approximately 10-15% is lost and released into water bodies (Ventura-camargo & Marin-morales, 2013). Subsequently, the presence of these constituents in industrial effluents can adversely affect aquatic ecosystems (Sabzoi *et al.*, 2018).

Azo dyes are favourable for industrial applications as they are versatile, resilient, and cost-effective agents. Due to these characteristics, azo dyes account for approximately 70% of all dyes utilised within industrial processes (Benkhaya et al., 2020). These compounds are chemically represented as R–N=N-R', where –N=N- is the azo group linked to phenyl and naphthyl radicals (Table 2.5). The diversity of the vivid colours usually arises from the replacement of the radicals with combinations of functional groups: amino ($-NH_2$), chlorine (-Cl), hydroxyl (-OH), methyl ($-CH_3$), nitro ($-NO_2$), sulphonic acid and sodium salts (SO_3Na) (Chung, 2016). Unfortunately, several studies have mentioned that the uncontrollable discharge of azo constituents into the environment is unnerving due to the genotoxic, mutagenic, and carcinogenic properties of these dyes and their biotransformation products (Puvaneswari et al., 2006). In addition, these pollutants create undesirable turbidity in aquatic bodies, reducing sunlight penetration and thereby restricting the nourishment of marine life (Ismail et al., 2019). Therefore, maintaining a sustainable concentration of dyes in industrial effluents, or the development of efficient methods for the treatment of polluted waters, is vital for the environment.

Table 2.5: Examples of different azo dyes and their respective chemical structures

Azo Dye	Abbreviation	Structure	λ (nm)
Methyl Orange	MO		464
Remazol Brilliant Red	RBR		542
Tartrazine	Tart		425

2.8.2. Advanced Oxidation Processes

The degradation of dye residues as a form of wastewater treatment is a promising way to combat the accumulation of these harmful substances in water bodies. Currently, several physical and chemical degradation methods exist, such as filtration, reverse osmosis, ozonation, electrolysis, oxidation, adsorption, coagulation-flocculation, ion exchange, and precipitation (Mahmood, 2022). However, these processes are often criticised for the high production of solid waste and secondary contamination.

Advanced oxidation processes (AOPs) have been vastly applied in refractory pollutant degradation as they are simple, highly efficient, environmentally compatible, and capable of oxidising a wide range of contaminants (mineralisation to CO_2, H_2O, and inorganic ions) (Saratale *et al.*, 2011). More specifically, generated free radicals such as hydroxyl radicals ($^\bullet OH$), superoxide radicals ($O_2^{\bullet -}$), and sulfate radicals ($SO_4^{\bullet -}$) play a substantial role in degrading recalcitrant micro-contaminants including hormones, pharmaceuticals, herbicides, and dyes (Brienza et al., 2014; Q. Zhang et al., 2015; Ahmed et al., 2014; D. Wang et al., 2015; Bagheri et al., 2019). Despite the dominant focus and abundant research, $^\bullet OH$-based AOPs are known to be accompanied by several limitations (Kurian, 2021):

- H_2O_2 instability
- Necessitates acidic process conditions (pH 2 – 4)
- Production of sludge.

Among the aforementioned AOPs, sulfate radicals have recently become of interest as they possess relatively longer lifetimes (30–40 µs), greater redox potential ($E_0 = 2.5 - 3.1$ V vs NHE) than that of $^{\bullet}OH$ ($E_0 = 1.8 - 2.7$ V vs NHE), more moderate reactional pH conditions (pH 2 – 8), and higher oxidation capacity in both carbonate and phosphate buffer solutions compared to the latter (Guerra-Rodríguez et al., 2018). Hence, sulfate-radical AOPs are regarded as the most promising for the removal of pollutants from water. Familiar sources for the generation of sulfate radicals are peroxymonosulfate (PMS: HSO_5^-) and persulfate (PS: $S_2O_8^{2-}$), where the compounds require activation through either (1) conventional heating, (2) ultraviolet irradiation, (3) ultrasonic waves, (4) alkaline activation, (5) strong oxidisers, (6) electrochemistry activation, or (7) transition metal nanoparticles (Yang *et al.*, 2007). Generally, peroxymonosulfate is considered a more favourable reactant as it retains the ability to produce both sulfate and hydroxyl radicals when its peroxide bond (-O-O-) is homolytically cleaved (Brienza & Katsoyiannis, 2017).

Various heterogeneous materials, such as Fe-, Co-, Ag-, Cu-, Mn-, Ru-, and Ni-based catalysts, have been reported to effectively activate PMS/PS for the removal of contaminants (Rao et al., 2014; M. Zhang et al., 2015; Zhang et al., 2020; Shan et al., 2021). Compared with other activation methods such as microwave, thermal, ultrasonic, and illumination, activation by heterogeneous materials has its advantages, including requiring less energy, ease of scaling up, and having high reactivity (Chowdhury et al., 2015). Transition metals can initiate the decomposition of PMS/PS through the mechanisms depicted in equations 3 and 4 (Xiao et al., 2018):

$$M^{n+} + S_2O_8{}^{2-} \rightarrow M^{(n+1)+} + SO_4{}^{\bullet-} + SO_4{}^{2-} \tag{3}$$

$$M^{n+} + HSO_5{}^- \rightarrow M^{(n+1)+} + SO_4{}^{\bullet-} + OH^- \tag{4}$$

In a recent study, Nagar & Devra (2019) displayed the successful activation of PMS through *Azadirachta indica*-mediated silver nanocatalysts, where the resulting sulfate radicals induced the degradation of Acid orange 10 (AO10) and Acid orange 52 (AO52). The maximum degradation efficiency of AO10 reached 84% in 32 minutes, while 90% in 15 minutes was achieved with AO52 (Nagar & Devra, 2019). Similarly, the spontaneous generation of $SO_4{}^{\bullet-}$ was demonstrated using a combination of green Co_3O_4-NPs and peroxymonosulfate. The mixture was applied in the degradation of a model compound Acid orange 7, resulting in 12% removal within 60 minutes (D. Wang et al., 2015).

2.9. Photo-nanocatalysis

Another interesting procedure for the degradation of dyes is an environmentally-benign technique involving the conversion of light energy into chemical energy; this process is known as photocatalysis. Initially, the nanoparticles come into contact with light, where photons are absorbed onto the surface of the nanostructure, thereby generating electron-hole pairs (h_{vb}^+/e_{cb}^-) as the electrons are transferred from the valence to the conduction band (Figure 2.9). Depending on the nanoparticle, the electron-hole pairs react in the solution to form free radicals that violently interact with the undesirable dye, oxidising the stable organic compound into reactive intermediates and inhibiting the h_{vb}^+/e_{cb}^- recombination process. The surface charge of the photocatalyst then speeds up the mineralisation of the intermediate species into CO_2, H_2O, and less toxic inorganic acids (Ijaz et al., 2017; Prakash et al., 2018).
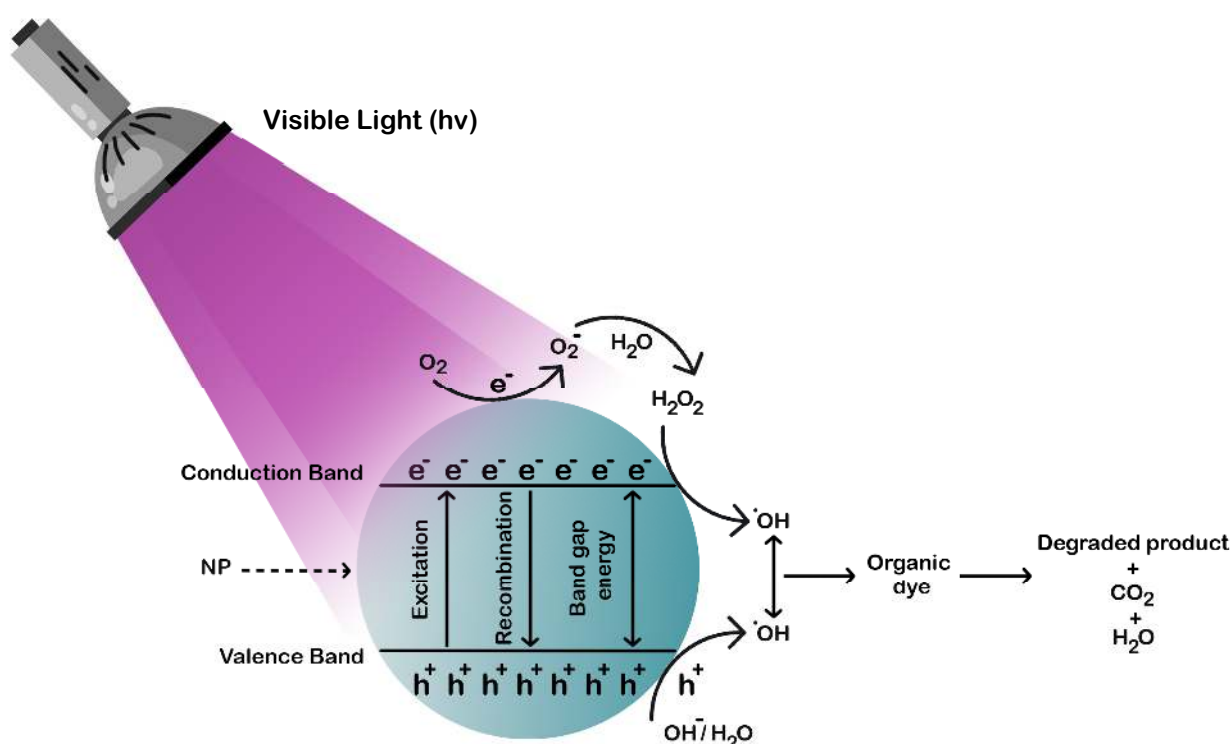
Figure 2.9: The general mechanism for the photo-induced degradation of pollutants through nanoparticles

Furthermore, the combination of metallic nanoparticles and ultraviolet illumination has proven beneficial to the degradation of pollutants by numerous researchers. The addition of this factor allows for the enhanced activation of PMS/PS, thereby increasing the available radicals in the system (Fan et al., 2019). Zazouli and co-authors (2017) compared the PMS-induced degradation of Brilliant Blue FCF (BBF) between solitary Fe_3O_4-TiO_2 nanoparticles and the nanostructures in conjunction with UV light. The research displayed interesting results, as the Fe-Ti-based nanoparticles alone only achieved 60% degradation; however, with the introduction of UV irradiation, complete decolourisation of the dye was accrued (Zazouli et al., 2017).

Moreso, the photocatalytic efficiency of $ZnFe_2O_4$ nanocomposites, coupled with PMS, was tested against Orange II (Zhu et al., 2016). The study observed virtually negligible deterioration of the azo dye in the NP/PMS system, while complete degradation was attained through the application of UV radiation therapy. Therefore, it can be deduced that majority of the radical generation was carried out by the UV-activated PMS. Despite the success of the irradiation, the nanomaterials mentioned above were initially deemed as unreactive substances in the presence of PMS; hence, a substantial efficiency hike was expected (Sun et al., 2021). Nonetheless, integrating several AOPs into one system is an ideal strategy for improving pollutant removal efficiencies.

2.10. Conclusion

It is clear that biological nanoparticle synthesis routes show promise in negating the adverse aspects of physical and chemical techniques through the utilisation of natural precursors. As mentioned in this section, despite the degradation upon roasting, spent coffee retains a substantial number of bioactive compounds that possess potent reductive capabilities. Furthermore, nanoparticles used for the activation of PMS in advanced oxidation processes have displayed enhanced reactivity towards pollutant removal compared to other methods. Hence, this study focuses on the green synthesis of Co_3O_4-NPs from spent coffee and evaluates the catalytic/photocatalytic properties in the degradation of an azo dye.

Chapter 3

3.1. Introduction

In this chapter, the materials, equipment, and procedures employed have been divided into relevant sections and discussed. This includes:

1. The extraction of phytochemicals from spent coffee
2. The synthesis and analysis of cobalt oxide nanoparticles from the spent coffee extract
3. The characterisation of the cobalt oxide nanoparticles
4. The catalytic/photocatalytic activity of the cobalt oxide nanoparticles against Tartrazine dye
5. A detailed study of the nanoparticles

All experiments were conducted at the Cape Peninsula University of Technology's Chemical Engineering and Chemistry Building in lab 1.27.

3.2. Extraction and Analysis of Phytochemicals from Spent Coffee

The extraction of phytochemicals was carried out through simple maceration, which is considered an effective solid-liquid extraction technique (Abubakar & Haque, 2020). The experiments were conducted to evaluate the effect of varying the extraction parameters on the solution's phytochemical concentration and antioxidant capacity. These tests include the effect of drying on the spent coffee grains. All experiments were performed in duplicates.

3.2.1. Materials

Arabica Coffee Beans, Folin-Ciocalteu reagent, Sodium carbonate (Na_2CO_3), Gallic acid, 1,1-diphenyl-2-picrylhydrazyl (DPPH), and methanol were all analytical grades. Deionised (DI) water, obtained from the laboratory purification system, was used to prepare all solutions.

3.2.2. Equipment

The following apparatuses were utilised in the extraction of the phytochemicals:

- A Mellerware Coffee machine was used to maintain the quality and consistency of spent coffee being generated.

- An incubator maintained temperatures over extended periods to remove any remaining liquid within the samples.

- The combination of a heating mantle, 500 mL round-bottom flask, condenser, and water-cooler was utilised as a closed system for the extraction of the phytochemicals from the spent coffee.

- A 1 L Büchner flask and funnel, coupled with a vacuum, were employed to clear the solution from unwanted debris.

- The CECIL CE2000 Spectrophotometer was used to analysis the extract through absorbance.

3.2.3. Experimental Procedure for the Spent Coffee Generation

1. Coffee beans were manually ground into fine granules in preparation for the coffee machine.
2. 100 g of the fresh coffee grains were introduced into the coffee machine with 1 L of tap water to simulate realistic consumer waste.
3. The spent coffee obtained from the machine was then evenly placed on a tray and inserted in an incubator with a designated temperature (30°C, 60°C, 90°C) for 18 hours.
4. The spent coffee grounds were then stored in an air-tight container at room temperature.

Table 3.1: The experimental runs for spent coffee drying temperature.

Run	Drying Temperature (°C)
A1	30
A2	60
A3	90

3.2.4. Experimental Procedure of Phytochemical Extraction

1. The water-cooler and heating mantle were powered on and set to their respective temperatures.
2. 200 mL of deionised H_2O was measured and deposited into the round-bottom flask, where it was heated to the required temperature (25°C, 50°C, 100°C) using a heating mantle.
3. The desired mass of the dried spent coffee was accurately measured for concentrations of either 25 or 50 g/L.
4. Using a funnel, the spent coffee was inserted into the round-bottom flask and briefly stirred to ensure equal extraction throughout the liquid.
5. The extraction was allowed to proceed for either 10 or 30 minutes.
6. After completion, the solution was immediately decanted into a suitable beaker to halt the process.
7. The Büchner flask and funnel filtered the remaining spent coffee particles from the extract.
8. The spent coffee extract (SCE) was then stored in the appropriate glass bottles at a temperature of 2°C.

Run	Concentration (g/L)	Temperature (°C)	Time (min)
B1	25	50	10
B2	50	50	10
B3	50	25	10
B4	50	50	10
B5	50	100	10
B6	50	50	10
B7	50	50	30

3.2.5. Experimental Procedure for the Analysis of the Extract

3.2.5.1. Total Phenolic Content

The concentration of total phenolic content was determined using a modified method introduced by Singleton & Rossi (1965). Initially, a 10 mL vial was used to host 0.2 mL of SCE with 1 mL DI-H$_2$O. The solution was then mixed with 0.2 mL of Folin-Ciocalteu reagent and left to settle for 5 minutes before 1 mL of a saturated sodium carbonate solution (8% w/v) was added (Singleton & Rossi, 1965). The solution was then incubated for 30 minutes at room temperature in the absence of light. Thereafter, the sample was centrifuged for 15 minutes at 4000 rpm to remove any turbidity. The resulting liquid was measured at a wavelength of 765 nm through the spectrophotometer. The sample blank was generated by replacing the SCE with the equivalent volume of distilled water. The following equation depicts how the true absorbance was calculated:

$$A = A_s - A_b \tag{5}$$

Where A$_s$ = the absorbance of the sample and A$_b$ = the absorbance of the blank. The results were presented as mg gallic acid equivalent/mL (mg GAE/mL) of coffee extract, on the basis of a standard curve of gallic acid (25-150mg/L, $Y = 0.006x - 0.1619, R^2 = 0.9935$)

3.2.5.2. DPPH Free Radical Scavenging Activity

This analysis enabled the quantification of the antioxidant activity against the stable free-radical DPPH. The assay was done per the method of Hemalatha et al. (2010) with minor alterations (Hemalatha et al., 2010). The test samples comprised 1 mL of the spent coffee extract and 3 mL of 0.1 mM DPPH-Methanol solution, with an additional 5 mL of methanol for further dilution. The samples were then immediately investigated at a wavelength of 517 nm using the CECIL CE2000 spectrophotometer. The SCE was replaced with methanol in order to obtain the absorbance of the control. The radical scavenging activity was calculated from the control sample using the equation 6:

$$Radical\ Scavenging\ Activity\ (\%) = \left(\frac{A_c - A_s}{A_c}\right) \times 100 \tag{6}$$

Where A_c and A_s are the absorbances of the control and sample, respectively.

3.3. Co_3O_4 Nanoparticle Synthesis from Spent Coffee Extract

The synthesis of the cobalt oxide nanoparticles was carried out using the SCE that displayed the optimal total phenolic content and antioxidant activity. However, the phytochemical extraction was scaled up, with each batch generating a 5 L solution for further application. These experiments were conducted to investigate different nanoparticle synthesis parameters and how they affect catalytic efficiencies. All experiments were performed in duplicates.

3.3.1. Materials

Optimal spent coffee extract, Cobalt nitrate hexahydrate ($Co(NO_3)_2 \cdot 6H_2O$), Sodium hydroxide (NaOH), Hydrochloric acid (HCl), Tartrazine ($C_{16}H_9N_4Na_3O_9S_2$), and Oxone ($KHSO_5$). Stock solutions were made using deionised water.

3.3.2. Equipment

The equipment involved in the synthesis process was as follows:

- Appropriate volumetric cylinders and pipettes were employed to accurately measure solutions, with the addition of a water bath to maintain the temperatures of the mixtures.

- A 500 mL glass beaker was used to house the synthesis reaction, coupled with a hotplate magnetic stirrer and thermometer for temperature control.

- An Ohaus Frontier 50 mL centrifuge was selected for primary solid-liquid separation.

- A Scientific series 2000 oven was brought into practice for further solid-liquid separation.

- A Labotec Precision furnace was used to elevate and maintain temperatures beyond 200°C.

3.3.3. Experimental Procedure for Co$_3$O$_4$ Nanoparticle Synthesis

1. A 0.06 M Co(NO$_3$)$_2$·6H$_2$O stock solution was made.

2. The required volume of the SCE and metallic salt (MS) solutions were accurately measured using volumetric cylinders.

3. The reaction vessel was then covered with aluminium foil and heated to the desired temperature (25°C, 50°C, 75°C) in a water bath.

4. Thereafter, the two solutions were poured into a beaker with their respective SCE to MS ratios (4:1, 1:1, 1:4).

5. The pH of the mixture was immediately adjusted to the required value (3, 7, 11) by adding either 30% HCl or 0.1 M NaOH solutions.

6. The resulting liquid was then transferred onto a hotplate, where the temperature was maintained for the duration of the reaction while continuous stirring commenced.

7. After completion, the solution was centrifuged at 6000 rpm for 15 minutes. This was repeated 3 times with the addition of DI water to ensure thorough rinsing of the nanoparticle precipitate.

8. The samples were then dehydrated in an oven at 60°C over a 12-hour period.

9. Finally, the remaining product was transferred into a suitable crucible, which was annealed in a furnace for 3 hours.

10. The nanomaterials were then stored in vials at room temperature.

Table 3.3: The experimental runs for Co$_3$O$_4$-NP synthesis.

Run	Temperature (°C)	Concentration (SCE:MS)	Time (h)	pH	Calcination Temperature (°C)
C1	25	1:1	2	7	400
C2	50	1:1	2	7	400
C3	75	1:1	2	7	400
C4	50	4:1	2	7	400
C5	50	1:1	2	7	400
C6	50	1:4	2	7	400
C7	50	1:1	2	7	400
C8	50	1:1	4	7	400
C9	50	1:1	8	7	400
C10	50	1:1	2	3	400
C11	50	1:1	2	7	400
C12	50	1:1	2	11	400
C13	50	1:1	2	7	200
C14	50	1:1	2	7	400
C15	50	1:1	2	7	800

3.3.4. Experimental Procedure for the Analysis of Co_3O_4 Nanoparticles

1. Stock solutions of 30 mg/L Co_3O_4-NPs, 0.1 mM Tartrazine, and 0.02 M Oxone were made.
2. The nanoparticles were resuspended using an ultrasonic bath set to 25°C for 15 minutes.
3. In a quartz cuvette, 1.5 mL of the NP solution was mixed with 0.5 mL of the dye solution and allowed to rest until equilibrium was reached.
4. The degradation reaction was then initiated through the addition of 1.5 mL Oxone solution.
5. The mixture was immediately placed in the UV-vis spectrophotometer, where the reaction commenced without light.
6. The absorbance of the solution was taken at 1-minute intervals.

3.4. Characterisation of the Co$_3$O$_4$ Nanoparticles

The characterisation of the nanoparticles was carried out to create a more detailed study of the optimal nanoparticles synthesised in section 3.3. In other words, the nanoparticles with the highest degradation efficiency were deemed optimal and, thus, studied further.

3.4.1. Ultraviolet-visible (UV-vis) Spectroscopy

The UV-vis spectrum of the cobalt oxide nanoparticles was carried using a GBC Cintra 2020 at a wavelength range of 200 to 600 nm.

3.4.2. Transmission Electron Microscopy (TEM)

The size and morphology of the nanoparticles were determined using the FEI F20 TEM situated at the University of Cape Town. The instrument was coupled with a Bruker Quanta 200 XFlash 6 EDX spectrometer capable of giving spectra that indicate which elements are present in the area illuminated by the electron beam. The image recording system is a Direct Electron DE-16 camera featuring continuous streaming at up to 92 frames per second. It features a DDD sensor with 16.8 million-6.5 um pixels optimised for 200 kV, delivering high-resolution images.

3.4.3. X-Ray Diffraction (XRD)

The crystallographic structure, chemical composition, and physical properties of the nanoparticles were studied at the University of Cape Town using the Bruker D8 Advance. The machine is capable of 0D, 1D, and 2D detection modes for identifying both crystalline and amorphous phases and determining specimen purity. In addition, the quantitative analysis of both crystalline and amorphous phases in multiphase mixtures. The software, coupled with the equipment, was PLAN.MEASURE. ANALYSE and DIFFRAC.SUITE.

3.4.4. Fourier-Transform Infrared Spectroscopy (FTIR)

The PerkinElmer Spectrum Two was used to obtain the infrared spectrum of the optimal nanoparticles. The resolution of the scan was 1 cm^{-1} with a range from 4000 to 400 cm^{-1}, using 60 scans. Dry atmosphere samples were analysed at room temperature.

3.5. Catalytic Activity of Co_3O_4 Nanoparticles

After characterisation, the optimal nanoparticles were synthesised in bulk using the experimental setup displayed in Figure 3.1 and employed in the catalytic activation of peroxymonosulfate (PMS) for the degradation of Tartrazine dye. Reaction parameters were varied to determine the effects on reaction rates and efficiencies (calculated using equation 7).

$$Dye\ removal\ \% = \left(\frac{C_0 - C_t}{C_0}\right) \times 100 \tag{7}$$

Where C_0 is the initial concentration of the dye solution and C_t is the concentration after time t. All experiments were performed in triplicates and with the absence of light.
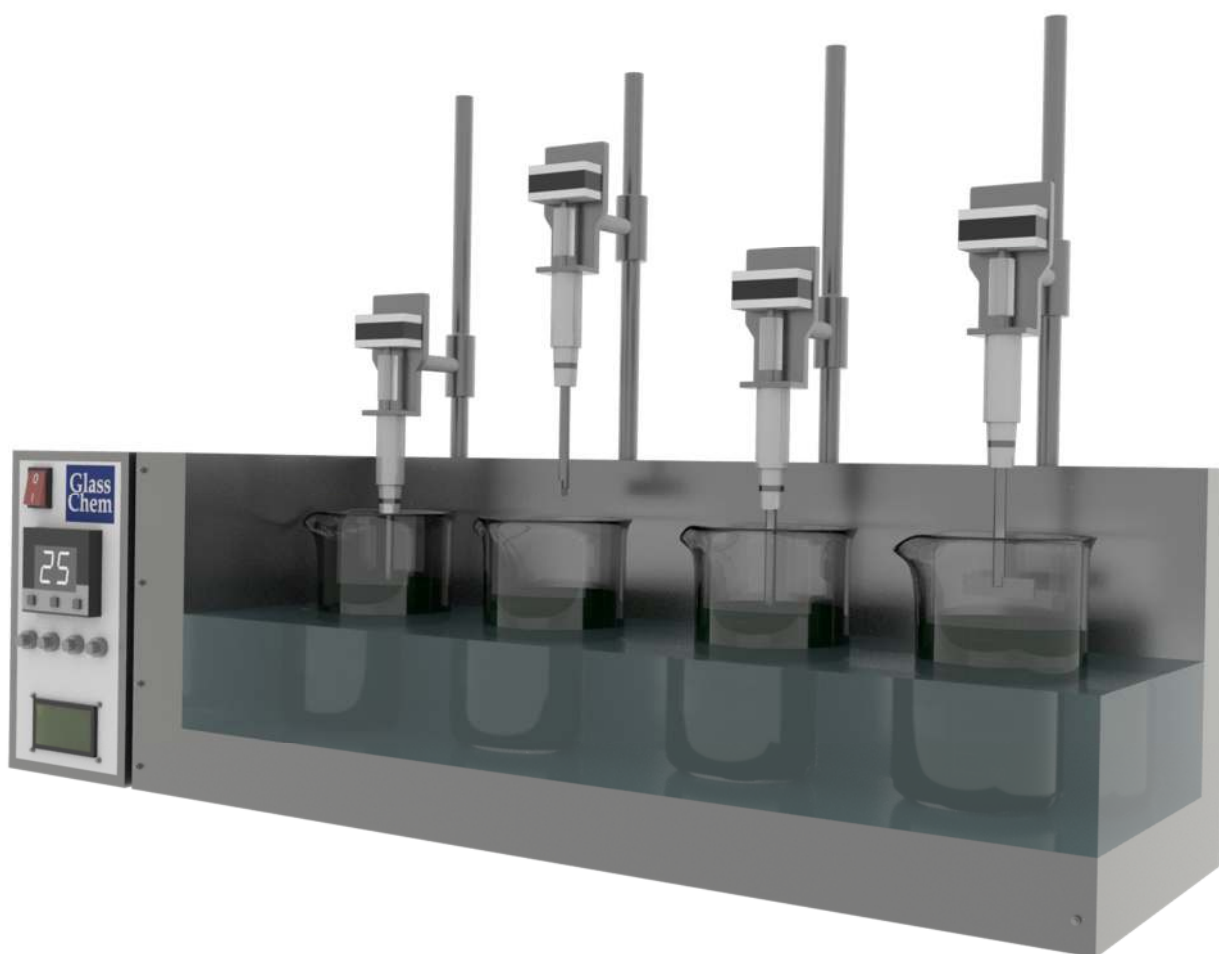
Figure 3.1: The experimental setup for the bulk synthesis of the optimal Co_3O_4 NPs

3.5.1. Materials

Optimal Co_3O_4-NPs, Tartrazine, Oxone, and a 0.1 M phosphate buffer solution.

3.5.2. Equipment

The following apparatus was utilised in the degradation of Tartrazine dye:

- A Kern balance to accurately measure the required mass of the substances for stock solutions.

- Several 100 mL beakers were used to house the respective reactions

- MRC Ultrasonic bath was used to resuspend the nanoparticles in a solution.

- A pH meter was used to determine the pH of the reaction solution.

- The Cintra UV-vis was used to analyse the solution at certain time intervals.

3.5.3. Experimental Procedure for Catalytic Activity

1. A 0.1 mM stock solution of Tartrazine was prepared.
2. 100 mL of the Tartrazine solution was measured using a volumetric cylinder and transferred to a beaker with an equivalent volume.
3. A known mass of the nanoparticles was measured using a balance and introduced into the Tartrazine solution.
4. The mixture was inserted into the sonicator and set to 25°C for 15 minutes for nanoparticle resuspension.
5. Thereafter, the solution was placed onto a hotplate magnetic stirrer and heated to the desired temperature while under constant agitation.
6. Once the required temperature was obtained, Oxone was mixed into the existing solution, initiating the reaction.
7. The pH of the reaction was adjusted using a 0.1 M Phosphate buffer solution where necessary.
8. 1.5 mL of the reaction mixture was extracted at 2-minute intervals until equilibrium was reached.
9. The analysis was completed using the UV-vis spectrophotometer.

Table 3.4: The experimental runs for the catalytic activity of the Co$_3$O$_4$-NPs.

Run	NP Concentration (mg/L)	Oxone Concentration (mg/L)	Temperature (°C)	pH
D1	2	100	25	2-3
D2	5	100	25	2-3
D3	10	100	25	2-3
D4	5	50	25	2-3
D5	5	100	25	2-3
D6	5	200	25	2-3
D7	5	100	25	2-3
D8	5	100	40	2-3
D9	5	100	60	2-3
D10	5	100	25	2-3
D11	5	100	25	7

3.6. Kinetic Study

All adsorption phenomena may follow one combination from different pathways, such as mass transfer, diffusion, and chemical reactions. Analysing the experimental data at various time intervals makes it possible to calculate the kinetic parameters and retrieve valuable information for designing and modelling adsorption processes. Therefore, the kinetic modelling of Tartrazine removal through Co$_3$O$_4$ NP-activated PMS was determined using the best fit of either:

The first-order kinetic model,

$$\ln[C_t] = -kt + \ln[C_0] \tag{8}$$

or the second-order kinetic model:

$$\frac{1}{[C_t]} = kt + \frac{1}{[C_0]} \tag{9}$$

In equations 8 and 9, C$_0$ is the initial concentration of the dye, C$_t$ is the concentration of the dye at time t (min), and k is the reaction-order-rate constant for the degradation of Tartrazine.

3.7. Reusability Study

These tests were carried out to evaluate the efficiency of the optimal nanoparticles after withstanding several batch-degradation processes. Therefore, an estimate could be made whether the catalyst could be viable for industrial use.

Due to the mass of the nanoparticles employed in the conventional degradation reaction, retrieving the catalyst was strenuous. Therefore, the test was altered by increasing the reaction's volume, along with the mass of the reactants, to enable a swift nanomaterial recovery. More specifically, the volume of 0.1 mM Tartrazine was 300 mL, and the concentration of Co_3O_4 nanoparticles was 70 mg/L, with 15 mg of Oxone added to commence the reaction. The recovery was accomplished by centrifuging the reaction mixture after equilibrium was reached.

3.8. Quenching Tests

The quenching study aimed to determine the active radicals responsible for the degradation of the Tartrazine dye, with the chemical species in question being hydroxyl ($^\bullet OH$) and sulfate ($SO_4^{\bullet -}$) radicals. Therefore, 2 mL of methanol or isopropyl alcohol was added to their respective mixtures at the start of the reaction. Reference process parameters (5 mg/L NPs, 100 mg/L Oxone, 25°C, and pH 2-3) were utilised for each run. Experiments were performed in duplicates.

3.9. Industrial Effluent Simulation

This test was used to determine the efficiency of the optimal nanoparticles when faced with an industrial dye effluent. Therefore, a mixture with equal volumes of 0.1 mM Tartrazine, 0.1 mM Methyl Orange, and 0.1 mM Remazol Brilliant Red was constructed to replicate an industrial effluent. All stock solutions were made with deionised water, and reference parameters were utilised for the reaction.

3.10. Chemical Oxygen Demand (COD) Study

The COD tests employed the HANNA Multiparameter Photometer to detect the concentrations within the reference degradation reaction of Tartrazine dye. The samples (2 mL) were withdrawn from the mixture at the start and finish of the reaction, where they were inserted into their respective COD test vials. The vials were then incubated at 180°C for 2 hours. Thereafter, the samples were analysed using the photometer, and the data was recorded.

3.11. Cobalt Leaching Study

The University of Cape Town conducted the cobalt leaching study in the Hair and Skin Research Lab. The equipment employed to detect elemental cobalt within the catalytic degradation reaction was the Agilent Technologies 7800 ICP-MS. Only ICPMS-grade plastic

wares were used for the assay as quality assurance measures. IV-STOCK-27 (Inorganic Ventures) was used as a stock solution for elemental analysis. ICPMS was tuned and calibrated before the run with blanks and quality control samples analysed after each sample. Quality control variations were less than 2%. All samples were analysed in duplicate, and average values were reported alongside their standard deviation values.

3.12. Photocatalytic Study

The light study was accomplished using the reference degradation mixtures, and the experiments were performed without ambient light. Initially, the azo dye and nanoparticle mixture was allowed to reach equilibrium, with the light source placed 5.0 cm away from the reaction vessel. After the addition of the Oxone, samples were analysed using the UV-vis spectrophotometer at 2-minute intervals. All experiments were performed in triplicates.

The following equipment was introduced for the light study:

- A 100 mL cubic quartz cuvette was utilised to contain the degradation reaction.

- The Autolab optical bench was used to provide artificial visible light to the reaction.

- A Sciencetech 300W arc lamp was employed to simulate solar light exposure.

3.12.1. Photocatalytic Activity under Natural Solar Illumination

The photocatalytic properties of the cobalt oxide nanoparticles were also evaluated using sunlight using the experimental setup in Figure 3.2. The nanoparticle and PMS mixture was placed on magnetic stirrers wrapped with aluminium foil to enhance UV irradiation. The degradation reaction was analysed at 5-minute intervals.

Figure 3.2: The experimental setup for the photocatalytic evaluation of solar illumination

3.13. Conclusion

A detailed description of spent coffee extraction and nanoparticle synthesis techniques have been included in this chapter, along with the characterisation methods utilised to determine the properties of the cobalt oxide nanostructures. In addition, the catalytic and photocatalytic procedures for the degradation of azo dyes were disclosed. The methods for an in-depth study of the Co_3O_4-NPs were also introduced.

Chapter 4

Results & Discussion

4.1. Introduction

The methodologies described in the previous chapter were employed to synthesise, optimise, and characterise the spent-coffee-mediated Co_3O_4 nanoparticles. Furthermore, experimentation was conducted to evaluate the feasibility of the nanostructures in catalytic/photocatalytic oxidation processes for the removal of azo dyes from water. The results presented within this chapter are divided into the following sections:

1. Spent coffee analysis
2. Synthesis and analysis of Co_3O_4-NPs from spent coffee
3. Characterisation of Co_3O_4 nanoparticles
4. The catalytic/photocatalytic activity of Co_3O_4 nanoparticles

4.2. Spent Coffee Analysis

The effect of various parameters on the oxidising strength of spent coffee (SC) was investigated. The main objective of this section was to preserve most of the fresh coffee's reductive capabilities for further application. The analysis was conducted using the techniques presented in section 3.2.5.

4.2.1. Effect of Drying Temperature on Spent Coffee

The analysis of samples through FTIR spectroscopy allows for accurate and rapid detection of the subtle differences in composition and concentration of the compounds in coffee. The FTIR analysis of coffee, situated in Figure 4.1, displays similar characteristics to other reported literature, where the peaks of interest associated with various chemical compounds such as caffeine, chlorogenic acids, proteins, carbohydrates, and water have been identified (Craig et al., 2011; Linlin et al., 2017; Q. Zhang et al., 2015; Chou et al., 2012).

According to Linlin and co-authors (2017), the emergence of the broad absorption band located at 3200-3600 cm^{-1} may be linked to the stretching vibration of hydroxyl groups (phenols, alcohols, carboxylic acids, or water). The sharp peaks expressed at 2840-2920 cm^{-1} were assigned to C-H asymmetric and symmetric stretch of the methylene (CH$_2$) and methyl (CH$_3$) groups, where lipids and caffeine may be substantial contributors to the intensity of the peaks (Craig et al., 2015). Furthermore, while unique for each organic molecule, the fingerprint region of the spectra (1600-1000 cm^{-1}) is a complex area of C-H, C-O, C-N, and P-O vibrations, which makes it challenging to analyse (Saragih et al., 2022). However, specific compounds in coffee have been narrowed down, and assumptions can be made due to the particular bonds within the molecules.

Flores-Valdez et al., (2020) reported that the ester group OC=O of quinic acids gave rise to steep peaks found at 1746 cm^{-1}. Also, caffeine and chlorogenic acids have been detected in the range of 1600-1650 cm^{-1} due to the stretching vibration of C=O groups (Reis et al., 2017). The bending vibrations of the C-H bond in aliphatic groups, such as phenols, resulted in fingerprint bands at 1377-1460 cm^{-1} (Lyman et al., 2003). Furthermore, chlorogenic acids were also identified to lie between 1155 and 1300 cm^{-1} (Guzmán et al., 2018). More specifically, 1060, 1160, and 1260 cm^{-1} are known to be characteristic peaks of CGA and its derivatives, which are related to the vibrations of the C-O bonds found in the compound (Abreu et al., 2020). Lastly, peaks from 650 to 900 cm^{-1} have been mentioned to be associated with proteins and amino acids (Singh et al., 1998).
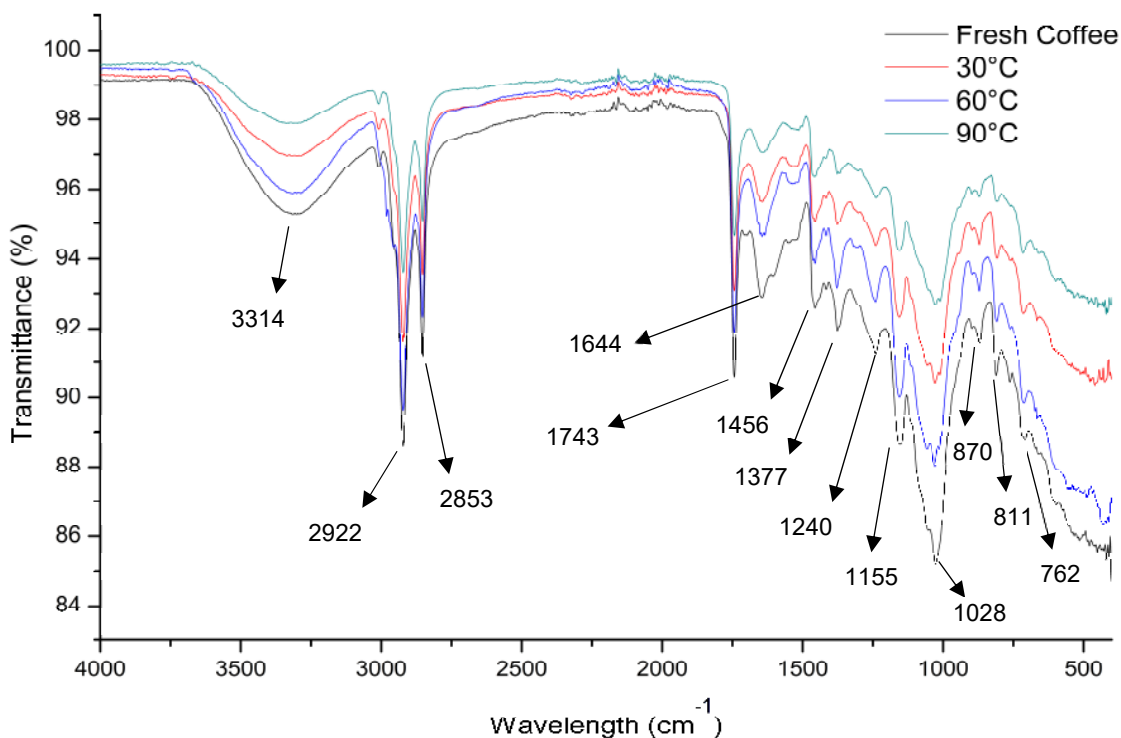
Figure 4.1: The FTIR spectra of spent coffee at different drying temperatures

The FTIR (Figure 4.1) presents the various peaks and transmittance obtained for fresh coffee and spent coffee dried at 30, 60, and 90°C. The deterioration of bioactive compounds found in coffee is distinctly evident in all the spent coffee samples. However, there are definitive discrepancies amongst the various drying temperatures in biochemicals such as caffeine (1644, 2853, and 2922 cm^{-1}), chlorogenic acids (1028, 1155, 1240, 1377, and 1743 cm^{-1}) and other phenols (811, 870 cm^{-1}). By virtue of its thermal instability, chlorogenic acid, along with minor phenolic compounds, underwent severe dilapidation through heat application. On the other hand, the caffeine content of the spent coffee has proven to be slightly more resistant, where the characteristic bands of the substance remained prominent.

From the data gathered, the SC dried at 90°C experienced the greatest degradation of its constituents. Similar consequences were observed by Kieu Tran and co-authors (2020), where it was mentioned that increased thermal activity in the presence of air promotes the oxidation of some phenolic compounds due to oxygen exposure combined with high temperatures. This can be witnessed while inspecting the more moderate drying conditions herein; however, 60°C revealed peak strengths closely related to fresh coffee. Therefore, minimal degradation was observed, with most essential substances still intact.

However, the moisture content (3314 cm^{-1}) of the spent coffee gave interesting results, as higher temperatures should increase the evaporation rate of water. In spite of this, 60°C gave a stronger band compared to 30°C, which could be attributed to the slight differences in the thickness of the spent coffee layer on the drying tray (Martinez, 2019).

4.2.2. Total Phenolic Content

The total phenolic content of fresh coffee extract (FCE) and spent coffee extract (SCE) was determined to grasp the effect of roasting on the samples' reducing capabilities. In addition, tests performed on coffee were a good indication of the concentrations of CGA, CGA derivatives, and CGA degradation by-products, as they are substantial contributors to the phenolic content of the extract (Nosal et al., 2022). The analytics in Figure 4.2 display the total phenolic content of FCE (154.25 mg GAE/g) and SCE (57.91 mg GAE/g), which exhibits a 62.5% decline. However, this was expected due to the multiple heat treatments and thermal instability of the compounds. The SCE obtained in this study is commendable due to the abundance of phenolic content and lack of degradation compared to other reports using similar extraction methods (Boyadzhieva et al., 2018; Díaz-Hernández et al., 2022).
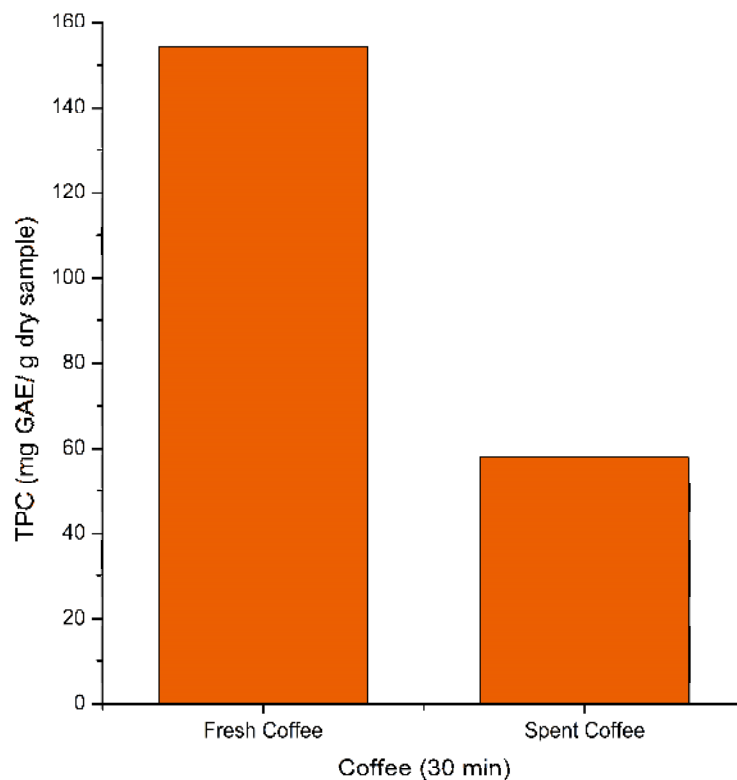
Figure 4.2: The total phenolic content of fresh and spent coffee. (30-minute extraction times were used for all experiments unless stated otherwise)

The impact of extraction parameters on TPC was also investigated, including the spent coffee concentration, extraction temperature, and reaction time. It can be noticed from Figure 4.3-a that the concentration of SC had a positive linear effect on the TPC, where higher concentrations experienced greater TPC outcomes (18.56 mg GAE/g of sample) compared to the latter (8.70 mg GAE/g of sample). These findings could be due to the abundance of spent coffee as a source of phytochemicals, resulting in more phenolic compounds in the extraction mixture (Do et al., 2014; Hou et al., 2016).

Furthermore, the temperature was directly correlated to the phenolic concentration of the solution (Figure 4.3-b), with optimal TPC obtained at 100°C (46.87 mg GAE/g of sample), essentially roasting the coffee grounds twice as conventional roasting temperatures are approximately 80°C. The enhancing ability of the parameter was in agreement with previous research, where it was reported that the yield of phenolic compounds increased with an increase in temperature (Thoo et al., 2010; Tan et al., 2013). This may be attributed to the elevated diffusivity of the solvent into the cells of the biomaterial while simultaneously increasing the solubility of phenolic compounds (Jiménez-Moreno et al., 2019). In addition, raised extraction temperatures increases mass transfer of phytochemicals and reduces surface tension and solvent viscosity, thus promoting the extraction of phenolic compounds (Ibañez et al., 2003; Liyana-Pathirana & Shahidi, 2005). It is also noteworthy to mention that

the denaturation of polyphenols may commence if certain temperatures are exceeded (Mokrani & Madani, 2016).

Regarding the duration of the procedure, 30-minute extraction periods were favoured, with phenolic concentrations reaching 25.2 mg GAE/g of sample (Figure 4.3-c). Rajha et al. (2014) stated that higher temperatures and shorter reaction times could avoid the significant degradation of phenolic compounds (Rajha et al., 2014). On the other hand, with prolonged periods, the effects are inverted as severe oxidation or degradation becomes imminent (Chirinos et al., 2007). This can be seen in the following section (Figure 4.4-c); hence, extraction times surpassing 30-minute periods were not studied.
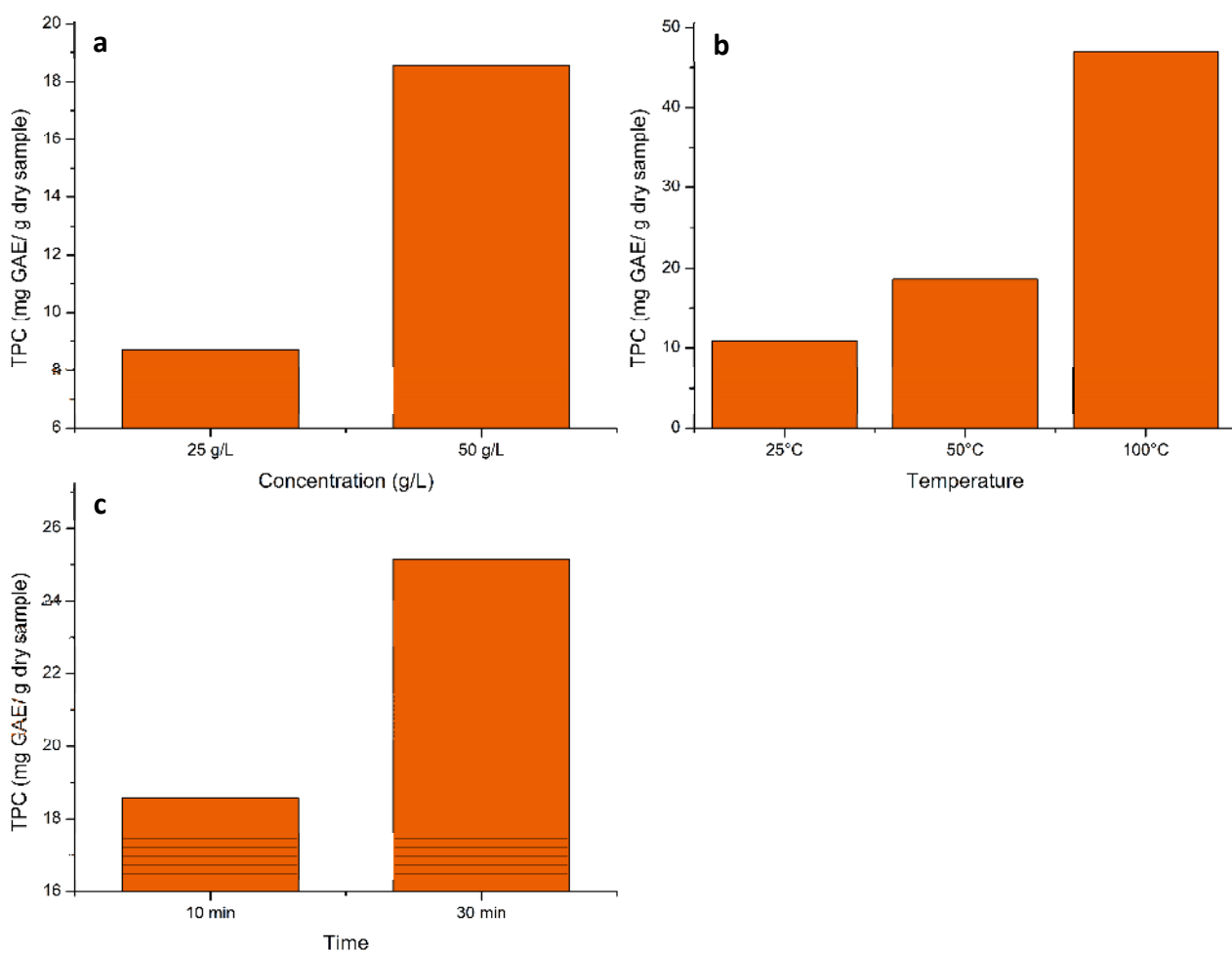
Figure 4.3: Total Phenolic Content – The effect of a) spent coffee concentration, b) extraction temperature, and c) reaction time

4.2.3. Antioxidant Capacity

It is known that phenolic compounds exhibit strong reducing capabilities, and the total phenolic content is the sum of their reaction potential, including radical scavenging and metal-chelating properties (Saeed et al., 2012). Despite playing a major role in reduction, polyphenols are not the sole contributors. Therefore, antioxidant assays have assisted this matter by depicting the combined effect of all radical scavenging components (Niroula et al., 2019). For coffee, the presence of antioxidant compounds such as chlorogenic acids, caffeine, Maillard reaction products, and other minor phenolic and non-phenolic compounds have been known to contribute to this assay (Gigliobianco et al., 2020). Nonetheless, previous researchers have still reported a distinct correlation between the antioxidant capacity (AOC) and total phenolic content of extracts (Kumar et al., 2014; Paixão et al., 2007).

The range of antioxidant activity achieved in this study was analogous to the results of the spent coffee analysis carried out by Bravo et al. (2012), ranging from 46.0 – 57.8%. From the data gathered in Figure 4.4-a, variations in the AOC can be observed when concentrations of the coffee material are altered. With a 25.0 g/L solution, the antioxidant activity was examined to be 49.59%, while doubling the concentration only led to a 4.68% increase in AOC.

Furthermore, the free radical scavenging activity of the spent coffee saw a drastic increase with higher temperatures, from 34.88 to 54.57% for 25 and 100°C, respectively (Figure 4.4-b). However, temperatures exceeding 50°C started to experience a slope in oxidative strength, considering the substantial temperature hike. Mokrani and Madani, (2016) stated that applying > 60°C of heat during extraction significantly reduces the total flavonoid content of the solution, which could explain the deterioration of the AOC as flavonoids are conspicuous donators to the volume of the assay. In spite of this, increased temperatures were still favoured, and these results have been backed by several studies that reported the enhancement of AOC through the introduction of heat (Farida et al., 2014; Vatai et al., 2009; Dorta et al., 2012).

Lastly, the phytochemical extraction time was the only parameter that encountered adverse effects as the variable increased (Figure 4.4-c). However, the 20-minute difference only accounts for a 2.64% change in AOC. This could be explained by Fick's second law of diffusion, which predicts the inevitability of equilibrium between solute concentrations in the solid matrix and bulk solution after a particular time.

In conclusion, spent coffee is far from being exhausted, with its extracts containing significant amounts of antioxidants ready for utilisation. For the remainder of the study, spent coffee extracts were optimised to obtain the highest TPC and AOC possible; therefore, concentrations and temperatures of 50 g/L and 100°C were employed with 30-minute periods.
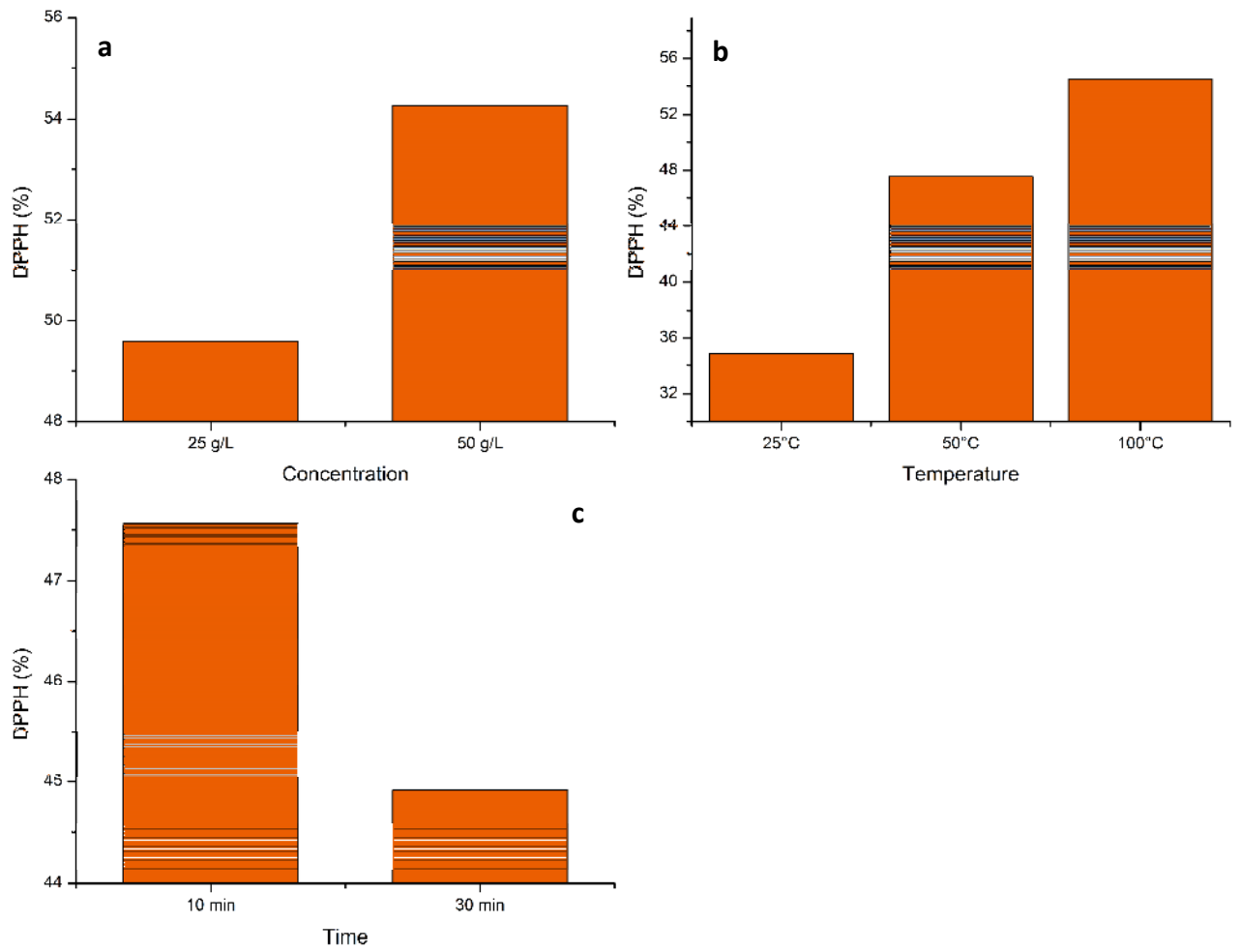
Figure 4.4: Antioxidant Capacity – The effect of a) spent coffee concentration, b) extraction temperature, and c) reaction time

4.3. Synthesis of Co₃O₄ Nanoparticles

The formation of Co_3O_4-NPs occurs in two stages: (1) the generation of nuclei and (2) the growth of the nanoparticle. Therefore, optimising synthesis process parameters for faster fabrication and slower growth is crucial. The nanostructures were synthesised using the method described in section 3.3, where the ideal spent coffee extract was utilised. All nanoparticle samples were analysed through their Tartrazine degradation efficiency. The optimal nanoparticles obtained from the experimentation in this section will be further studied.

4.3.1. Effect of Precursor Concentration

The concentration of reaction components, such as plant substances and metallic precursors, plays a vital role in the production of green nanoparticles. Despite the exact effect of this property being unpredictable, one aspect remains constant: the reaction necessitates sufficient antioxidants for the reduction of metallic ions (Kaningini et al., 2022). According to Bala and co-authors (2014), an insufficient amount of bioactive compounds lowers the yield of NPs generated, while sufficient phytochemicals should effectively reduce all available ions in the solution, thereby producing higher nanoparticle yields (Bala et al., 2014). However, surpassing this optimal concentration will decline the overall conversion rate, subsequently lowering the yield. This is caused by the excess number of biomolecules present, where primary reduction (nucleation) becomes overpowered by secondary reduction (growth) (Nagar & Devra, 2018). Therefore, as depicted in Figure 4.5, the 20% and 80% spent coffee mixtures experienced lower yields when compared to the 42 mg of Co_3O_4-NPs obtained from the 1:1 extract to metallic precursor (E:M) ratio.
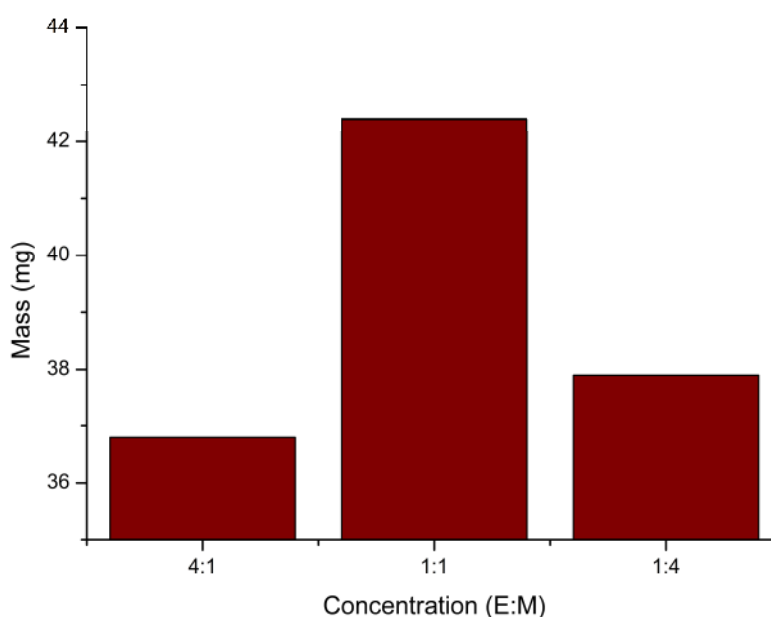
Figure 4.5: The Co_3O_4-NP yield obtained from varying precursor concentrations

Regarding the size and morphology of the nanoparticles, previous researchers have revealed distinct outcomes where an increase in reactant concentration led to smaller particle diameters. For instance, Ehrampoush et al. (2015) synthesised iron nanoarchitectures from tangerine peel extract. It was found that varying the concentration of the fruit extract from 2 to 6% resulted in a substantial reduction of NP size from 200 to 50 nm. The effect was contradicted by increasing the concentration beyond 6%, where the nanoparticles witnessed a gradual size increase due to aggregation (Ehrampoush et al., 2015). Furthermore, Nagar & Devra (2018) mentioned that an increase in the precursor salt concentration results in larger quantities of metallic nuclei and, ultimately, smaller particle sizes. However, an excess of nuclei will be generated at high reactant concentrations, subsequently aggregating the nuclei and initiating the growth of the nanoparticles (Mohammadi & Ghasemi, 2018). Other authors reported similar results in the field, where an increase in either reactant led to a decrease in particle size. However, with excessive concentrations, the diameters tend to increase (L. B. Anigol et al., 2017; Iravani & Zolfaghari, 2013; Ebrahiminezhad et al., 2018).
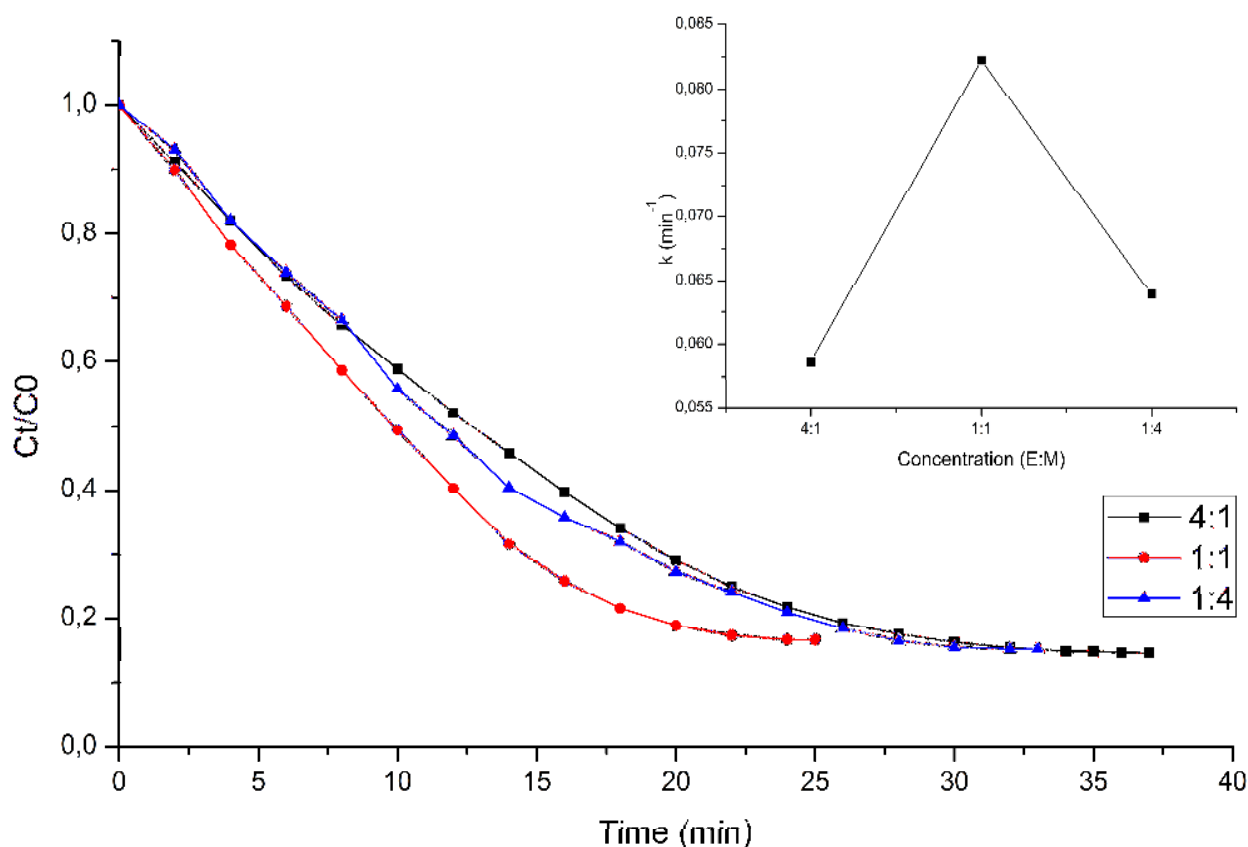
Figure 4.6: The effect of precursor concentration on Co_3O_4-NPs, analysed against the degradation of Tartrazine dye

This study was no different from the research mentioned above, where an extract-to-precursor ratio of 1:1 was favoured due to superior dye degradation (Figure 4.6), indicating the presence of smaller nanoparticles with higher reactivities. The batch synthesis of Co_3O_4-NPs using higher concentrations of reactants resulted in weaker degradation efficiencies, which suggests that the structures have greater diameters or have undergone aggregation.

4.3.2. Effect of Reaction Temperature

The influence of temperature on the cobalt oxide nanoparticles was studied using three different reaction temperatures: 25, 50, and 75°C. Previous researchers have demonstrated positive outcomes by altering this process parameter, where higher temperatures have been deemed essential for achieving greater ionic conversion with plant-based reduction, thereby increasing the overall nanoparticle yield (Zheng et al., 2013). These results were in coordination with the yield obtained in this study, where the product mass increased from 5.4 mg at 25°C to 83.0 mg at 75°C (Figure 4.7).
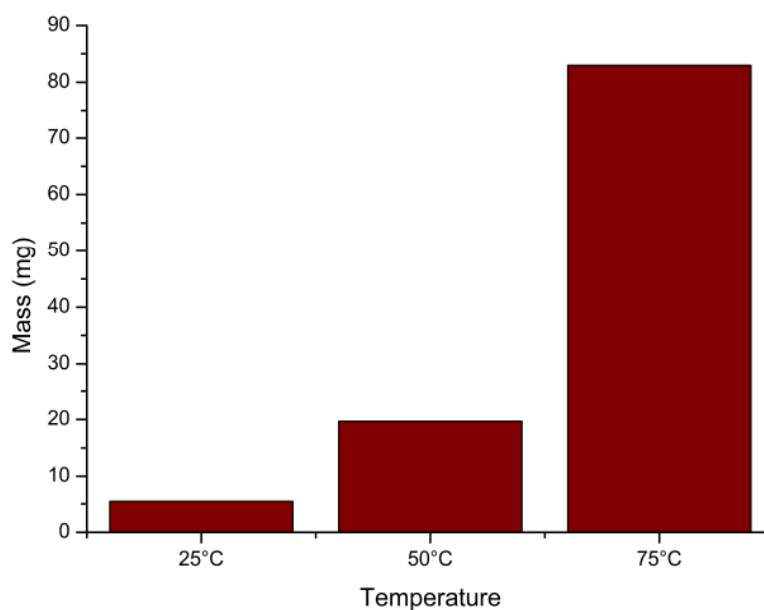
Figure 4.7: The Co_3O_4-NP yield obtained from varying the reaction temperature

Moreover, prior temperature evaluation on the size of nanoparticles has brought about some mixed conclusions. Iravani & Zolfaghari (2013) analysed their *Pinus eldarica*-mediated silver nanoparticles after varying reaction temperatures. It was noted that an increase in temperature upped the production of colloidal silver along with the rate of reaction, while the particles experienced a sharp decrease in diameter. This could be attributable to the rapid reduction rate and the subsequent homogeneous nucleation of metallic ions, allowing for the formation of smaller nanoparticles (Zhan et al., 2011; Khalil et al., 2014; Vanaja et al., 2013). The effect on the nucleation rate caused by temperature outweighs that of the growth rate due to most of

the ions being consumed by the initial nucleation process, thereby stalling nucleic growth (Bharadwaj et al., 2016). In other words, high temperatures promote nucleation, while low temperatures are conducive to growth. However, extreme temperatures enhance the surface activity of nuclei and, in turn, encourages agglomeration (Zheng et al., 2013).

On the other hand, some researchers have encountered opposing results to the effects above. For instance, silver nanoparticles synthesised using *Pulicaria glutinosa* experienced negative thermal consequences, where diameters effectively increased with an increase in temperature (Sun et al., 2014). Like the nucleation rate, the temperature can potentially increase secondary reduction, provided sufficient precursor exists. In theory, the nanoparticles' growth rate is only limited to the amount of precursor available, as the ions present could grow abundantly on the crystal nuclei, thereby increasing particle diameters (Liu et al., 2020).
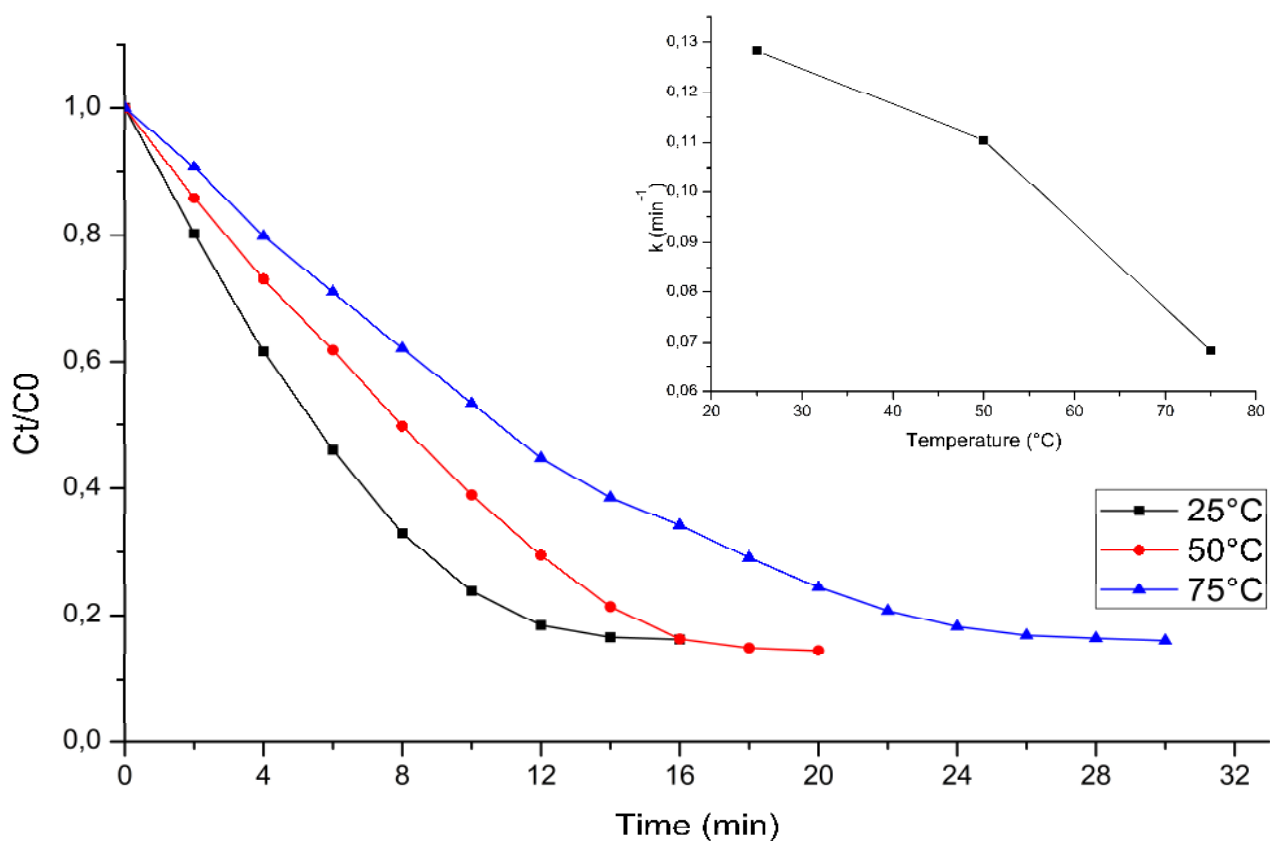
Figure 4.8: The effect of reaction temperature on Co$_3$O$_4$-NPs, analysed against the degradation of Tartrazine dye

Herein, it may be assumed that each synthesis reaction contained sufficient precursor as degradation efficiencies decreased with an increase in temperature (Figure 4.8), stipulating that particle growth and aggregation were evident with elevated reaction temperatures (50 and 75°C). This may have resulted from the high Co (III) conversion rate and the abundance of ions that readily form nuclei and, subsequently, larger colloids (Mamdooh & Naeem, 2022). Therefore, lower temperatures were favoured due to minimal ionic conversion, allowing primary reduction to be the main focus of nanoparticle synthesis where smaller diameters are retained.

4.3.3. Effect of Reaction Time

The reaction time for the green synthesis of nanoparticles was investigated by extending fabrication periods to 2, 4, and 8 hours. Previous research on this subject revealed that contact time undeniably affected the elected nanoparticles' concentration and size. Within this study, the yield of the nanoparticles increased alongside the reaction time (Figure 4.9). These findings may have been the outcome of the drawn-out nucleation and growth periods, therefore allowing the nanoparticles to increase in concentration (Behravan et al., 2019). This was in agreement with the data obtained from previous reports (Ahmad et al., 2016; Cao et al., 2022).
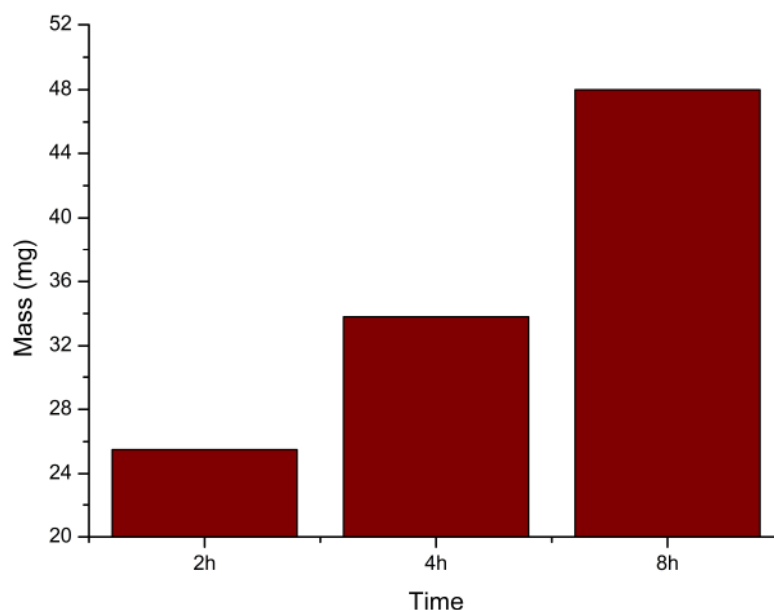
Figure 4.9: The Co$_3$O$_4$-NP yield obtained from varying the reaction time

Regarding the size of the nanostructures, it has been mentioned that higher reaction times enhance nucleation and particle growth processes, inducing the formation of larger diameters (Karade et al., 2018). On the other hand, Elemike and co-authors (2017) observed a decrease in particle sizes as time progressed; however, the diameter of the structures increased after exceeding 45 minutes, indicating the occurrence of agglomeration (ELEMIKE et al., 2017). Herein, the slower degradation efficiency of the 8-hour nanoparticle sample may illustrate aggregation due to the overwhelming concentration of colloids (Figure 4.10) (Jain & Mehata, 2017). The lower contact times of 2 and 4 hours display like-degradation capabilities, which could stem from the similar size and stability of Co_3O_4 nanoparticles (Ibrahim, 2015). Nevertheless, using a higher reaction time is unjustifiable due to increased operating costs.
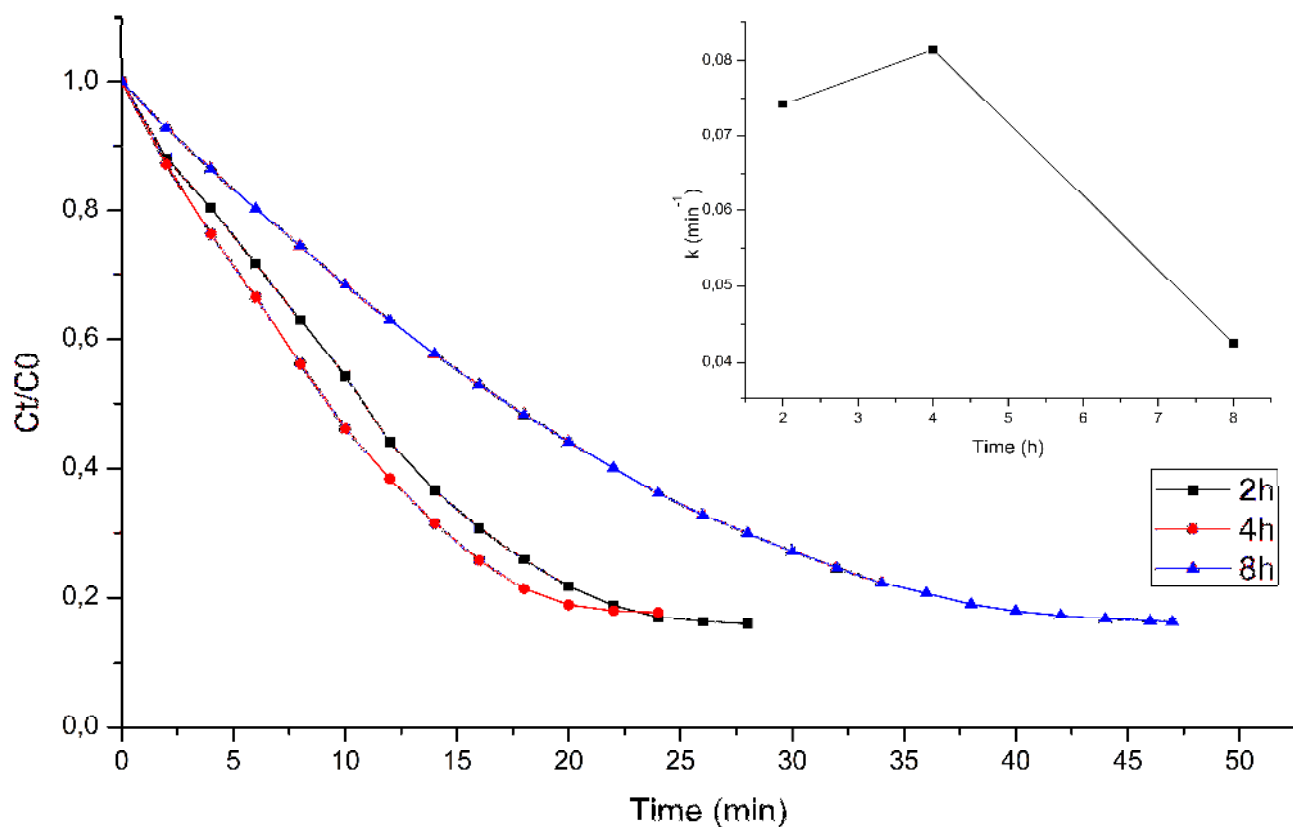
Figure 4.10: The effect of reaction time on Co₃O₄-NPs, analysed against the degradation of Tartrazine dye

4.3.4. Effect of pH

The solution pH is a critical factor in controlling the concentration and size of green nanoparticles. By virtue of its effect, numerous studies have investigated this parameter for enlightenment on the subject. Herein, the synthesis pH of 2-3, 7, and 11 were utilised in the fabrication of cobalt oxide nanoparticles. Initially, as seen in Figure 4.11, the unadjusted solution (pH 2-3) resulted in negligible product mass, with the yield accumulating to 0.5 mg; therefore, the samples could not be further analysed.

On the other hand, a neutral pH obtained 51.7 mg of annealed nanostructures, while the alkaline solution experienced extreme results, with the yield amounting to 576.1 mg. This data was in agreement with multiple other reports (Ramesh et al., 2015; Aziz & Jassim, 2018; Al-Radadi, 2019). According to Ghaffari-Moghaddam & Hadi-Dabanlou (2014), the presence of pH-adjusting additives was correlated to the stability of the nanoparticles as hydroxide ions can alter the surface charge of the material. At alkaline pH, the stability of the nanoarchitectures was enhanced due to the complete charging of the clusters, thus maximising the repulsive electrostatic/electrosteric interactions and increasing colloid formation (Ghaffari-Moghaddam & Hadi-Dabanlou, 2014; Anigol et al., 2017).
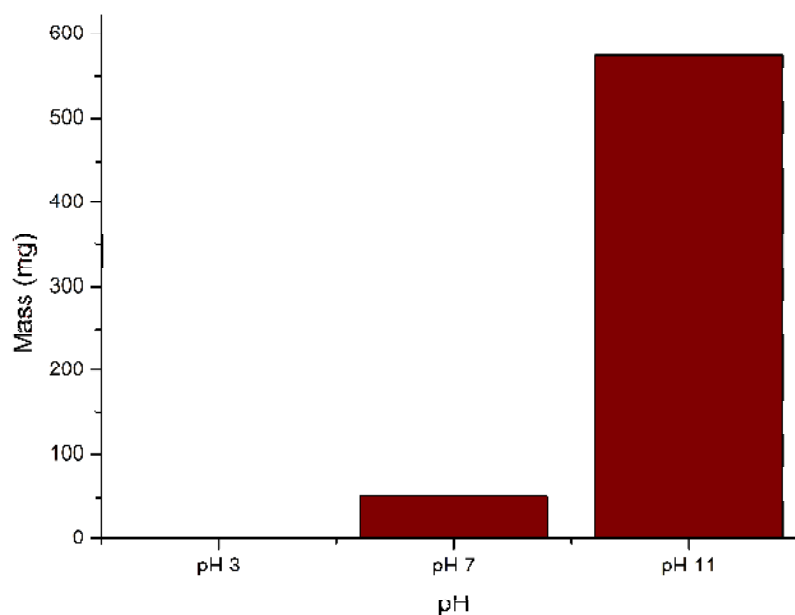
Figure 4.11: The Co$_3$O$_4$-NP yield obtained from varying the pH of the solution

Looking at Figure 4.12, it can be assumed that the drastic decrease in degradation efficiency from pH 7 to 11 was associated with the enlargement of particle sizes. Similar results were obtained by Traiwatcharanon and co-authors (2016), where reaction solutions of pH 6 and 10 were prepared, which resulted in the expansion of average diameters. In addition, a neutral pH was also favoured during the production of colloidal copper nanoparticles (Nagar & Devra, 2018), where an increase in concentration and reduction rate was observed with basic mediums. This indicated that acidic pH suppresses the synthesis of the nanomaterial due to the inactivity of the biomolecules (Kredy, 2018). At neutral pH, the availability of functional groups for ionic binding led to the fabrication of smaller nanoparticles. Furthermore, elevated pH solutions were found to be efficient in generating NPs; however, agglomeration negatively impacts the structures by forming larger particles as growth is favoured over nucleation (Singh & Srivastava, 2015; Iravani & Zolfaghari, 2013).
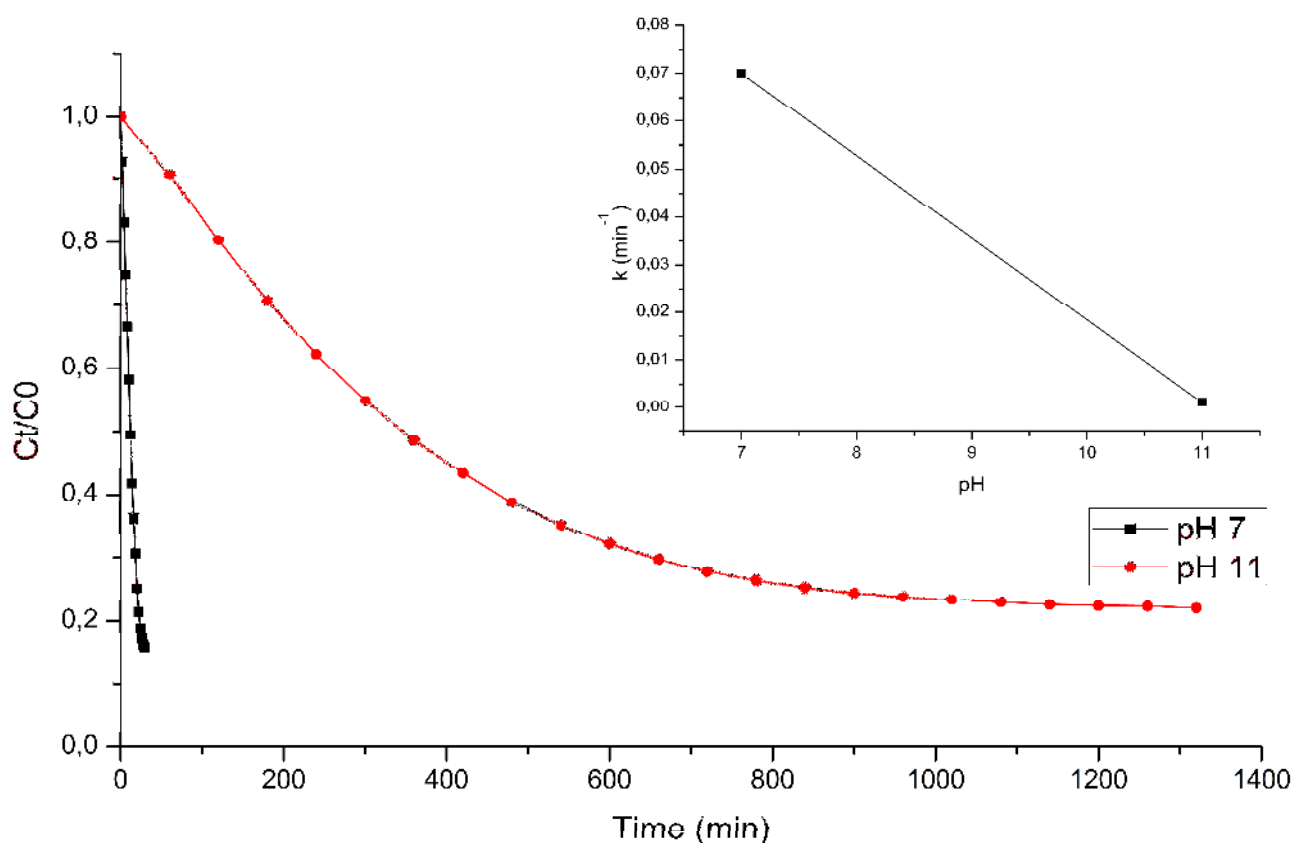
Figure 4.12: The effect of pH on Co$_3$O$_4$-NPs, analysed against the degradation of Tartrazine dye

4.3.5. Effect of Calcination Temperature

Calcination temperatures are considered capable of enhancing the electrical and optical properties of green nanoparticles through extreme heat treatment. Within this research, calcination temperatures of 200, 400, and 800°C were utilised. The yield retrieved from the fabrication process is depicted in Figure 4.13, where the lowest annealing temperature achieved the greatest accumulation of Co_3O_4-NPs (80.9 mg). On the other hand, temperatures exceeding 200°C witnessed a drastic decrease in mass, with 400 and 800°C amounting to 36.2 and 39.4 mg, respectively. These developments could be the consequence of the remaining phytochemicals that showed considerable resilience towards heat treatment at 200°C. In spite of this, higher temperatures were able to surpass the biological threshold and decompose impurities, thereby obtaining pure Co_3O_4 nanoparticles (Syahirah Kamarudin et al., 2018).
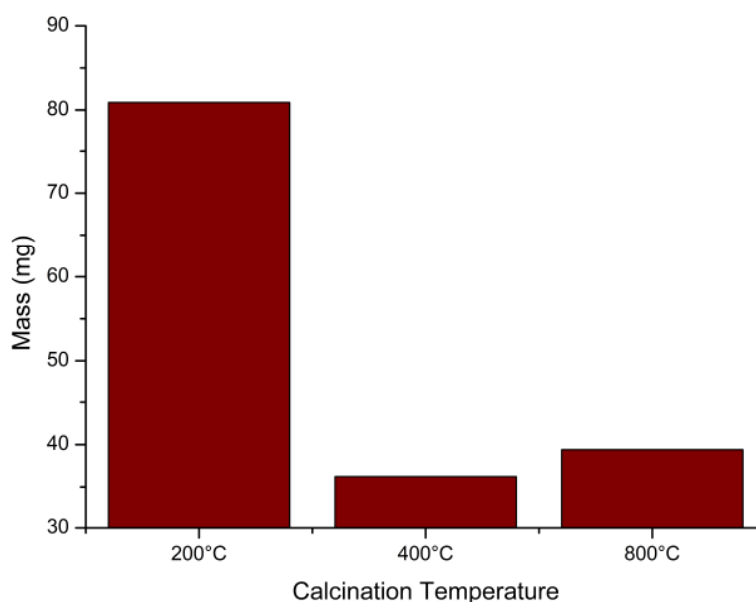
Figure 4.13: The Co₃O₄-NP yield obtained from varying the calcination temperature

Furthermore, the response of size and morphology through the alteration of annealing temperature has been investigated by several studies. For example, Bano and Pillai (2020) found that crystallite sizes tend to increase at higher temperatures due to the coalescence of grains with heat treatment. The larger particles stem from the movement of atoms to more favourable positions, thus merging into adjacent particles. In addition, defects in the crystal lattice were also detected; however, these flaws decreased as calcination approached higher temperatures, thus generating a more crystalline structure (Govindasamy et al., 2021). Similar results were experienced by Ariyanta and co-authors (2021), where lower annealing temperatures displayed a weak NP crystalline phase, while higher temperatures indicated a

strong crystalline phase with increased crystallite sizes due to thermally promoted growth (Ariyanta et al., 2021).

Moreover, Tijani et al. (2019) mentioned that the sintering temperature significantly affected nanoparticle morphology and agglomeration rate. According to their results, the increase from 250 to 650°C produced larger particles with minimal aggregation. The direct linear relationship between the particle size and calcination temperature may have been induced by the stepwise disappearance of crystal defects, thereby enhancing the crystalline nature of the nanoarchitectures (Tijani et al., 2019). Several other investigations have displayed relatable findings, where increased thermal energy led to heightened crystallinity and enlarged particle sizes (Moorthy et al., 2015; da Silva et al., 2019; Karam & Abdulrahman, 2022).
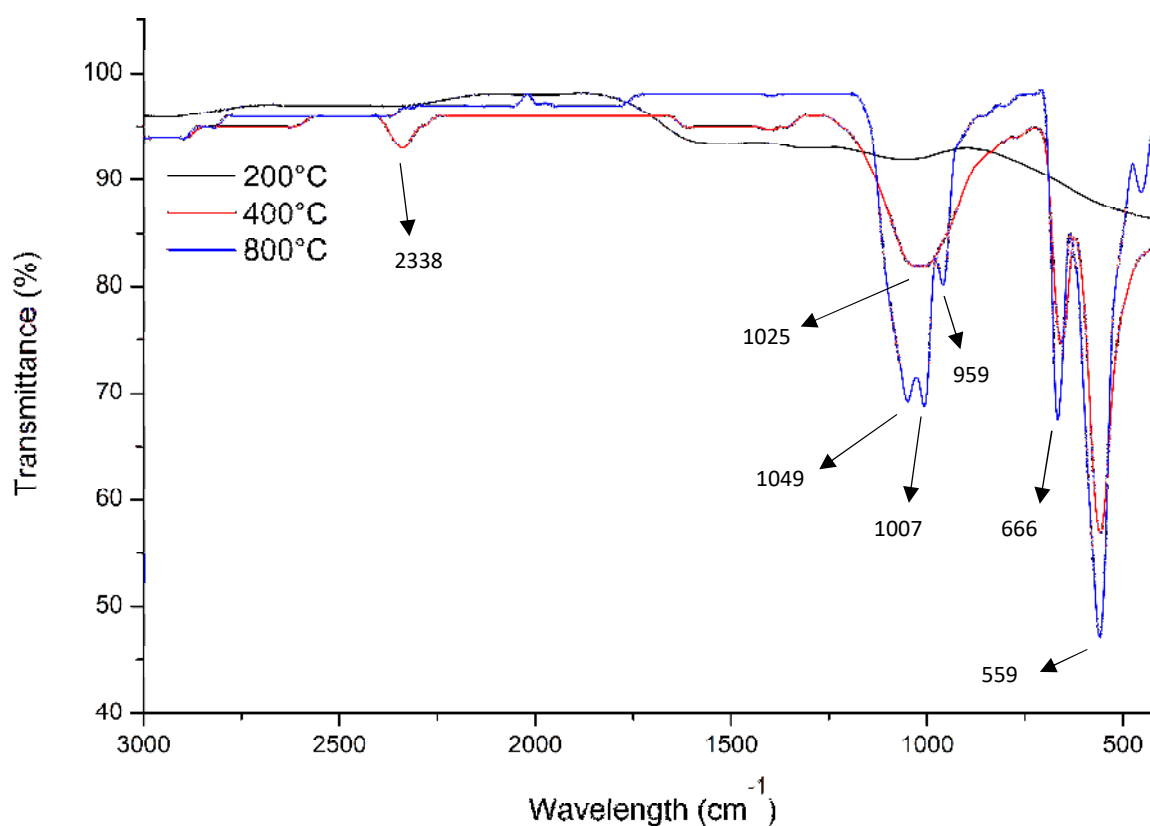
Figure 4.14: The redrawn FTIR spectra of spent-coffee mediated Co$_3$O$_4$-NPs at different calcination temperatures

Herein, the catalytic properties of the Co_3O_4-NPs fabricated using 200°C could not be analysed due to their inability to redisperse in the reaction solution. However, the FTIR spectrum was employed to analyse all nanoparticle samples (Figure 4.14), where no characteristic bands for cobalt oxide were detected at the lowest calcination temperatures. The data retrieved from 200°C closely corresponds to uncalcined nanoparticles as a result of insufficient thermal energy for the completion of the synthesis process (Rameli et al., 2018). Nonetheless, 400 and 800°C have strong peaks at 559 and 666 cm^{-1}. These bands are associated with Co-O stretching vibration and the bridging vibration of O-Co-O bonds (Bhargava et al., 2018). The increase in peak intensity with temperature may have also indicated a greater degree of particle crystallinity (Kombaiah et al., 2018). Furthermore, little differences in degradation efficiencies were observed despite doubling the calcination temperature (Figure 4.15), thereby deeming 800°C an unnecessary increase in energy consumption.
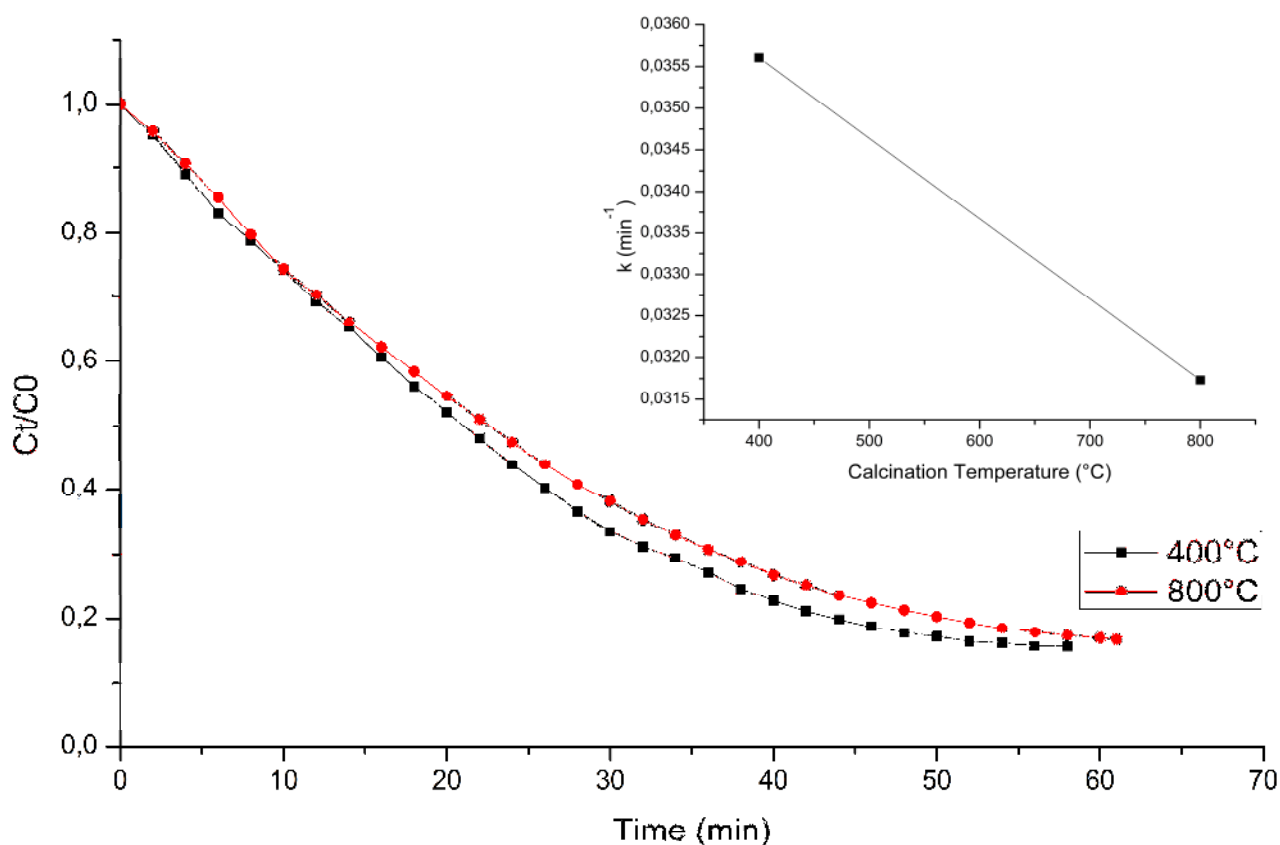
Figure 4.15: The effect of calcination temperature on Co_3O_4-NPs, analysed against the degradation of Tartrazine dye

4.4. Characterisation of Co_3O_4 Nanoparticles

The cobalt oxide nanoparticles within this section were chosen according to the optimal catalytic efficiencies achieved in section 4.3 while simultaneously minimising the energy usage throughout the process. Therefore, the nanoparticles were synthesised using a 1:1 extract to precursor volume at 25°C, with a neutral pH and a 2-hour reaction time. The calcination of the nanomaterial was done at 400°C for 3 hours. Nanoparticles were characterised using XRD, TEM, and UV-vis analysis techniques.

4.4.1. X-ray Powder Diffraction

The confirmation of the spent-coffee mediated Co_3O_4-NPs was carried out through x-ray diffraction techniques. As observed in Figure 4.16, the 2θ peaks at approximately 22.06°, 36.42°, 42.99°, 45.00°, 52.45°, 65.53°, 70.07°, and 77.36° correspond to the (111), (220), (311), (222), (400), (422), (511), and (440) cubic crystal planes of cobalt oxide (JCPDS card file No. 01-080-1533). However, no sharp peaks were detected in the analysis, indicating that the Co_3O_4 nanostructures were poorly crystalline.
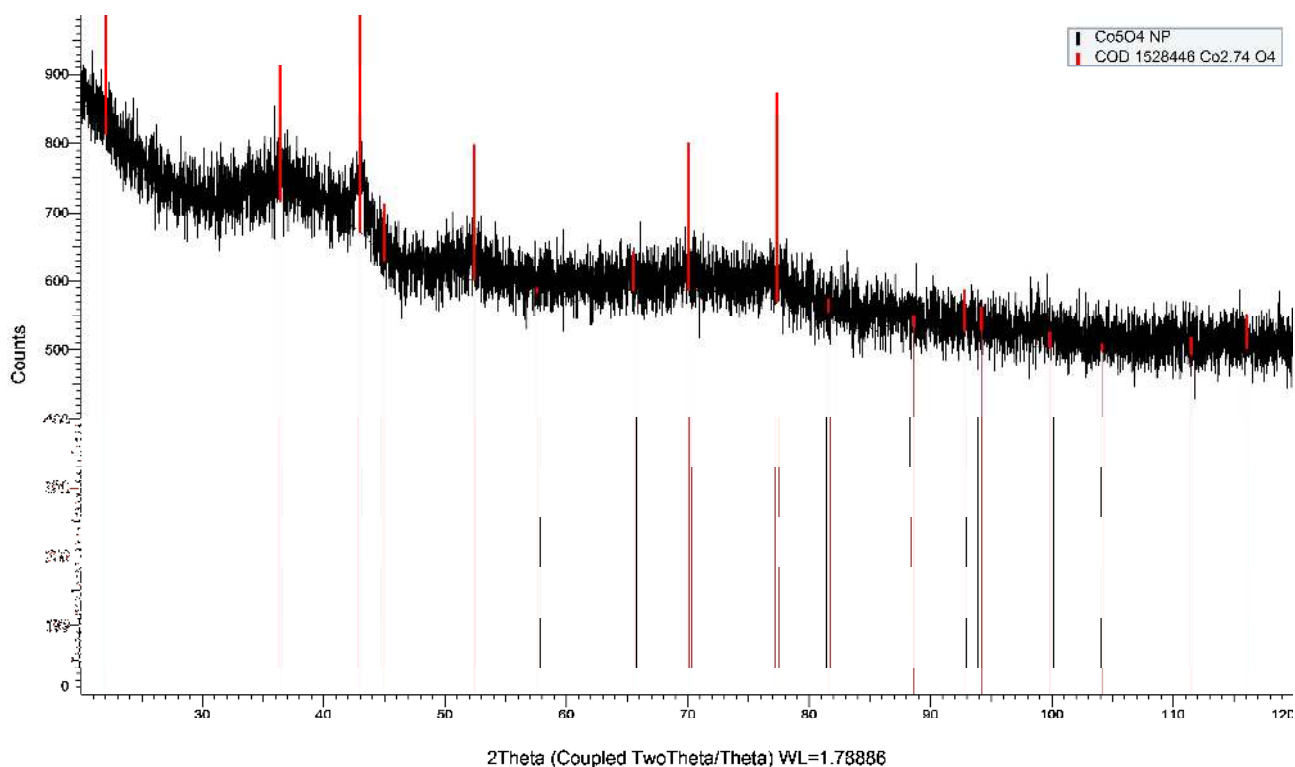
Figure 4.16: The XRD characterisation of the optimal Co_3O_4-NPs

4.4.2. Transmission Electron Microscopy

Electron microscopy was employed to determine the size and morphology of the cobalt oxide nanoparticles. It was discovered that the nanostructures were significantly clustered, with a mixture of spherical and irregularly shaped colloids (Figure 4.17a – c). A study was done on the diameters of the architectures using ImageJ software, where the lengths of the particles ranged from 12.08 – 69.05 nm with a narrow size distribution (Figure 4.17-d). The average diameter of the individual nanoparticles displayed in the TEM images was 29.01 nm, which was well in line with other reports on cobalt oxide nanoparticles (Muhammad et al., 2020; Jeong et al., 2015; Chekin et al., 2016).
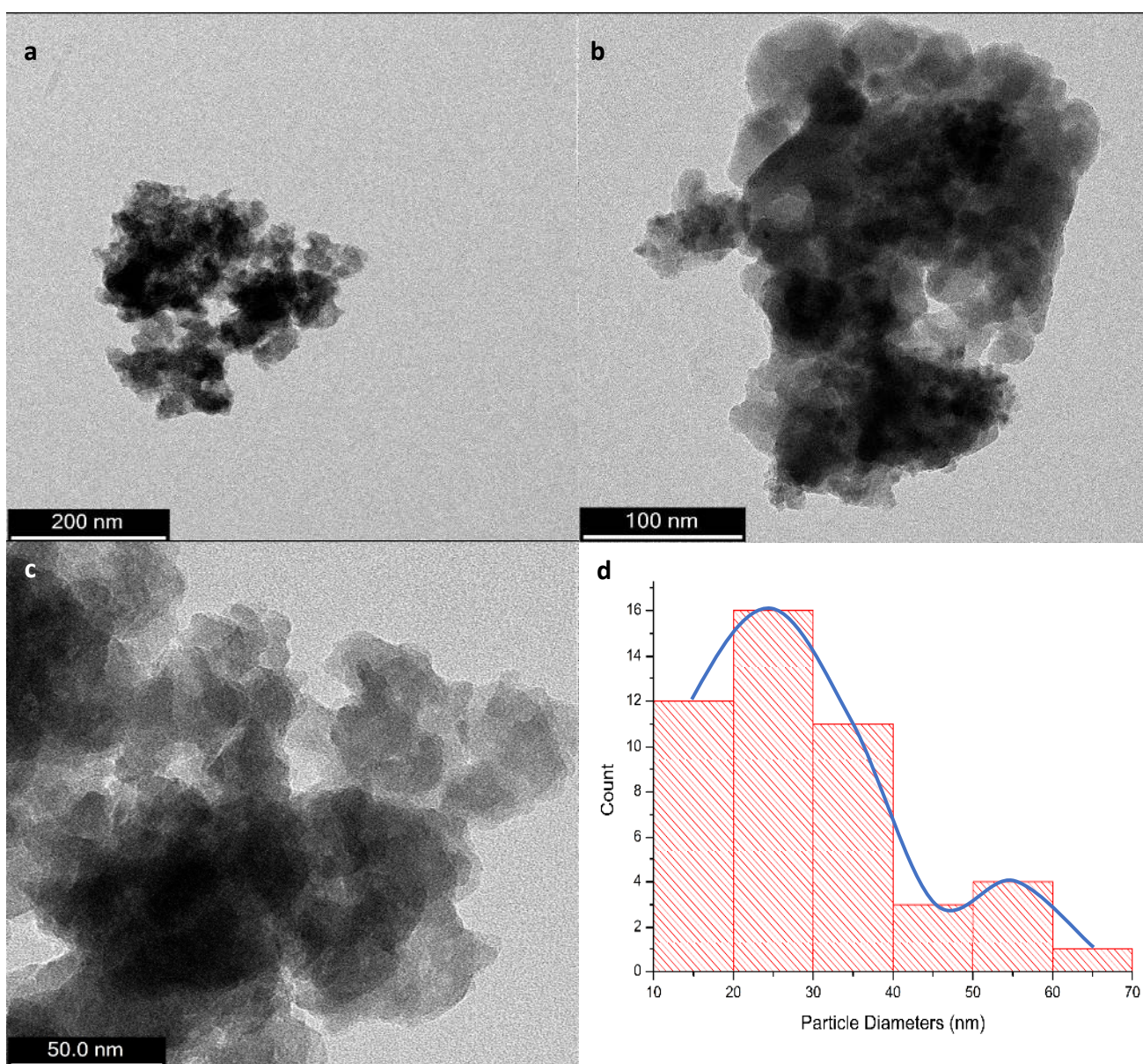
Figure 4.17: The TEM images of the Co_3O_4-NPs at (a) 200 nm, (b) 100 nm, and (c) 50 nm magnifications, with (d) the particle size distribution

4.4.3. UV-Visible Spectroscopy

The origin of light absorption by metallic nanoparticles arises from the consistent oscillation of electrons in the conduction band induced by the interaction of an electromagnetic field (Bibi et al., 2017). Therefore, the optical analysis of the cobalt oxide nanoparticles was accomplished through UV-vis spectroscopy. The absorption profile, depicted in Figure 4.18, reveals two peaks: the appearance of the first band is situated from 300 – 320 nm, while the overshadowing second peak is located between 410 – 440 nm. The peaks derive from the charge transfer processes of $O^{2-} \rightarrow Co^{2+}$ and $O^{2-} \rightarrow Co^{3+}$, respectively. Hence, further confirming the presence of Co_3O_4 nanostructures (Dewi et al., 2019; Yarestani et al., 2014). According to previous literature, these results agree with the characteristic bands of Co_3O_4-NPs, which range between 300 and 550 nm (Alrehaily et al., 2013; Bala et al., 2004; Bhargava et al., 2018; Dubey et al., 2018).
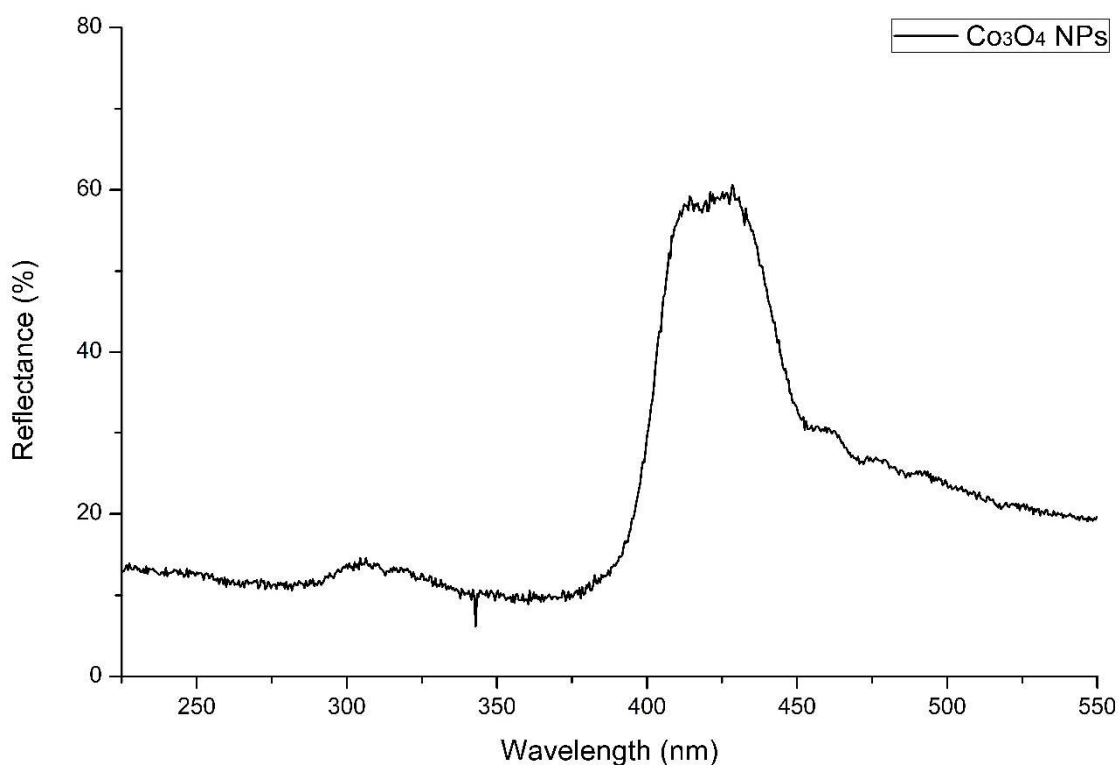
Figure 4.18: The UV-vis spectra of the Co_3O_4-NPs

The band gap energy of a material describes the energy needed to excite an electron from the valence band to the conduction band (Qiao et al., 2013). For an estimation of this value, the Tauc relation may be utilised:

$$(F(R_\infty) \cdot hv)^n = B(hv - E_g)$$ (10)

Where hv is the photon energy, E_g is the band gap energy, and B is a constant, $F(R_\infty)$ is the Kubelka-Munk function, and n is the factor dependent on the electron transition's nature. For Co_3O_4, direct-allowed transition bands are employed; therefore, n = 2 (Bhargava et al., 2018). In addition, the Kubelka-Munk function can be expanded as follows:

$$F(R_\infty) = \frac{K}{S} = \frac{(1-R_\infty)^2}{2R_\infty}$$ (11)

Where $R_\infty = \frac{R_{sample}}{R_{standard}}$ is the reflectance of an infinitely thick specimen, while K and S are the absorbance and scattering coefficients, respectively (Makuła et al., 2018). According to previous literature, the band gap for the bulk material of cobalt oxide was reported to be 2.85 eV for the transitions from the valence band to the cobalt ion sub-bands (Sarfraz & Hasanain, 2014). It is known that the band gaps generally increase with a decrease in particle size; this is a result of electron-hole pairs being significantly closer together, and the Coulombic interaction between them can no longer be neglected, thereby leaving an overall higher kinetic energy and initiating the effect of quantum confinement (M. Singh et al., 2018). Hence, the energy difference between the filled and empty states widens the band gap and further restricts the movement of electrons. Within this study, the band gap energy of spent-coffee-mediated Co_3O_4-NPs was approximately 3.09 eV (Figure 4.19), thus confirming the effects of quantum confinement. The results obtained were in agreement with findings published by previous researchers (Yarestani et al., 2014; Vennela, 2019).
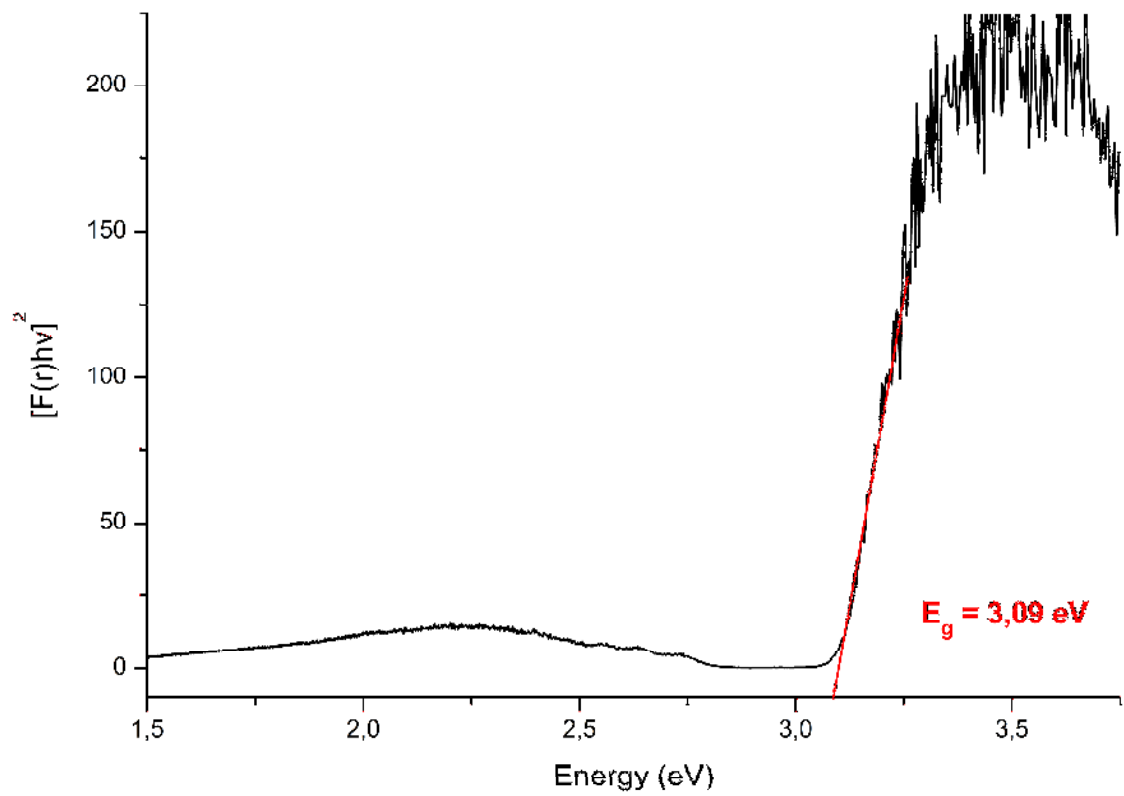
Figure 4.19: The band gap energy of the Co_3O_4 NPs

4.5. Catalytic Activity of Co$_3$O$_4$ Nanoparticles

The spent coffee-mediated nanoparticles were utilised for the remediation of dye-polluted water, where the efficiency was tested against Tartrazine dye. The adsorption kinetic study of the data was accomplished through first-order kinetics (Figure 4.20), as it displayed the strongest correlation (R^2 = 0.9837) when concentrations were plotted accordingly: ln [C] vs t.

Equation	y = a + b*x	
Adj. R-Squar	0,98371	
	Value	Standard Error
Ln [C] Intercept	3,83488	0,04195
Ln [C] Slope	-0,07174	0,00238
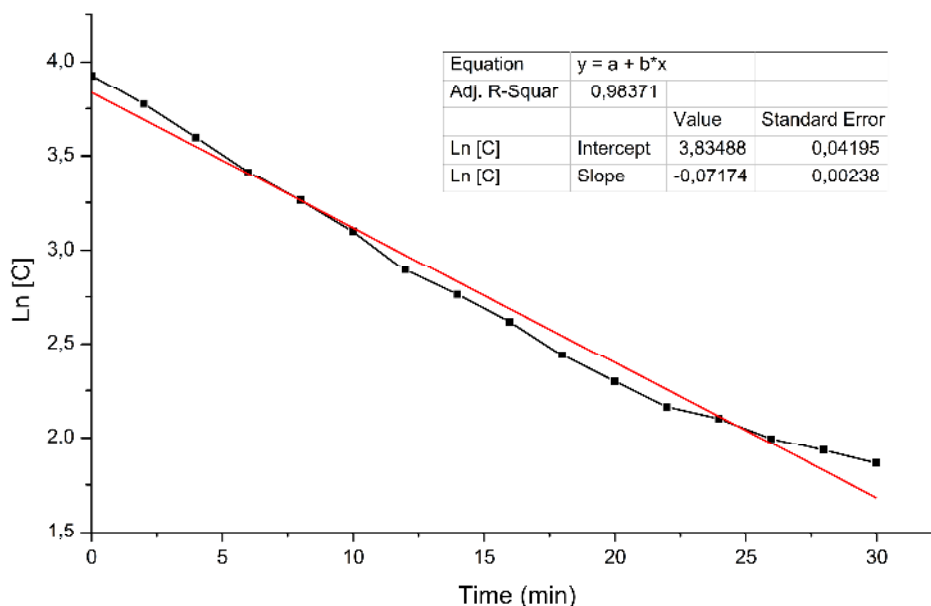
Figure 4.20: The first-order kinetics for the degradation of Tartrazine dye

Initially, the degradation of Tartrazine was investigated by separately introducing each reaction component, as seen in Figure 4.21-a. Alone, the Co$_3$O$_4$ nanoparticles experienced the lowest efficiency, with a minor accumulation of 2.12%, suggesting that the contribution of adsorption to Tart was weak as a result of the relatively small particle sizes (Dai et al., 2021). Furthermore, peroxymonosulfate is a strong oxidant with a redox potential of 1.82 V and has been employed in a wide range of oxidation reactions (Zhang et al., 2017). However, adding PMS to the dye solution only brought about 12.93% decolourisation. On the other hand, the nanostructures coupled with PMS resulted in 89.01% degradation of the Tartrazine within 30 minutes, thereby indicating the excellent catalytic performance of the Co$_3$O$_4$ nanoparticles for PMS activation and, ultimately, sulfate radicals ($SO_4^{\bullet-}$) generation.

Moreover, the reproducibility of nanoparticle synthesis and catalytic dye degradation procedures is one of the fundamental problems faced by researchers (Cukic et al., 2006). Improving this aspect is considered crucial for applications in research and industrial fields. Herein, a remarkable degree of repeatability with high accuracy was achieved, indicating that the unique properties of the nanoparticles were preserved during synthesis (Figure 4.21-b).
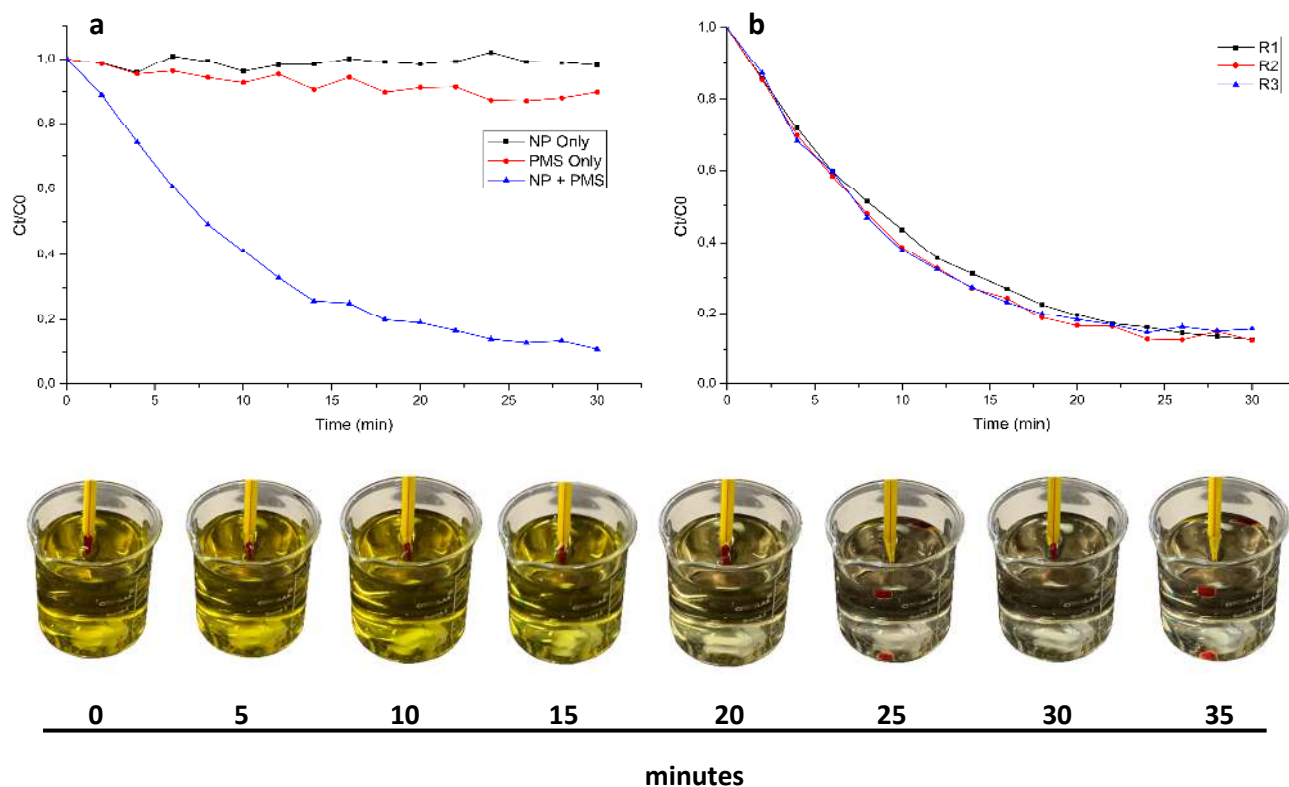
Figure 4.21: The (a) degradation kinetics of Tartrazine dye and (b) repeatability of the decolourisation process

4.5.1. Influence of Temperature

Previous research has reported that various degradation temperatures have had profound effects on the rate and efficiency of the process (Tan et al., 2022). The results of this study strongly correlate with this statement. Depicted in Figure 4.22 are temperatures of 25, 40, and 60°C with efficiencies of 93.86, 96.10, and 99.42%, respectively. Despite the differences being minuscule, the time taken to achieve equilibrium drastically diminishes. Therefore, unprecedented degradation rate (k) values were produced: 0.09, 0.21, and 0.34 min^{-1} for 25, 40, and 60°C, correspondingly. Due to higher temperatures, molecules in the solution possess elevated thermal energies, raising the collision frequency between the nanoparticles and the dye molecules and initiating a higher rate of reaction (Salama et al., 2018). In addition, an increased rate of sulfate radical generation is simultaneously experienced alongside valent cobalt species, further accelerating the dye degradation rate (Siddique et al., 2018). Also, with the enhanced activity at the surface, free radicals are allured to the surrounding film of the nanoparticle. Subsequently, fast-cracking reactions of the dye molecules take place (Rafique et al., 2019).

Parameter	Time (min)	Efficiency (%)	k (min^{-1})
25°C	22	93,86	0,0909
40°C	10	96,10	0,2092
60°C	2	99,42	0,3371
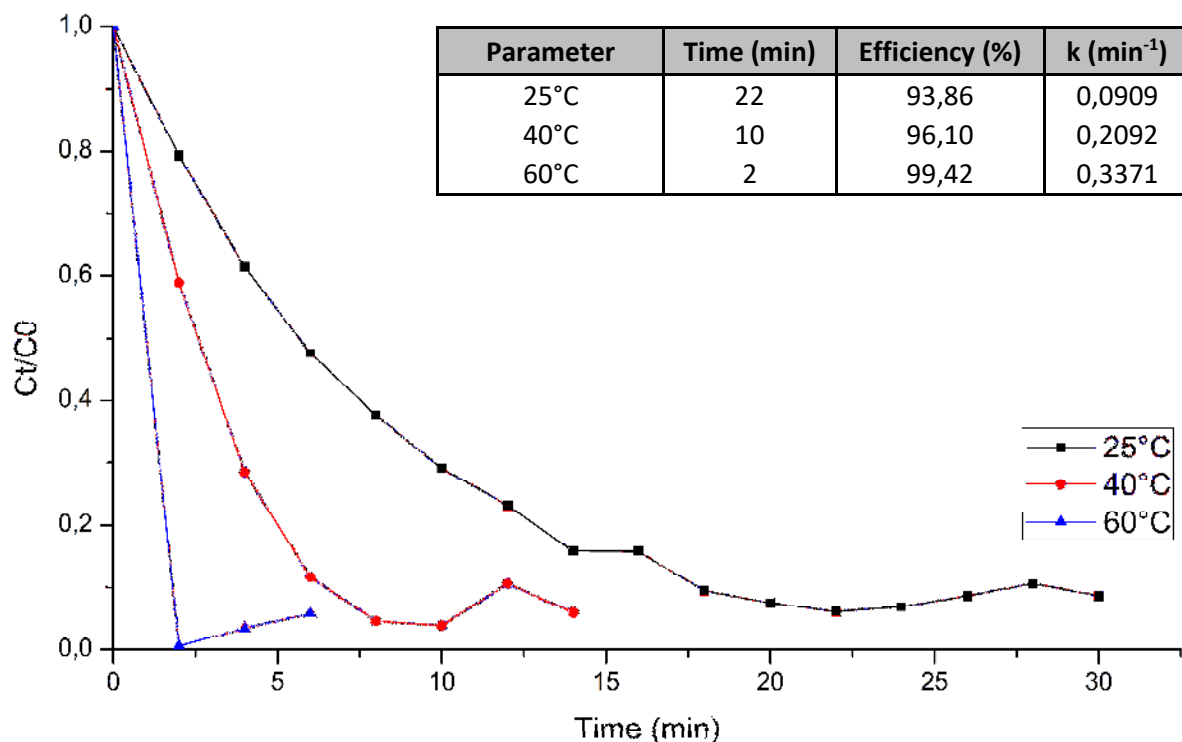
Figure 4.22: The effect of temperature on the degradation of Tartrazine dye

Another imperative factor is the proportion of reactant molecules that possess sufficient energy to react. This means: the greater the difference between the energy and the activation energy, the faster the reaction rate will be. The Arrhenius equation was utilised to determine the activation energy of the Tartrazine degradation through Co_3O_4-NPs.

$$k = Ae^{(-E_a/RT)}$$

(12)

Where A is the pre-exponential factor and $e^{(-E_a/RT)}$ represents the fraction of collisions that have enough energy to overcome the activation barrier at temperature T. By rearranging the equation, a linear relation between ln [k] and 1/T may be drawn, with the slope of the graph equating to -E_a/R, where E_a is the activation energy (J/mol), R the ideal gas constant (8.3145 J/K.mol), T the temperature (K), and k the reaction rate constant. Therefore, from the data in Figure 4.23, the activation energy was calculated to be 30.61 KJ/mol. Similar investigations on cobalt oxide-based catalysts present activation energies ranging from 26.5 – 75.5 KJ/mol, suggesting that the energy barrier of the Co_3O_4-NPs obtained herein was relatively low (Shukla et al., 2011; Yao et al., 2012; Chowdhury et al., 2015).

Equation	y = a + b*x		
Adj. R-Squa	0,9156		
		Value	Standard Err
Ln [k]	Intercept	10,03453	2,46213
Ln [k]	Slope	-3681,41	772,73351
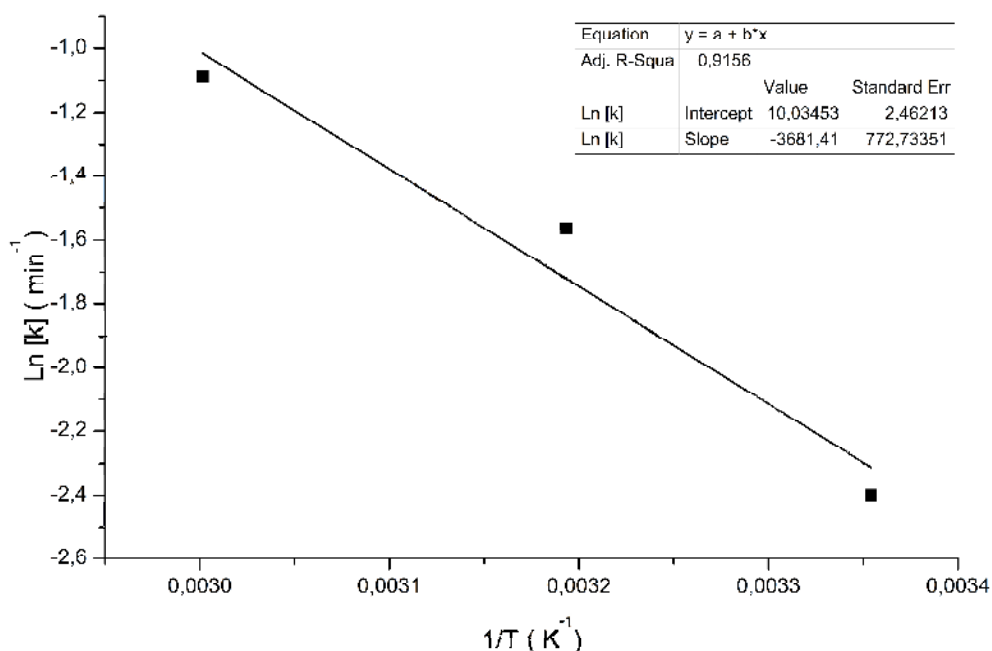
Figure 4.23: The activation energy of Tartrazine dye through the Co_3O_4-NPs

4.5.2. Influence of Catalyst Loading

The degradation of Tart dye through alterations of Co_3O_4-NP concentrations was examined. As delineated in Figure 4.24, increasing the cobalt oxide content from 2 to 5 mg/L slightly increases the reaction efficiency by approximately 6%. Catalyst loads surpassing 5 mg/L saw almost no increase in the overall decolourisation of the solution. Furthermore, elevated NP concentrations clearly display superior rates of azo dye degradation, with rate constants (k) estimated to be 0.032, 0.094, and 0.193 for 2, 5, and 10 mg/L, respectively.

The efficiency and reaction rate enhancement has been mentioned in preceding reports (Esmaeili et al., 2019; Dung et al., 2020). According to Ali and co-authors (2017), these observations can be rationalised by the increased availability of active sites for PMS activation, thus accelerating the oxidation of organic compounds through the generation of more sulfate radicals (Kuriechen & Murugesan, 2013).

Parameter	Time (min)	Efficiency (%)	k (min^{-1})
2 mg/L	60	87,91	0,0318
5 mg/L	24	93,84	0,0941
10 mg/L	10	93,91	0,1932
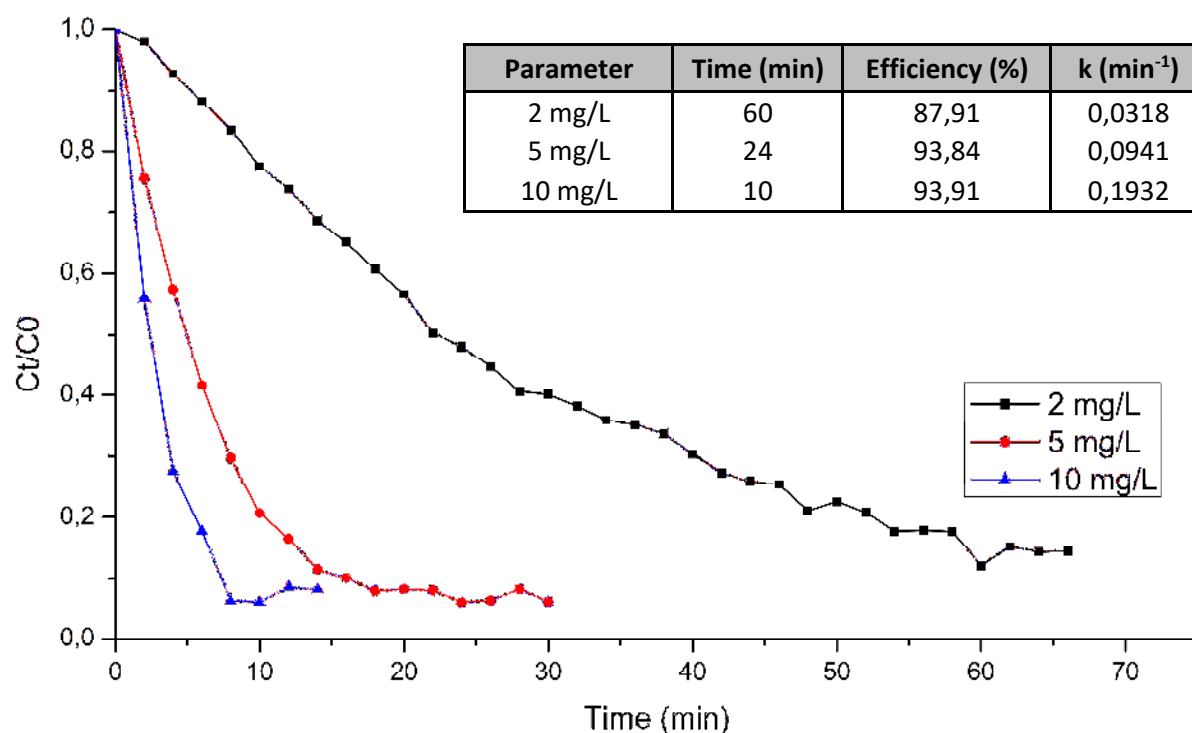
Figure 4.24: The effect of catalyst loading on the degradation of Tartrazine dye

4.5.3. Influence of PMS Dosage

In pursuance of oxidant dosage effects, assorted masses of peroxymonosulfate were introduced into the dye-nanoparticle mixture. As seen in Figure 4.25, the reaction rate significantly increased when Oxone concentrations were elevated from 50 to 100 mg/L; however, 200 mg/L solutions obtained slightly slower initial degradation rates than 100 mg/L. This phenomenon is consistent with several other heterogeneous catalytic reactions for the activation of PMS (Shi et al., 2022; Liu et al., 2017). Nonetheless, the highest PMS concentrations remained the most effective, with efficiencies amounting to 94.82% in 22 minutes.

At low concentrations of PMS, the increased decolourisation may have been induced by the increased production of reactive species, deeming that PMS prevails as the limiting factor. On the other hand, higher dosages experienced minimal increases in efficiency due to the limitations of available active sites for radical production (Mo et al., 2022). In addition, redundant radicals react with unused PMS in the self-quenching reactions exhibited in equations 13 and 14 (Ma et al., 2018):

$$SO_4^{\bullet-} + HSO_5^- \rightarrow SO_5^{\bullet-} + HSO_4^- \tag{13}$$

$$^{\bullet}OH + HSO_5^- \rightarrow SO_5^{\bullet-} + H_2O \tag{14}$$
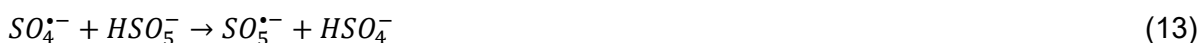
Therefore, an overdose of PMS molecules will inevitably lead to a decrease in the reactivity of the degradation system.

Parameter	Time (min)	Efficiency (%)	k (min^{-1})
50 mg/L	68	85,74	0,0231
100 mg/L	28	89,27	0,0713
200 mg/L	22	94,82	0,1256
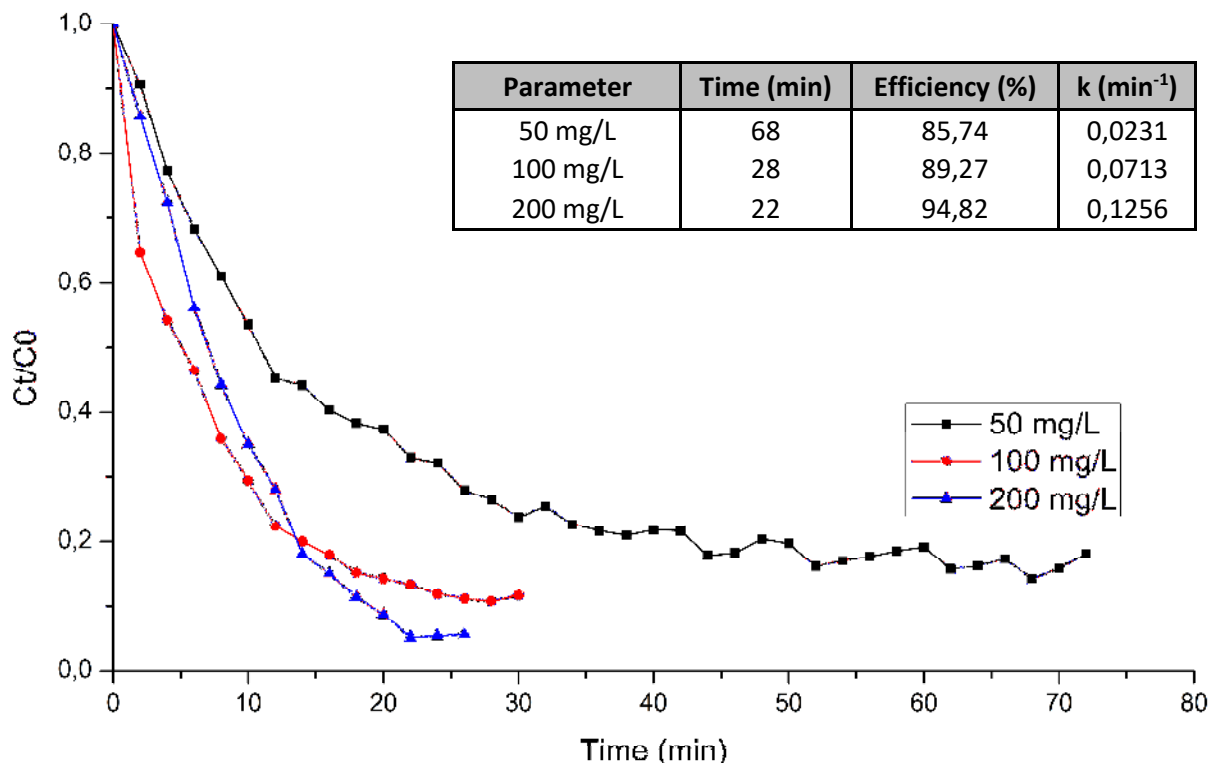
Figure 4.25: The effect of PMS dosage on the degradation of Tartrazine dye

4.5.4. Influence of Reaction pH

The pH of dye degradation reactions is a critical variable, as the concentration of cobalt ions and the speciation of free radicals are highly pH dependent. In order to obtain the optimal pH, a series of experiments were conducted in acidic (pH ±3.5) and neutral (pH 7) systems. Initially, the nanoparticles dispersed in the dye solution presented a pH of approximately 8.3. After adding PMS, the pH dropped to ±3.5 due to the acidic quality of the substance (Zazouli et al., 2017). The tests executed with the unadjusted pH displayed the most efficient outcome, resulting in 91.00% decolourisation within 22 minutes (Figure 4.26). However, modifying the pH to 7 brought about a dramatic decrease in the dye removal capabilities, with only 50.06% degraded after 30 minutes.

Nagar and Devra (2018) reported similar findings, where an increase in degradation was observed up to a pH of 6.5. This may have been attributed to the catalyst's surface charge and stability of PMS at acidic conditions. When dispersed in water, the surface of the nanoparticles becomes cationic, providing more coverage of hydroxyl groups (Keshta et al., 2022).

Therefore, the uncharged surface hydroxyl groups become the main active sites for generating radicals and, in turn, deteriorating pollutants (Huang et al., 2017; Lou et al., 2014). Furthermore, at a low pH, the dye degradation rate is only limited due to the H⁺ ion scavenging effects of the radicals $^\bullet OH$ and $SO_4^{\bullet-}$ (Eqn 15 – 16):

$$^\bullet OH + H^+ + e^- \rightarrow H_2O \tag{15}$$

$$SO_4^{\bullet-} + H^+ + e^- \rightarrow HSO_4^{\bullet-} \tag{16}$$

At a neutral pH, the surface of the catalyst transitions to anionic, and higher electron repulsion forces drive the reactive species away (Bouzayani et al., 2019). Consequently, fewer molecules reach the surface of the nanoparticles, decreasing the degradation rate (Ahmadi & Ghanbari, 2019). It is also noteworthy that Ball and Edwards (1956) witnessed the spontaneous decomposition of PMS in the range of 6.00 – 11.65; hence, no attempt was made to further adjust the reaction pH past 7. If the pH is increased from the natural one, then the degradation of the dye would only be accomplished by the self-decomposition of PMS (Madhavan et al., 2006).

Parameter	Time (min)	Efficiency (%)	k (min^{-1})
3-4	22	91,00	0,0712
7	30	50,06	0,0173
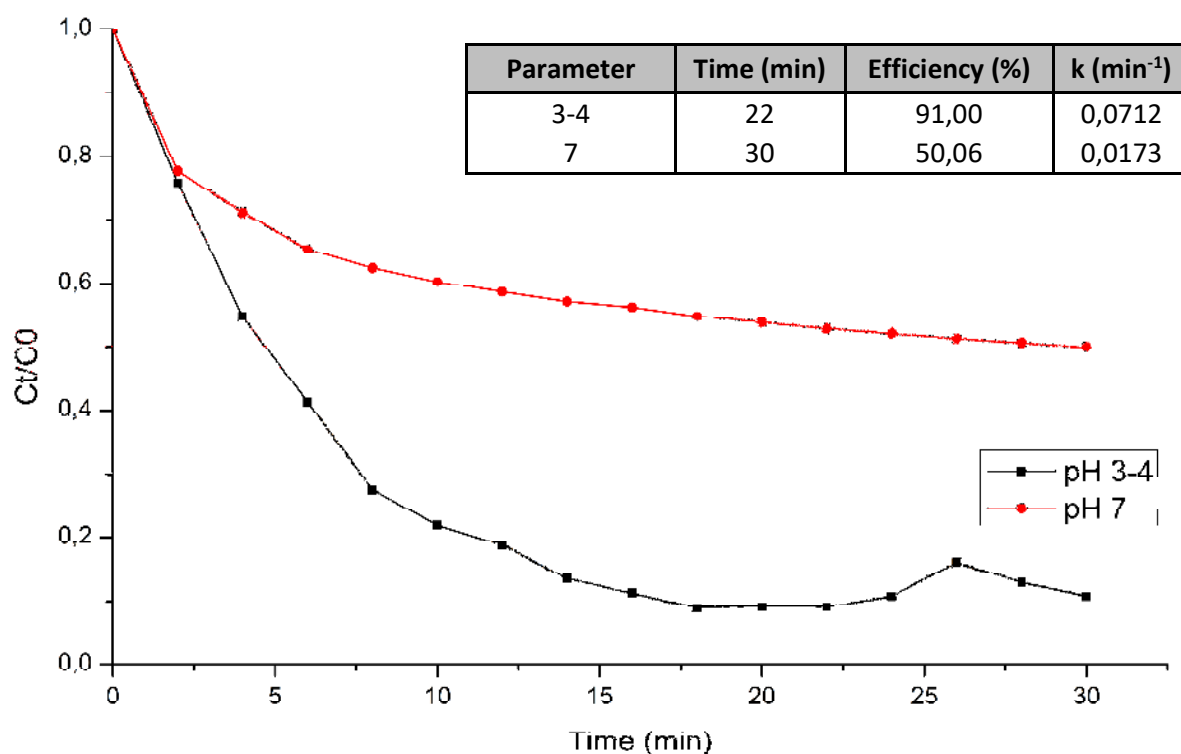
Figure 4.26: The effect of solution pH on the degradation of Tartrazine dye

4.5.5. Possible Activation Mechanism of PMS

During advanced oxidation processes, the generation of various radicals is crucial for the degradation of organic contaminants. Within the metal-catalysed activation of PMS, five main types of reactive species arise: sulfate radical ($SO_4^{•-}$), hydroxyl radical ($^{•}OH$), superoxide radical ($O_2^{•-}$), peroxysulfate radicals ($SO_5^{•-}$), and singlet oxygen ($^{1}O_2$) (Ghanbari & Moradi, 2017). In order to ascertain the dominating radicals in the Co_3O_4/PMS system, quenching experiments were conducted using methanol (MeOH) and isopropanol (IPA). It is well known that MeOH possesses the ability to scavenge both $SO_4^{•-}$ (k = 8 x 10^8 $M^{-1}s^{-1}$) and $^{•}OH$ (k = 1 x 10^{10} $M^{-1}s^{-1}$) radicals (Farooq et al., 2022), while IPA has been reported to effectively quench $^{•}OH$ reactive species 1000-fold higher than the rate of quenching occurring between IPA and $SO_4^{•-}$ (Govindan et al., 2020).

The evaluation of the Tartrazine removal rate in the presence of the radical scavengers is presented in Figure 4.27. The decrease in reaction rate from 0.0712 min^{-1} to 0.0385 (IPA, 50.0 mM) and 0.0219 min^{-1} (MeOH, 50 mM) substantiates the involvement of sulfate and hydroxyl radicals. This was further confirmed by the overall deterioration of the dye declining from 90.90% to 70.38 and 48.63% for IPA and MeOH, respectively. Also, since MeOH could not completely halt the degradation of the azo dye; therefore, the participation of the other reactive species ($O_2^{•-}$, $SO_5^{•-}$, and $^{1}O_2$) may be assumed.
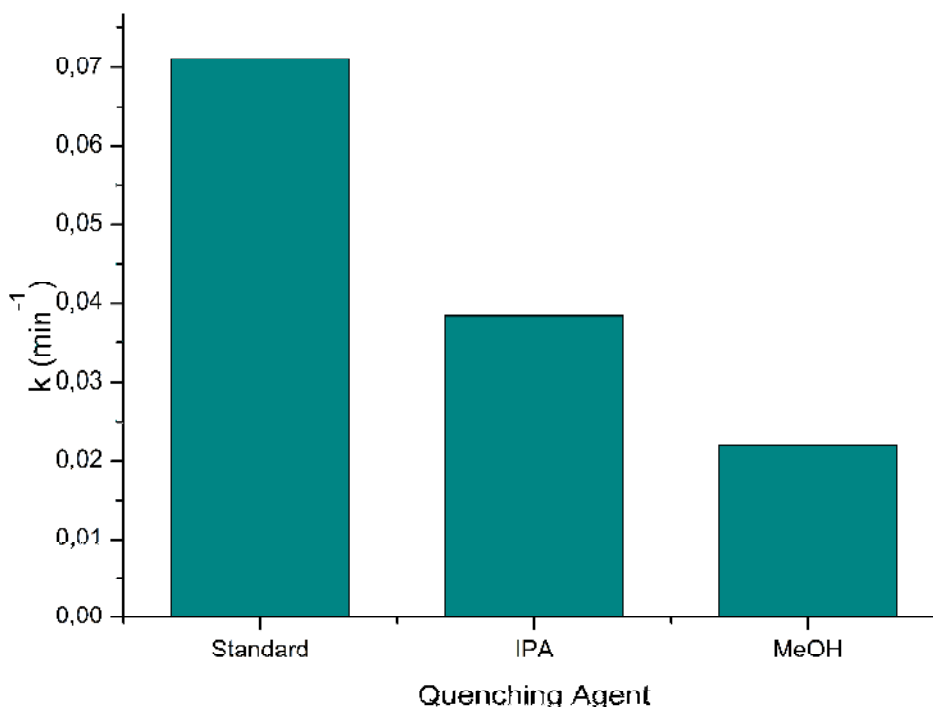
Figure 4.27: The quenching study on the degradation of Tartrazine dye

Based on the above results and previous studies, the possible mechanism for activating PMS through spent coffee-mediated Co_3O_4 nanoparticles is summarised by equations 17 – 30. In the presence of cobalt oxide nanostructures, PMS is activated to generate $SO_4^{\bullet-}$ and $SO_5^{\bullet-}$ radicals (Eqn 17 – 18). In addition, the same reactions describe the regeneration of Co^{2+} and Co^{3+} in the redox cycle (Cheng et al., 2020). Equations 19 – 20 indicate the reaction between the sulfate radicals and H_2O/OH^- to produce $^{\bullet}OH$ species. Furthermore, hydroxyl radicals may also be formed by the reaction between $SO_5^{\bullet-}$ and hydroxylated metallic sites ($M^{3+} - H_3O^+$) (Eqn 21 – 22) (Dung et al., 2020). In the oxidation system, PMS would be hydrolysed to produce $O_2^{\bullet-}$ (Eqn 23 – 24), with the dissolved oxygen also being able to contribute to $O_2^{\bullet-}$ concentrations (Eqn 25) (Mo et al., 2022). Moreover, the generated superoxide species can consume PMS and accelerate the production of $SO_4^{\bullet-}$ (Eqn 26), thereby improving the oxidation performance of the system (Peng et al., 2018). Equations 27 – 28 represent the formation of $^1O_2$ from the self-reaction of $SO_5^{\bullet-}$ and self-decomposition of PMS. Simultaneously, the reaction between $O_2^{\bullet-}/SO_5^{\bullet-}$ and water molecules would also generate singlet oxygen species (Eqn 29 – 30) (Kohantorabi, Moussavi & Giannakis, 2021). Lastly, the resulting radicals attack the Tart dye molecules, open the aromatic rings, and form intermediate products, which are ultimately mineralised into H_2O and CO_2.

$$Co^{2+} + HSO_5^- \rightarrow Co^{3+} + SO_4^{\bullet-} + OH^- \tag{17}$$

$$Co^{3+} + HSO_5^- \rightarrow Co^{2+} + SO_5^{\bullet-} + H^+ \tag{18}$$

$$SO_4^{\bullet-} + H_2O \rightarrow +H^+ + SO_4^{2-} \tag{19}$$

$$SO_4^{\bullet-} + OH^- \rightarrow {}^{\bullet}OH + SO_4^{2-} \tag{20}$$

$$M^{3+} - H_3O^+ + SO_5^{\bullet-} \rightarrow M^{3+} - \cdot OHOSO_3 + H_2O \tag{21}$$

$$M^{3+} - \cdot OHOSO_3 + 2e^- \rightarrow M^{2+} + SO_4^{\bullet-} + {}^{\bullet}OH \tag{22}$$

$$HSO_5^- \rightarrow SO_5^{2-} + H^+ \tag{23}$$

$$SO_5^{2-} + H_2O \rightarrow O_2^{\bullet-} + SO_4^{2-} + H^+ \tag{24}$$

$$O_2 + e^- \rightarrow O_2^{\bullet-} \tag{25}$$

$$HSO_5^- + O_2^{\bullet-} \rightarrow SO_4^{\bullet-} + O_2 + OH^- \tag{26}$$

$$SO_5^{\bullet-} + SO_5^{\bullet-} \rightarrow 2SO_4^{2-} + {}^1O_2 \tag{27}$$

$$HSO_5^- + SO_5^{2-} \rightarrow HSO_4^- + SO_4^{2-} + {}^1O_2 \tag{28}$$

$$2O_2^{\bullet-} + 2H_2O \rightarrow {}^1O_2 + H_2O_2 + 2OH^- \tag{29}$$

$$2SO_5^{\bullet-} + H_2O \rightarrow 2HSO_4^- + 1.5^1O_2 \tag{30}$$
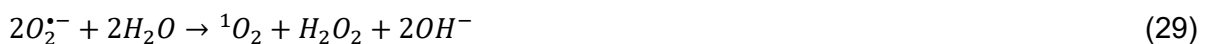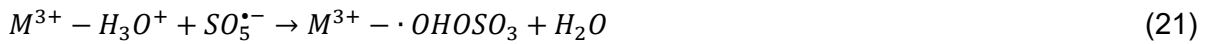
4.5.6. Reusability

Three recycling runs of the nano-Co_3O_4 catalyst were carried out to determine the performance and stability of the nanoparticles after use. Figure 4.28-a and -b depict the exponential deterioration of the efficiency of the degradation process, with the reaction rate decreasing by 95.03% from the first to the third cycle. These results were mainly caused by the difficulty of nanoparticle recovery for further use, as a substantial decrease in the yield was observed after each cycle. Therefore, it may be suggested that the nanostructures necessitate a growth template for easy retrieval. This aspect would be critical for the feasibility of the material within industry.
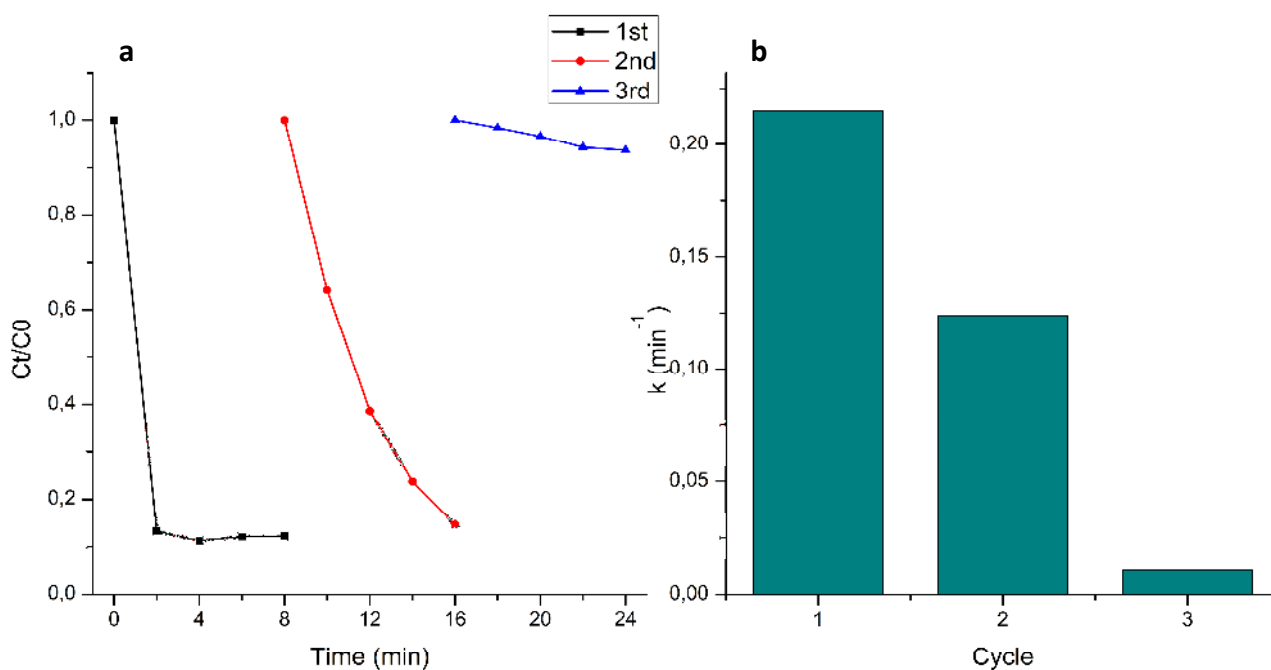
Figure 4.28: The reusability of the spent-coffee mediated Co_3O_4-NPs

4.5.7. Industrial Effluent Simulation

The efficiency of the spent coffee-mediated Co_3O_4-NPs was analysed against a mixture of three dyes that may mimic a typical industrial effluent (Kulasooriya et al., 2020). The mixture consisted of equal volumes of Tartrazine, Methyl Orange, and Remazol Brilliant Red, with concentrations of 0.1 mM (Figure 4.29).
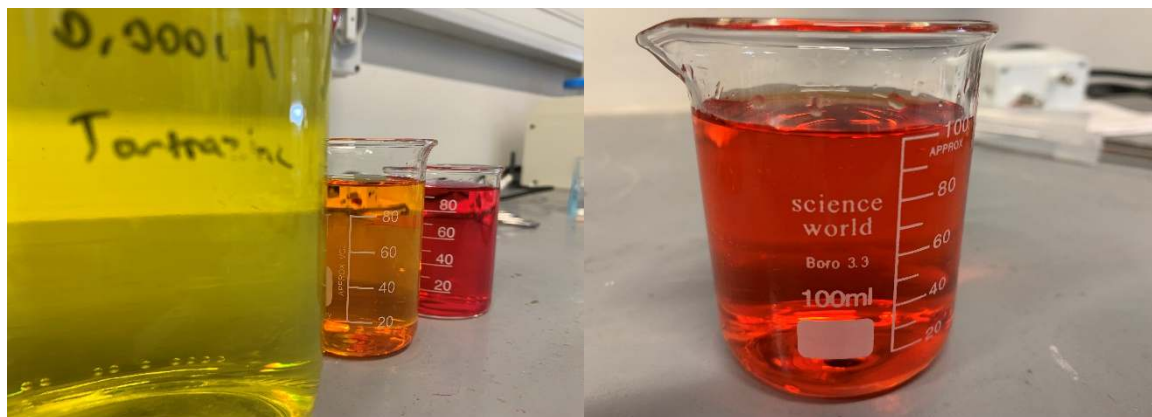
Figure 4.29: The images of the industrial dye simulation and its constituents

Figure 4.30 displays the UV-vis spectrum of the mixed dye degradation process. Compared to the average degradation of Tartrazine (k = 0.082 min^{-1}), the catalytic activity of the nanoparticles in the mixed dye solution presented promising results, with the reaction rate constant (k) equating to 0.086 min^{-1}. Therefore, a 4.65% increase in the reaction rate was observed. Moreover, the efficiency of decolourisation also witnessed a minor increase from 91.99 to 92.77% for the degradation of Tart and mixed dye solutions, respectively. This is an excellent indication that there was no substantial effect on the performance of the Co_3O_4 catalyst, despite the high load of organic pollutants with a wide variety of chemical compositions.
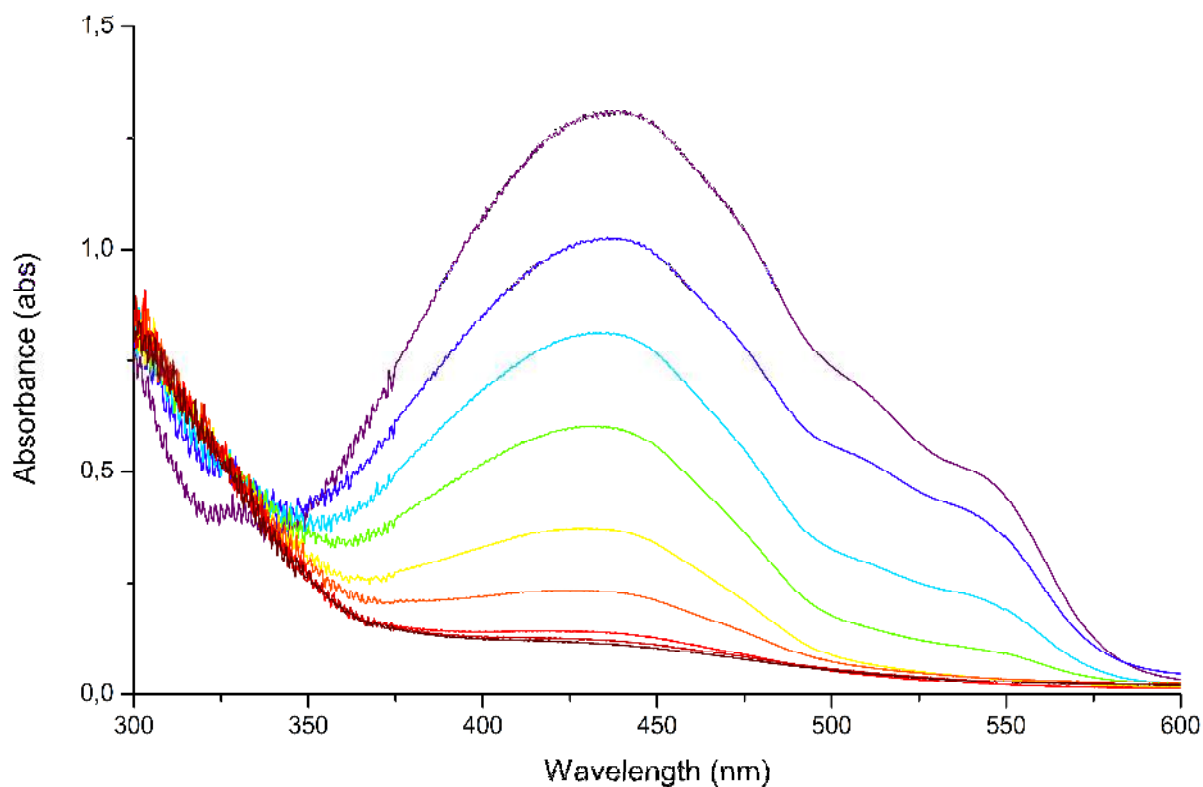
Figure 4.30: The UV-vis spectra of the industrial dye degradation through Co_3O_4-NPs and PMS

4.5.8. Stability of Co_3O_4 NPs

The leaching of redox metal ions is a major issue regarding cobalt-activated AOPs. Due to its toxicity, there is a dire need for strategies that can combat or prevent the release of cobalt ions during oxidation reactions. Typically, the permissible level for dissolved cobalt is 1 ppm or lower (Achola et al., 2020). In addition to the carcinogenic properties, ionic leaching may negatively impact the catalyst through gradual deterioration, thereby limiting the lifespan.

The leaching of Co^{2+} ions was studied during the degradation of Tartrazine dye, with the standard solution comprised of deionised water (Figure 4.31-a). These curves do not exhibit a clear trend in the dissolved cobalt concentrations; however, a peak of 0.86 µg/g can be observed at 25 minutes. This equates to approximately 0.0001% of the total cobalt in the reaction mixture, which is significantly lower than the cobalt leaching in similar reports (Gao et al., 2021; Lin & Lin, 2017; Zhang et al., 2016). Considering the low cobalt ion concentrations, it is suggested that the activation of PMS by Co_3O_4-NPs follows a heterogeneous pathway, indicating that the nanoparticles function as a stable cobalt source and accelerate the generation of sulfate radicals from PMS (Zhou et al., 2013). Nonetheless, it is worth noting that any measurable release of heavy metal ions into the reactant solution is a potential limitation for real-world applications.

Furthermore, the degradation of azo dyes is usually accompanied by the removal of chemical oxygen demand (COD). Figure 4.31-b demonstrates the decrease of 21.88% in COD after a

30-minute reaction period. Therefore, this implies that not only does the catalytic system degrade the azo dye linkage (–N=N–), but it could also decompose the reaction products (Shen et al., 2010). In spite of this, the removal of COD was relatively low compared to previous findings (Cai et al., 2015; Shi et al., 2012).
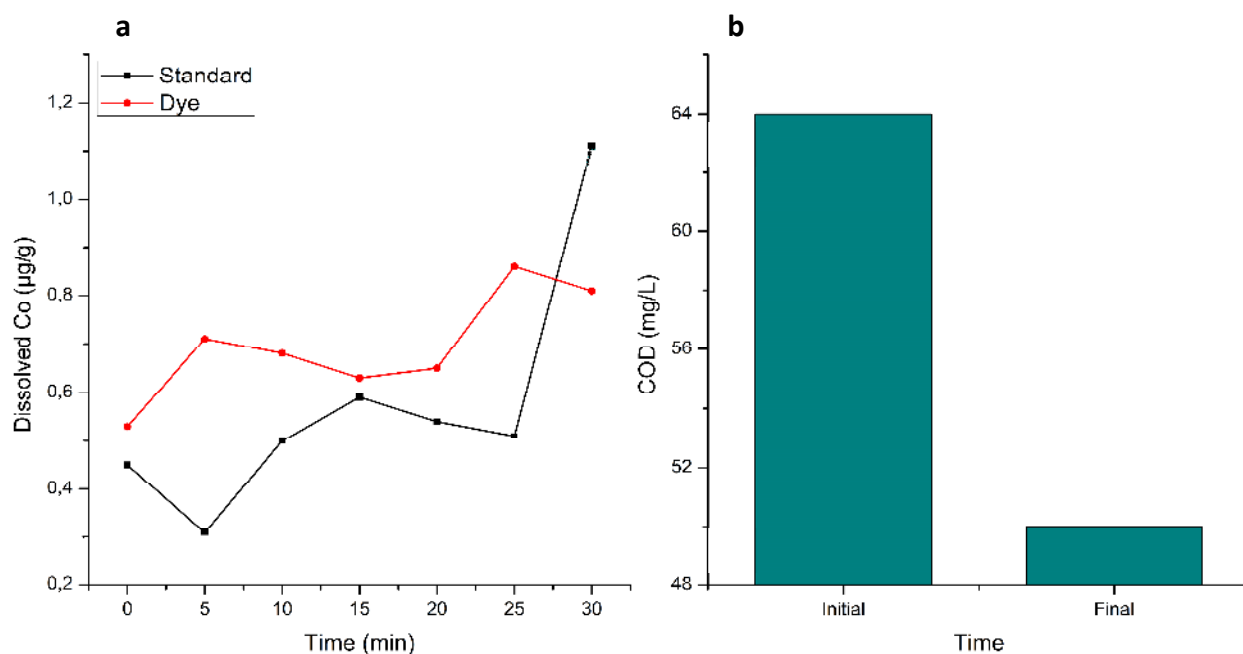
Figure 4.31: The (a) cobalt leaching of the Co_3O_4-NPs and the (b) COD removal of the dye degradation reaction

4.6. Photocatalytic Activity of Co$_3$O$_4$ Nanoparticles

The photocatalytic degradation of Tartrazine dye in the presence of spent-coffee mediated Co$_3$O$_4$ nanocomposites was investigated under two different light sources: a 6 W LED emitting white light and a solar simulator producing 100 W/m^2 UV irradiation, both situated 5.0 cm from the reaction cell (Figure 4.32).
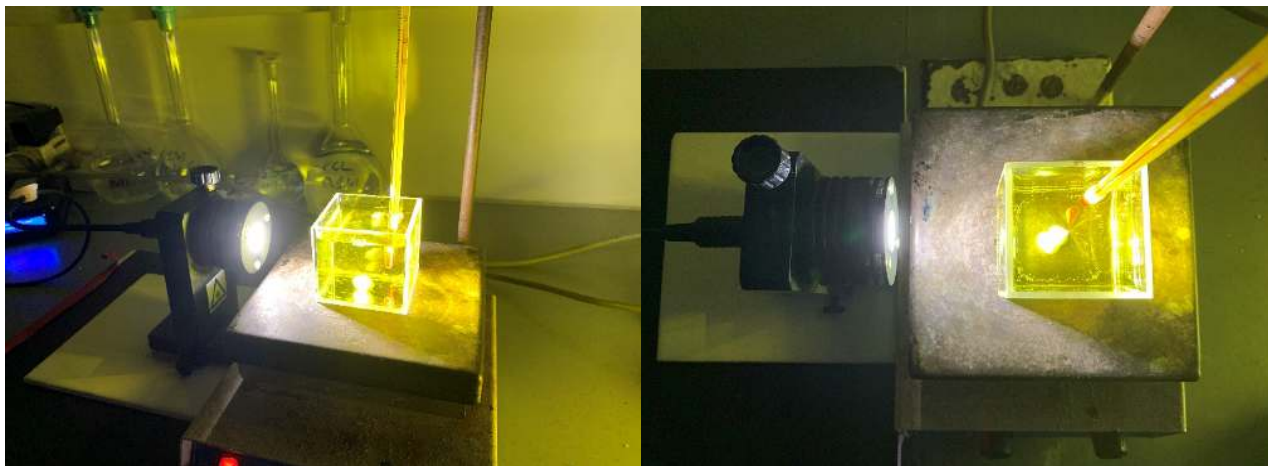
Figure 4.32: The experimental setup for the photocatalytic degradation of Tartrazine dye

As presented in Figure 4.33-a, the introduction of light had an apparent effect on the reaction rate of the system. As expected, the use of a UV light source resulted in a significant increase of 37.60%, while the LED accrued a relatively negligible increment of 6.04%. Therefore, only solar illumination was investigated from here-on out.

To better understand the mechanism, quenching tests were conducted on the photocatalytic degradation of Tart dye using the same reagents described in section 4.5.5 (50 mM IPA and 50 mM MeOH). Compared to the prior catalytic outcome, an overall increase in reaction rate was observed after adding the simulated solar light in quenched systems (Figure 4.33-b). Although both the employed radical scavengers resulted in a substantial drop in oxidation rate, it is clear that hydroxyl radicals may have been the dominating species in the UV-assisted reaction as dye deterioration was quenched by 51.81% (IPA). Nonetheless, the introduction of methanol confirmed the presence of sulfate radicals with a quenching accumulation of 67.63%. These findings were in accordance with the data obtained from similar research (Li et al., 2016; Mohamed Reda et al., 2017).
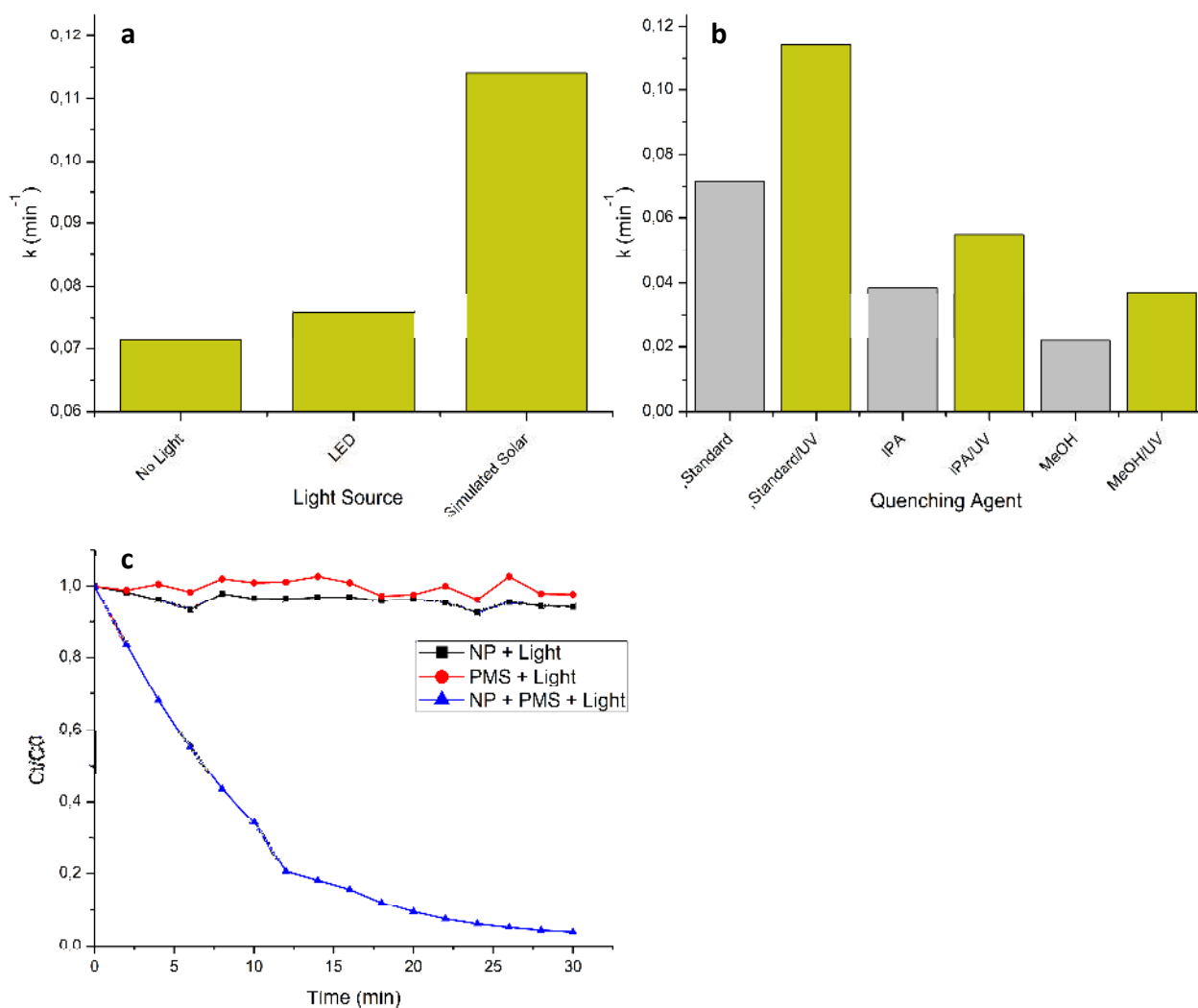
Figure 4.33: The (a) effect of light on the catalytic degradation of Tartrazine dye, (b) the quenching benchmarks of the UV-induced reaction, and (c) the photoinduced degradation kinetics of the azo dye

Based on the aforementioned results and previous reports, the proposed mechanism is shown in Figure 4.34. The enhanced efficiency of Co_3O_4-NPs under UV irradiation is possible due to the excitement of the valence band electrons to its conduction band, thus leaving corresponding holes in the valence band (Eqn 31) (Nagajyothi et al., 2020; Yang et al., 2005). Subsequently, PMS possesses the capability to capture the migrating electrons to generate $SO_4^{\bullet-}$ and reduce the quick recombination of electron-hole pairs (Eqn 32) (Meng et al., 2020). Depicted in equations 33, 34, and 39 are the possible paths the photoinduced holes may follow, where they react with H_2O/OH^-, PMS, or Tart molecules to produce hydroxyl radicals, peroxysulfate radicals, or CO_2 and H_2O as degradation products, respectively (Kohantorabi, Moussavi, Mohammadi, et al., 2021; Mahmoud et al., 2009). Therefore, the separation efficiency of photoinduced electron-hole pairs is effectively improved. Despite the minor role, superoxide radicals were also implicated in the photo-degradation of the azo dye, brought about by dissolved oxygen concentrations (Eqn 35) (Gao et al., 2018). Furthermore, the

activation of PMS through UV irradiation should not be neglected (Eqn 36). However, Figure 4.33-c presents argumentative results, as no degradation was observed after the addition of PMS in the UV system. According to Meng and co-authors (2020), this may have been the outcome of the solar simulator's high optical power density, as the increased presence of photons quenched the reactive oxygen species and decreased the performance. Lastly, in equations 37 – 38, the Tartrazine is inevitably mineralised into carbon dioxide and water after sufficient $SO_4^{\bullet-}$ and $^\bullet OH$ generation.

$$Catalyst + hv \rightarrow Catalyst\ (e_{CB}^- + h_{VB}^+) \tag{31}$$

$$e_{CB}^- + HSO_5^- \rightarrow SO_4^{\bullet-} + OH^- \tag{32}$$

$$h_{VB}^+ + H_2O/OH^- \rightarrow {}^\bullet OH \tag{33}$$

$$h_{VB}^+ + HSO_5^- \rightarrow SO_5^{\bullet-} + H^+ \tag{34}$$

$$e_{CB}^- + O_2 \rightarrow O_2^{\bullet-} \tag{35}$$

$$HSO_5^- + hv \rightarrow SO_4^{\bullet-} + {}^\bullet OH \tag{36}$$

$$SO_4^{\bullet-} + Tartrazine \rightarrow Intermediates \rightarrow CO_2 + H_2O + SO_4^{2-} \tag{37}$$

$${}^\bullet OH + Tartrazine \rightarrow Intermediates \rightarrow CO_2 + H_2O \tag{38}$$

$$h_{VB}^+ + Tartrazine \rightarrow (Tartrazine)^{\bullet+} \rightarrow CO_2 + H_2O \tag{39}$$
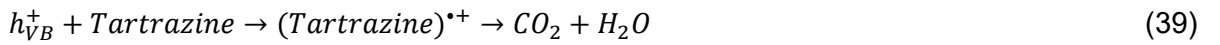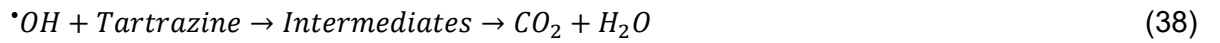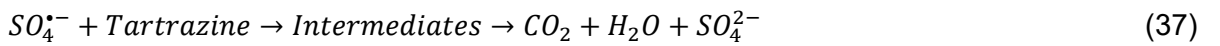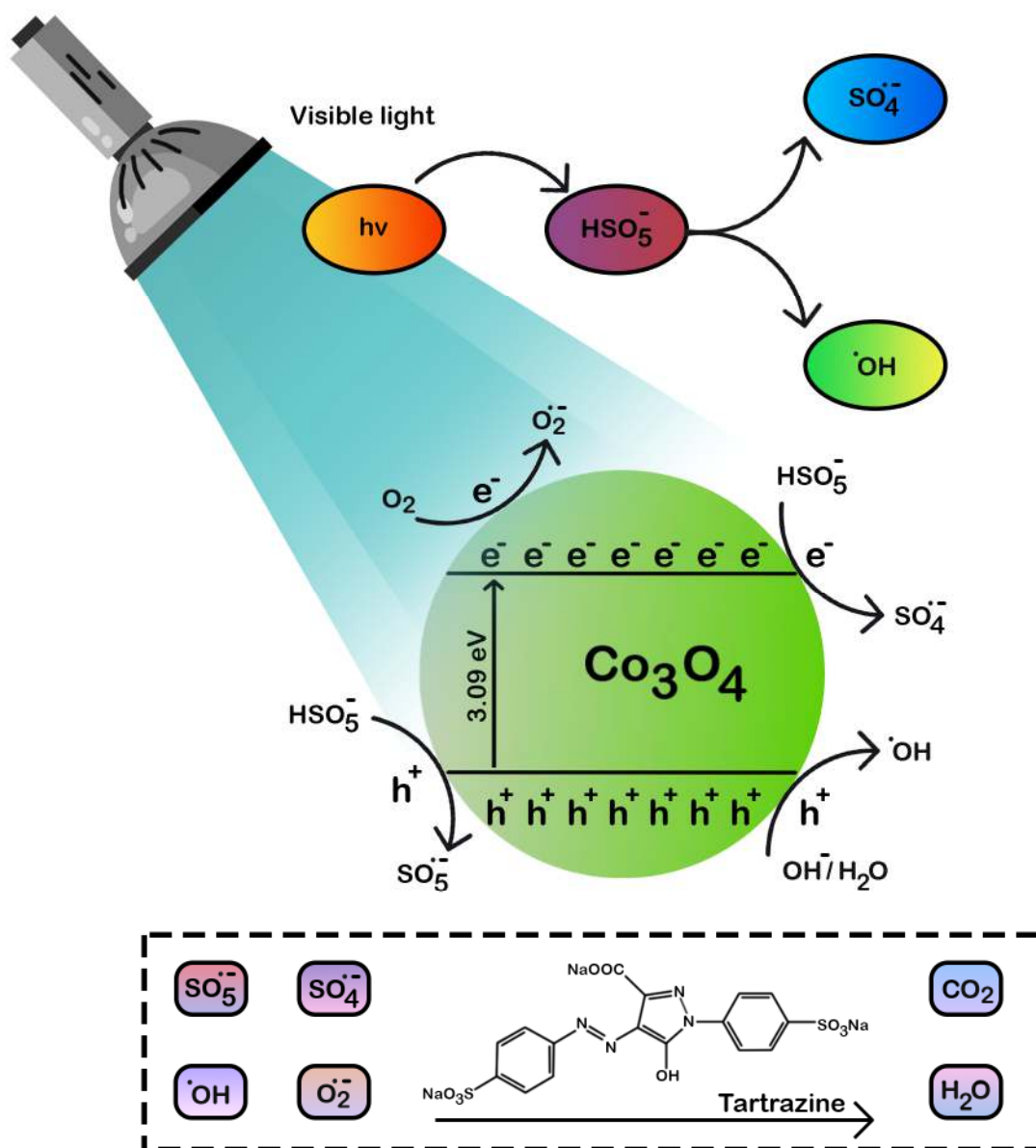
Figure 4.34: The possible mechanisms for the photocatalytic degradation of Tartrazine dye using Co₃O₄ NPs.

4.6.1. Techno-economic Analysis

At ambient temperature, the degradation of Tartrazine dye through Co_3O_4-NP-activated PMS resulted in 89.27% decolourisation within 30 minutes ($k = 0.0713$ min^{-1}), with continuous agitation being the only contributor to the operating costs of the process. On the other hand, the photocatalytic degradation of the azo dye involving the solar simulator exhibited an efficiency of 96.09% within the same period ($k = 0.1141$ min^{-1}). Therefore, this indicates a 6.82% increase in pollutant removal and a 37.60% increase in degradation rate. However, introducing artificial light to the advanced oxidation process is accompanied by additional electricity consumption, increasing operating costs. With a 300 W lamp employed for a 30-minute reaction, the energy expenditure accumulates to 0.15 kWh. In South Africa, the current price of electricity per kWh is R2.558, which brings the lamp's overall operating cost to 38 cents, ultimately deeming the introduction of a UV source an economically viable method for improving the efficiency of the degradation process.

Contrarily, UV irradiation from the sun could negate the need for artificial light sources. Herein, the decolourisation of Tartrazine dye was carried out in direct sunlight, with the weather conditions presented in Table 4.1.

Table 4.1: The apparent weather conditions for the sunlight-assisted degradation of Tartrazine dye.

Time	12:00 - 14:00
Temperature	30°C
UV Index	11
Wind	13 km/h
Precipitation	0 mm
Humidity	45%
Visibility	35 km
Pressure	1013 hPa

The results depicted in Figure 4.35-a and -b demonstrate the substantial influence sunlight has on the degradation of Tartrazine dye, with 97.11% decolourisation in 30 minutes ($k = 0.1306$ min^{-1}). Despite the abundance of UV light, the efficiency of pollutant removal may have also been attributed to the thermal energy introduced by the sun, thereby implementing another enhancing aspect of the degradation process. Therefore, artificial light is entirely replaceable by renewable energy radiating from the sun; however, the limitation of the earth's revolution should still be considered.
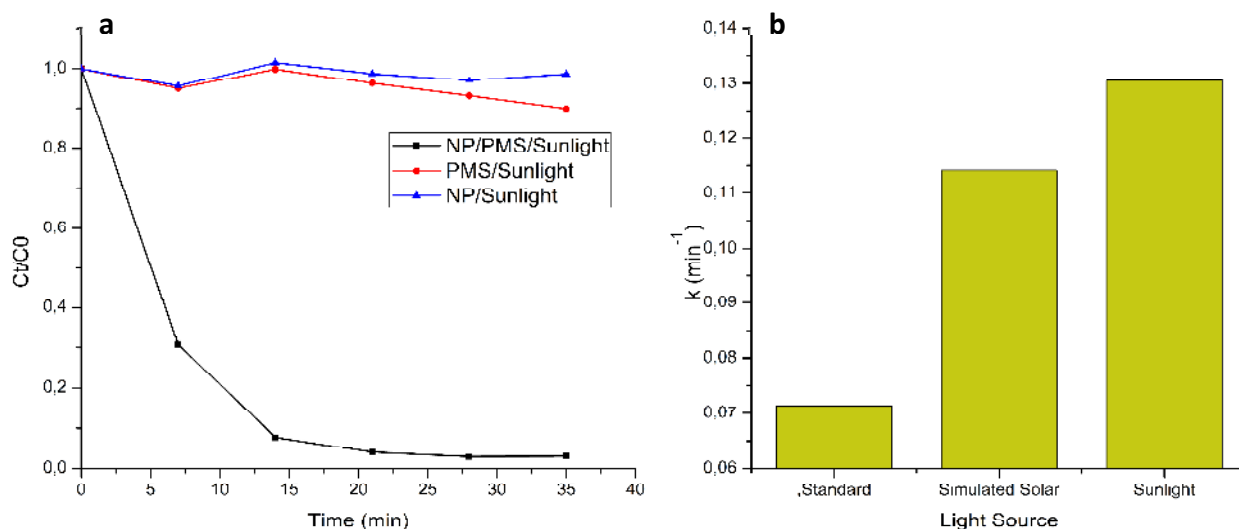
Figure 4.35: The (a) degradation kinetics of Tartrazine dye in direct sunlight and (b) reaction rate constant comparison between simulated solar light and sunlight.

4.7. Conclusion

This chapter has demonstrated the extraction of valuable phytochemicals from spent coffee while retaining potent oxidative capabilities as the extraction mixture successfully reduced metallic ions to form Co_3O_4-NPs. The cobalt oxide nanoparticles were characterised using FTIR, XRD, TEM, and UV-vis techniques, where they were found to be poorly crystalline, with spherical and irregular morphologies that possessed an average size of 29.01 nm. Also, the nanostructures exhibited exceptional catalytic performances against the degradation of Tartrazine dye, further enhanced through the addition of UV irradiation.

Chapter 5

<div align="right">

Conclusion & Future Recommendations

</div>

Herein, the successful synthesis of Co_3O_4-NPs with a remarkable degree of repeatability has been demonstrated, thereby deeming spent coffee an ideal waste material for developing a clean, nontoxic green approach for producing nanoparticles at ambient temperature. The characterisation of the cobalt oxide nanoparticles was accomplished using XRD, TEM, and UV-vis techniques. The XRD pattern displayed a poorly crystalline nanomaterial correlated with the cubic crystal planes of cobalt oxide. The TEM images indicated aggregates of spherical and irregular nanostructures with an average size of 29.01 nm. Moreso, the UV-vis spectrum further confirmed the formation of Co_3O_4-NPs and the band gap energy was calculated to be 3.09 eV.

The catalytic activity of the nanoparticles illustrated a highly efficient Co_3O_4 NP/PMS system, where 89.27% of the Tartrazine dye was degraded within 30 minutes. Throughout the reaction, a maximum of only 0.0001% of the cobalt leached into the solution. Therefore, the toxicity of the nanoparticles had negligible effects. Furthermore, the cobalt oxide nanostructures were not overwhelmed by the mixture of Tartrazine, Methyl orange, and Remazol brilliant red as they retained high decolourisation efficiencies and fast degradation rates, indicating a solid viability for industrial effluent treatment.

After the addition of simulated solar irradiation, the efficiency and rate of Tartrazine removal increased by 6.82 and 37.60%, respectively. Hence, indicating that the nanoparticles were photoactive. However, introducing this aspect required additional operating costs to the procedure. Therefore, sunlight was used as a natural replacement that achieved an overall Tartrazine degradation of 97.11% and a 45.41% increase in reaction rate compared to the standard oxidation process.

In conclusion, the Co_3O_4-NPs presented within this study displayed exceptional catalytic/photocatalytic performance for the remediation of dye-stained water and, due to the availability of the raw material, is an extremely cost-effective and environmentally sustainable procedure that is highly suitable for future industrial implementation.

Recommendations

In order to improve the viability of this study, the following should be considered:

- The use of a nanoparticle growth substrate is suggested to assist in the recovery of the catalyst.
- A sulphur leaching study should be considered.
- The efficiency of the nanoparticles should also be tested in a continuous flow system to simulate traditional wastewater treatment processes.
- A feasibility study for the full scale-up of the degradation process should be contemplated.

Bibliography

Abbasian, R. & Jafarizadeh-Malmiri, H. 2020. Green approach in gold, silver and selenium nanoparticles using coffee bean extract. *Open Agriculture*, 5(1): 761–767. https://doi.org/10.1515/opag-2020-0074.

Abd El-Aziz, A.R., Al-Othman, M.R. & Mahmoud, M.A. 2018. Degradation of DDT by gold nanoparticles synthesised using Lawsonia inermis for environmental safety. *Biotechnology and Biotechnological Equipment*, 0(0): 1–9. https://doi.org/10.1080/13102818.2018.1502051.

Abel, S., Tesfaye, J.L., Shanmugam, R., Dwarampudi, L.P., Lamessa, G., Nagaprasad, N., Benti, M. & Krishnaraj, R. 2021. Green Synthesis and Characterizations of Zinc Oxide (ZnO) Nanoparticles Using Aqueous Leaf Extracts of Coffee (*Coffea arabica*) and Its Application in Environmental Toxicity Reduction S. Rajeshkumar, ed. *Journal of Nanomaterials*, 2021: 3413350. https://doi.org/10.1155/2021/3413350.

Abreu, M.B., Marcheafave, G.G., Bruns, R.E., Scarminio, I.S. & Zeraik, M.L. 2020. Spectroscopic and Chromatographic Fingerprints for Discrimination of Specialty and Traditional Coffees by Integrated Chemometric Methods. *Food Analytical Methods*, 13(12): 2204–2212. https://doi.org/10.1007/s12161-020-01832-1.

Abubakar, A.R. & Haque, M. 2020. Preparation of Medicinal Plants: Basic Extraction and Fractionation Procedures for Experimental Purposes. *Journal of pharmacy & bioallied sciences*, 12(1): 1–10. https://pubmed.ncbi.nlm.nih.gov/32801594.

Achola, L.A., Ghebrehiwet, A., Macharia, J., Kerns, P., He, J., Fee, J., Tinson, C., Shi, J., March, S., Jain, M. & Suib, S.L. 2020. Enhanced visible-light-assisted peroxymonosulfate activation on cobalt-doped mesoporous iron oxide for orange II degradation. *Applied Catalysis B: Environmental*, 263: 118332. https://www.sciencedirect.com/science/article/pii/S0926337319310781.

Adekunle, A., Oyekunle, J., Durosinmi, L., Oluwafemi, O., Dare, S., Akinola, A., Olaoluwa, O., Akinyele, O. & temitope adekunle, A. 2019. Potential of cobalt and cobalt oxide nanoparticles as nanocatalyst towards dyes degradation in wastewater. *Nano-Structures & Nano-Objects*, 21: 100405.

Ahmad, T., Irfan, M., Bustam, M.A. & Bhattacharjee, S. 2016. Effect of Reaction Time on Green Synthesis of Gold Nanoparticles by Using Aqueous Extract of Elaise Guineensis (Oil Palm Leaves). *Procedia Engineering*, 148: 467–472. https://www.sciencedirect.com/science/article/pii/S1877705816309328.

Ahmadi, M. & Ghanbari, F. 2019. Organic dye degradation through peroxymonosulfate catalyzed by reusable graphite felt/ferriferrous oxide: Mechanism and identification of intermediates. *Materials Research Bulletin*, 111: 43–52. https://www.sciencedirect.com/science/article/pii/S0025540818323948.

Ahmed, M.M., Brienza, M., Goetz, V. & Chiron, S. 2014. Solar photo-Fenton using peroxymonosulfate for organic micropollutants removal from domestic wastewater: Comparison with heterogeneous TiO2 photocatalysis. *Chemosphere*, 117: 256–261. https://www.sciencedirect.com/science/article/pii/S0045653514009072 23 April 2019.

Ahmed, S.F., Mofijur, M., Rafa, N., Chowdhury, A.T., Chowdhury, S., Nahrin, M., Islam, A.B.M.S. & Ong, H.C. 2022. Green approaches in synthesising nanomaterials for environmental nanobioremediation: Technological advancements, applications, benefits and challenges. *Environmental Research*, 204: 111967. https://www.sciencedirect.com/science/article/pii/S0013935121012627.

Akhlaghi, N., Najafpour-Darzi, G. & Younesi, H. 2020. Facile and green synthesis of cobalt

oxide nanoparticles using ethanolic extract of Trigonella foenumgraceum (Fenugreek) leaves. *Advanced Powder Technology*, 31(8): 3562–3569. https://www.sciencedirect.com/science/article/pii/S092188312030337X.

Akhtar, M.S., Panwar, J. & Yun, Y.-S. 2013. Biogenic Synthesis of Metallic Nanoparticles by Plant Extracts. *ACS Sustainable Chemistry & Engineering*, 1(6): 591–602. https://doi.org/10.1021/sc300118u.

Akula, R. & Ravishankar, G.A. 2011. Influence of abiotic stress signals on secondary metabolites in plants. *Plant Signaling & Behavior*, 6(11): 1720–1731. https://doi.org/10.4161/psb.6.11.17613.

Al-Radadi, N.S. 2019. Green synthesis of platinum nanoparticles using Saudi's Dates extract and their usage on the cancer cell treatment. *Arabian Journal of Chemistry*, 12(3): 330–349. https://doi.org/10.1016/j.arabjc.2018.05.008.

Alavi, M. 2022. Bacteria and fungi as major bio-sources to fabricate silver nanoparticles with antibacterial activities. *Expert Review of Anti-infective Therapy*, 20(6): 897–906. https://doi.org/10.1080/14787210.2022.2045194.

Alharbi, N.S., Alsubhi, N.S. & Felimban, A.I. 2022. Green synthesis of silver nanoparticles using medicinal plants: Characterization and application. *Journal of Radiation Research and Applied Sciences*, 15(3): 109–124. https://www.sciencedirect.com/science/article/pii/S1687850722082024.

Ali, M. Ben, Barras, A., Addad, A., Sieber, B., Elhouichet, H., Férid, M., Szunerits, S. & Boukherroub, R. 2017. Co2SnO4 nanoparticles as a high performance catalyst for oxidative degradation of rhodamine B dye and pentachlorophenol by activation of peroxymonosulfate. *Physical Chemistry Chemical Physics*, 19(9): 6569–6578. http://dx.doi.org/10.1039/C6CP08576H.

Aliofkhazraei, M. & Ali, N. 2014. PVD Technology in Fabrication of Micro- and Nanostructured Coatings. In S. Hashmi, G. F. Batalha, C. J. Van Tyne, & B. B. T.-C. M. P. Yilbas, eds. Oxford: Elsevier: 49–84. https://www.sciencedirect.com/science/article/pii/B9780080965321007056.

Almadiy, A., Nenaah, G.E. & Shawer, D. 2018. Facile synthesis of silver nanoparticles using harmala alkaloids and their insecticidal and growth inhibitory activities against the khapra beetle. *Journal of Pest Science*, 91: 1–11.

Alrehaily, L.M., Joseph, J.M., Biesinger, M.C., Guzonas, D.A. & Wren, J.C. 2013. Gamma-radiolysis-assisted cobalt oxide nanoparticle formation. *Physical Chemistry Chemical Physics*, 15(3): 1014–1024. http://dx.doi.org/10.1039/C2CP43094K.

Alsamhary, K.I. 2020. Eco-friendly synthesis of silver nanoparticles by Bacillus subtilis and their antibacterial activity. *Saudi Journal of Biological Sciences*, 27(8): 2185–2191. https://www.sciencedirect.com/science/article/pii/S1319562X2030139X.

Altemimi, A., Lakhssassi, N., Baharlouei, A., Watson, D.G. & Lightfoot, D.A. 2017. Phytochemicals: Extraction, Isolation, and Identification of Bioactive Compounds from Plant Extracts. *Plants*, 6(4).

Amendola, V. & Meneghetti, M. 2009. Laser ablation synthesis in solution and size manipulation of noble metal nanoparticles. *Phys. Chem. Chem. Phys.*, 11(20): 3805–3821. http://dx.doi.org/10.1039/B900654K.

Amoruso, S., Bruzzese, R., Spinelli, N., Velotta, R., Vitiello, M., Wang, X., Ausanio, G., Iannotti, V. & Lanotte, L. 2004. Generation of silicon nanoparticles via femtosecond laser ablation in vacuum. *Applied Physics Letters*, 84(22): 4502–4504. https://doi.org/10.1063/1.1757014.

Anastopoulos, I., Hosseini-Bandegharaei, A., Fu, J., Mitropoulos, A.C. & Kyzas, G.Z. 2018. Use of nanoparticles for dye adsorption: Review. *Journal of Dispersion Science and Technology*, 39(6): 836–847. https://doi.org/10.1080/01932691.2017.1398661.

Anigol, L., Charantimath, J. & Gurubasavaraj, P. 2017. Effect of Concentration and pH on the Size of Silver Nanoparticles Synthesized by Green Chemistry. *Organic & Medicinal Chemistry International Journal*, 3(5): 124–128. https://ideas.repec.org/a/adp/jomcij/v3y2017i5p124-128.html 12 September 2022.

Anigol, L.B., Charantimath, J.S. & Gurubasavaraj, P.M. 2017. Effect of Concentration and pH on the Size of Silver Nanoparticles Synthesized by Green Chemistry. *Organic & Medicinal Chem*, 3(5): 1–5.

Anon. 2021. Global Nanotechnology Industry. *Report Linker*. https://www.reportlinker.com/p0326269/Global-Nanotechnology-Industry.html?utm_source=GNW 4 October 2021.

Arbain, R., Othman, M. & Palaniandy, S. 2011. Preparation of iron oxide nanoparticles by mechanical milling. *Minerals Engineering*, 24(1): 1–9. https://www.sciencedirect.com/science/article/abs/pii/S0892687510002244 5 August 2019.

Ariyanta, H.A., Ivandini, T.A. & Yulizar, Y. 2021. Novel NiO nanoparticles via phytosynthesis method: Structural, morphological and optical properties. *Journal of Molecular Structure*, 1227: 129543. https://www.sciencedirect.com/science/article/pii/S0022286020318585.

Arora, N. & Sharma, N.N. 2014. Arc discharge synthesis of carbon nanotubes: Comprehensive review. *Diamond and Related Materials*, 50: 135–150. https://www.sciencedirect.com/science/article/pii/S0925963514001952.

Aryal, S., Baniya, M.K., Danekhu, K., Kunwar, P., Gurung, R. & Koirala, N. 2019. Total Phenolic Content, Flavonoid Content and Antioxidant Potential of Wild Vegetables from Western Nepal. *Plants*, 8(4). /pmc/articles/PMC6524357/ 24 August 2022.

Ashkarran, A.A. 2010. A novel method for synthesis of colloidal silver nanoparticles by arc discharge in liquid. *Current Applied Physics*, 10(6): 1442–1447. https://www.sciencedirect.com/science/article/pii/S1567173910001446 7 August 2019.

Ashkarran, A.A., Iraji zad, A., Mahdavi, S.M. & Ahadian, M.M. 2009. ZnO nanoparticles prepared by electrical arc discharge method in water. *Materials Chemistry and Physics*, 118(1): 6–8. https://www.sciencedirect.com/science/article/abs/pii/S0254058409003848 7 August 2019.

Aziz, W.J. & Jassim, H.A. 2018. A novel study of pH influence on Ag nanoparticles size with antibacterial and antifungal activity using green synthesis. *World Scientific News*, 97(April): 139–152. www.worldscientificnews.com.

Baghaienezhad, M., Boroghani, M. & Anabestani, R. 2020. Silver nanoparticles Synthesis by coffee residues extract and their antibacterial activity. *Nanomedicine Research Journal*, 5(1): 29–34. http://www.nanomedicine-rj.com/article_38643.html.

Bagheri, M., Najafabadi, N.R. & Borna, E. 2019. Removal of reactive blue 203 dye photocatalytic using ZnO nanoparticles stabilized on functionalized MWCNTs. *Journal of King Saud University - Science*. https://www.sciencedirect.com/science/article/pii/S101836471830781X 23 April 2019.

Baig, N., Kammakakam, I. & Falath, W. 2021. Nanomaterials: a review of synthesis methods, properties, recent progress, and challenges. *Materials Advances*, 2(6): 1821–1871. https://pubs.rsc.org/en/content/articlehtml/2021/ma/d0ma00807a 5 October 2021.

Bala, N., Saha, S., Chakraborty, M., Maiti, M., Das, S., Basu, R. & Nandy, P. 2014. Green

synthesis of zinc oxide nanoparticles using Hibiscus subdariffa leaf extract: effect of temperature on synthesis, anti-bacterial activity and anti-diabetic activity. *RSC Advances*, 5(7): 4993–5003. https://pubs.rsc.org/en/content/articlehtml/2015/ra/c4ra12784f 5 September 2022.

Bala, T., Pushpakanth, S., Pasricha, R., Blv, P. & Sastry, M. 2004. Foam-based synthesis of cobalt nanoparticles and their subsequent conversion to CocoreAgshell nanoparticles by a simple transmetallation reaction. *J. Mater. Chem.*, 14: 1057–1061.

Banerjee, A. & Chattopadhyay, S. 2019. Synthesis and characterization of mixed valence cobalt(III)/cobalt(II) complexes with N,O-donor Schiff base ligands. *Polyhedron*, 159: 1–11. https://www.sciencedirect.com/science/article/pii/S0277538718306958.

Bano, S. & Pillai, S. 2020. Green synthesis of calcium oxide nanoparticles at different calcination temperatures. *World Journal of Science, Technology and Sustainable Development*, ahead-of-p.

Bao, Y., He, J., Song, K., Guo, J., Zhou, X. & Liu, S. 2021. Plant-Extract-Mediated Synthesis of Metal Nanoparticles D. Pasini, ed. *Journal of Chemistry*, 2021: 6562687. https://doi.org/10.1155/2021/6562687.

Baptista, A., Silva, F., Porteiro, J., Míguez, J. & Pinto, G. 2018. Sputtering Physical Vapour Deposition (PVD) Coatings: A Critical Review on Process Improvement and Market Trend Demands. *Coatings*, 8(11). https://www.mdpi.com/2079-6412/8/11/402.

Barua, S., Geng, X. & Chen, B. 2020. Graphene-based nanomaterials for healthcare applications. In S. ki B. T.-P. for T. and I. Choi, ed. *Micro and Nano Technologies*. Elsevier: 45–81. https://www.sciencedirect.com/science/article/pii/B9780128178409000035.

Baruwati, B., Kumar, D.K. & Manorama, S. V. 2006. Hydrothermal synthesis of highly crystalline ZnO nanoparticles: A competitive sensor for LPG and EtOH. *Sensors and Actuators B: Chemical*, 119(2): 676–682. https://www.sciencedirect.com/science/article/pii/S0925400506000463 12 August 2019.

Becker, M.F., Brock, J.R., Cai, H., Henneke, D.E., Keto, J.W., Lee, J., Nichols, W.T. & Glicksman, H.D. 1998. Metal nanoparticles generated by laser ablation. *Nanostructured Materials*, 10(5): 853–863. https://www.sciencedirect.com/science/article/pii/S0965977398001214 6 August 2019.

Behera, A., Mallick, P. & Mohapatra, S.S. 2020. Nanocoatings for anticorrosion: An introduction. In S. Rajendran, T. A. N. H. Nguyen, S. Kakooei, M. Yeganeh, & Y. B. T.-C. P. at the N. Li, eds. *Micro and Nano Technologies*. Elsevier: 227–243. https://www.sciencedirect.com/science/article/pii/B9780128193594000131.

Behravan, M., Hossein Panahi, A., Naghizadeh, A., Ziaee, M., Mahdavi, R. & Mirzapour, A. 2019. Facile green synthesis of silver nanoparticles using Berberis vulgaris leaf and root aqueous extract and its antibacterial activity. *International Journal of Biological Macromolecules*, 124: 148–154. https://doi.org/10.1016/j.ijbiomac.2018.11.101.

Benchettara, Abdelhakim & Benchettara, Abdelkader. 2015. Electrochemical Sensor Based on Nanoparticles of Cobalt Oxides for Determination of Glucose. *Materials Today: Proceedings*, 2(8): 4212–4216. https://www.sciencedirect.com/science/article/pii/S2214785315007890 8 April 2019.

Benelmekki, M. 2015. An introduction to nanoparticles and nanotechnology. In *Designing Hybrid Nanoparticles*. 2053-2571. Morgan & Claypool Publishers: 1–14. http://dx.doi.org/10.1088/978-1-6270-5469-0ch1.

Benkhaya, S., M'rabet, S. & El Harfi, A. 2020. Classifications, properties, recent synthesis

and applications of azo dyes. *Heliyon*, 6(1): e03271.
https://www.sciencedirect.com/science/article/pii/S240584402030116X.

Bera, D., Kuiry, S.C., McCutchen, M., Kruize, A., Heinrich, H., Meyyappan, M. & Seal, S.
2004. In-situ synthesis of palladium nanoparticles-filled carbon nanotubes using arc-
discharge in solution. *Chemical Physics Letters*, 386(4–6): 364–368.
https://www.sciencedirect.com/science/article/abs/pii/S0009261404001526 7 August
2019.

Beyene, A. & Sabally, K. 2013. Determination of Chlorogenic Acids (CGA) in Coffee Beans
using HPLC. , 2013: 78–91.

Bharadwaj, M.S., Prem, K., Satyanandam, K. & Raju, A.I. 2016. Green Synthesis of Iron
Nanoparticles using Albizia lebbeck leaves for Synthetic Dyes decolorization. *Int. J. Sci.
Eng. Technol. Research*, 5(12): 3429–3434.

Bhargava, R., Khan, S., Ahmad, N. & Ansari, M.M.N. 2018. Investigation of structural, optical
and electrical properties of Co3O4 nanoparticles. *AIP Conference Proceedings*,
1953(1): 30034. https://aip.scitation.org/doi/abs/10.1063/1.5032369.

Bhatnagar, S., Goel, A., Sharma, B. & Satz, S. 2014. Biosynthesis of manganese oxide
nanoparticles using Lawsonia innermis extract and their effect on the growth of Cicer
Arietinum. *Journal of Nanomedicine & Nanotechnology*, 05(05): 5.
https://www.walshmedicalmedia.com/proceedings/biosynthesis-of-manganese-oxide-
nanoparticles-using-lawsonia-innermis-extract-and-their-effect-on-the-growth-of-cicer-
arietinum-26675.html 20 November 2022.

Biacuana, G. 2017. OPINION: Leveraging off South Africa's growing coffee culture | IOL
Business Report. *Business Report*. https://www.iol.co.za/business-report/opinion-
leveraging-off-south-africas-growing-coffee-culture-11549580 17 April 2019.

Bibi, I., Nazar, N., Iqbal, M., Kamal, S., Nawaz, H., Nouren, S., Safa, Y., Jilani, K., Sultan, M.,
Ata, S., Rehman, F. & Abbas, M. 2017. Green and eco-friendly synthesis of cobalt-oxide
nanoparticle: Characterization and photo-catalytic activity. *Advanced Powder
Technology*, 28(9): 2035–2043.
https://www.sciencedirect.com/science/article/pii/S0921883117302121.

Biswas, P. & Wu, C.-Y. 2005. Nanoparticles and the Environment. *Journal of the Air & Waste
Management Association*, 55(6): 708–746.
https://doi.org/10.1080/10473289.2005.10464656.

Van Boekel, M.A.J.S. 2006. Formation of flavour compounds in the Maillard reaction.
Biotechnology Advances, 24(2): 230–233.

Bogireddy, N.K.R., Martinez Gomez, L., Osorio-Roman, I. & Agarwal, V. 2017. Synthesis of
gold nanoparticles using Coffea Arabica fruit extract. *Advances in Nano Research*, 5(3).

Bogireddy, N.K.R., Pal, U., Gomez, L.M. & Agarwal, V. 2018. Size controlled green synthesis
of gold nanoparticles using Coffea arabica seed extract and their catalytic performance
in 4-nitrophenol reduction. *RSC Advances*, 8(44): 24819–24826.

Bomatí-Miguel, O., Mazeina, L., Navrotsky, A. & Veintemillas-Verdaguer, S. 2008.
Calorimetric Study of Maghemite Nanoparticles Synthesized by Laser-Induced
Pyrolysis. *Chemistry of Materials*, 20(2): 591–598. https://doi.org/10.1021/cm071178o.

Boone, D.H. 1986. Physical vapour deposition processes. *Materials Science and
Technology*, 2(3): 220–224. https://doi.org/10.1179/mst.1986.2.3.220.

Böttger, A., Vothknecht, U., Bolle, C. & Wolf, A. 2018. *Lessons on caffeine, cannabis & Co.*
http://link.springer.com/10.1007/978-3-319-99546-5.

Bouzayani, B., Rosales, E., Pazos, M., Elaoud, S.C. & Sanromán, M.A. 2019. Homogeneous and heterogeneous peroxymonosulfate activation by transition metals for the degradation of industrial leather dye. *Journal of Cleaner Production*, 228: 222–230. https://www.sciencedirect.com/science/article/pii/S0959652619313046.

Boyadzhieva, S., Angelov, G., Georgieva, S. & Yankov, D. 2018. Characterization of polyphenol content and antioxidant capacity of spent coffee grounds. *Bulgarian Chemical Communications*, 50.

Bravo, J., Juániz, I., Monente, C., Caemmerer, B., Kroh, L.W., De Peña, M.P. & Cid, C. 2012. Evaluation of spent coffee obtained from the most common coffeemakers as a source of hydrophilic bioactive compounds. *Journal of agricultural and food chemistry*, 60(51): 12565–12573. https://pubmed.ncbi.nlm.nih.gov/23214450/ 29 August 2022.

Brienza, M. & Katsoyiannis, I.A. 2017. Sulfate Radical Technologies as Tertiary Treatment for the Removal of Emerging Contaminants from Wastewater. *Sustainability* , 9(9).

Brienza, M., Mahdi Ahmed, M., Escande, A., Plantard, G., Scrano, L., Chiron, S., A. Bufo, S. & Goetz, V. 2014. Relevance of a photo-Fenton like technology based on peroxymonosulphate for 17β-estradiol removal from wastewater. *Chemical Engineering Journal*, 257: 191–199. https://www.sciencedirect.com/science/article/pii/S1385894714009516 23 April 2019.

Brown, P. 2018. Cobalt transition metal Chemistry cobalt(II)Co2+ complex ions stabilised ligand substitution cobalt(III) Co3+ complexes redox chemical reactions +2 +3 principal oxidation states GCE AS A2 IB A level inorganic chemistry revision notes. http://www.docbrown.info/page07/transition07Co.htm 25 April 2019.

Budryn, G., Nebesny, E. & Oracz, J. 2015. Correlation Between the Stability of Chlorogenic Acids, Antioxidant Activity and Acrylamide Content in Coffee Beans Roasted in Different Conditions. *International Journal of Food Properties*, 18(2): 290–302. https://doi.org/10.1080/10942912.2013.805769.

Burger, T. 2018. Coffee Industry Focus: Want To Open A Coffee Shop? | JTB Consulting. *JTB Consulting*. http://jtbconsulting.co.za/coffee-industry-want-to-open-a-coffee-shop/ 17 April 2019.

Cai, C., Zhang, H., Zhong, X. & Hou, L. 2015. Ultrasound enhanced heterogeneous activation of peroxymonosulfate by a bimetallic Fe–Co/SBA-15 catalyst for the degradation of Orange II in water. *Journal of Hazardous Materials*, 283: 70–79. https://www.sciencedirect.com/science/article/pii/S030438941400716X.

Calle, L.C. & López, M.E.L. 2017. Green synthesis of silver nanoparticles using green coffee bean extract. *IFMBE Proceedings*, 60(February): 217–220.

Cao, X., Zhu, L., Bai, Y., Li, F. & Yu, X. 2022. Green one-step synthesis of silver nanoparticles and their biosafety and antibacterial properties. *Green Chemistry Letters and Reviews*, 15(1): 28–34. https://doi.org/10.1080/17518253.2021.2018506.

Castro-Longoria, E., Vilchis-Nestor, A.R. & Avalos-Borja, M. 2011. Biosynthesis of silver, gold and bimetallic nanoparticles using the filamentous fungus Neurospora crassa. *Colloids and surfaces. B, Biointerfaces*, 83(1): 42–48. https://pubmed.ncbi.nlm.nih.gov/21087843/ 18 April 2022.

Chauhan, A., Anand, J., Parkash, V. & Rai, N. 2022. Biogenic synthesis: a sustainable approach for nanoparticles synthesis mediated by fungi. *Inorganic and Nano-Metal Chemistry*: 1–14. https://doi.org/10.1080/24701556.2021.2025078.

Chekin, F., Vahdat, S.M. & Asadi, M.J. 2016. Green synthesis and characterization of cobalt oxide nanoparticles and its electrocatalytic behavior. *Russian Journal of Applied*

Chemistry, 89(5): 816–822. https://doi.org/10.1134/S1070427216050219.

Cheng, X., Li, P., Liu, W., Luo, C., Wu, D., Zhou, W., Zheng, L., Zhu, X. & Liang, H. 2020. Activation of peroxymonosulfate by metal oxide nanoparticles for mitigating organic membrane fouling in surface water treatment. *Separation and Purification Technology*, 246: 116935. https://www.sciencedirect.com/science/article/pii/S138358662031409X.

Chhabra, V., Pillai, V., Mishra, B.K., Morrone, A. & Shah, D.O. 1995. Synthesis, Characterization, and Properties of Microemulsion-Mediated Nanophase TiO2 Particles. *Langmuir*, 11(9): 3307–3311. https://doi.org/10.1021/la00009a007.

Chien, H., Kuo, C., Kao, L., Lin, G. & Chen, P. 2019. Polysaccharidic spent coffee grounds for silver nanoparticle immobilization as a green and highly efficient biocide. *International journal of biological macromolecules*, 140: 168–176. https://pubmed.ncbi.nlm.nih.gov/31422193/ 30 September 2021.

Chin, P.P., Ding, J., Yi, J.B. & Liu, B.H. 2005. Synthesis of FeS2 and FeS nanoparticles by high-energy mechanical milling and mechanochemical processing. *Journal of Alloys and Compounds*, 390(1–2): 255–260. https://www.sciencedirect.com/science/article/abs/pii/S0925838804010783 5 August 2019.

Chirinos, R., Rogez, H., Campos, D., Pedreschi, R. & Larondelle, Y. 2007. Optimization of extraction conditions of antioxidant phenolic compounds from mashua (Tropaeolum tuberosum Ruíz & Pavón) tubers. *Separation and Purification Technology*, 55(2): 217–225. https://www.sciencedirect.com/science/article/pii/S1383586606004151.

Chiu, H.-C. & Yeh, C.-S. 2007. Hydrothermal Synthesis of SnO2 Nanoparticles and Their Gas-Sensing of Alcohol. *The Journal of Physical Chemistry C*, 111(20): 7256–7259. https://doi.org/10.1021/jp0688355.

Choi, W.K., Liew, T.H., Chew, H.G., Zheng, F., Thompson, C.V., Wang, Y., Hong, M.H., Wang, X.D., Li, L. & Yun, J. 2008. A Combined Top-Down and Bottom-Up Approach for Precise Placement of Metal Nanoparticles on Silicon. *Small*, 4(3): 330–333. https://doi.org/10.1002/smll.200700728.

Choi, W.Y., Lee, D.K., Kim, H.-T., Choi, J.W. & Lee, J.W. 2019. Cobalt oxide-porous carbon composite derived from CO2 for the enhanced performance of lithium-ion battery. *Journal of CO2 Utilization*, 30: 28–37. https://www.sciencedirect.com/science/article/pii/S221298201830948X 17 April 2019.

Chorkendorff, I. & Niemantsverdriet, H. 2005. Concepts of modern catalysis and kinetics. *SERBIULA (sistema Librum 2.0)*.

Chou, W.-L., Wang, C.-T., Huang, K.-Y., Chang, Y.-C. & Shu, C.M. 2012. Investigation of indium ions removal from aqueous solutions using spent coffee grounds. *International journal of physical sciences*, 7: 2445–2454.

Chowdhury, M., Oputu, O., Kebede, M., Cummings, F., Cespedes, O., Maelsand, A. & Fester, V. 2015. Rapid and large-scale synthesis of Co3O4 octahedron particles with very high catalytic activity, good supercapacitance and unique magnetic properties. *RSC Advances*, 5: 104991–105002.

Chung, K.-T. 2016. Azo dyes and human health: A review. *Journal of Environmental Science and Health, Part C*, 34(4): 233–261. https://doi.org/10.1080/10590501.2016.1236602.

Craig, A.P., Franca, A.S. & Oliveira, L.S. 2011. Discrimination between immature and mature green coffees by attenuated total reflectance and diffuse reflectance Fourier transform infrared spectroscopy. *Journal of food science*, 76(8). https://pubmed.ncbi.nlm.nih.gov/22417580/ 22 August 2022.

Craig, A.P., Franca, A.S., Oliveira, L.S., Irudayaraj, J. & Ileleji, K. 2015. Fourier transform infrared spectroscopy and near infrared spectroscopy for the quantification of defects in roasted coffees. *Talanta*, 134: 379–386. https://www.sciencedirect.com/science/article/pii/S0039914014009308.

Crista, D.M.A., El Mragui, A., Algarra, M., Esteves da Silva, J.C.G., Luque, R. & Pinto da Silva, L. 2020. Turning Spent Coffee Grounds into Sustainable Precursors for the Fabrication of Carbon Dots. *Nanomaterials (Basel, Switzerland)*, 10(6): 1209. https://pubmed.ncbi.nlm.nih.gov/32575837.

Cukic, T., Holena, M., Linke, D., Herein, D. & Dingerdissen, U. 2006. Approaching the preparation of Pd-Al2O3 catalyst systematically: one step closer to reproducible catalyst synthesis. In E. M. Gaigneaux, M. Devillers, D. E. De Vos, S. Hermans, P. A. Jacobs, J. A. Martens, & P. B. T.-S. in S. S. and C. Ruiz, eds. *Scientific Bases for the Preparation of Heterogeneous Catalysts*. Elsevier: 195–202. https://www.sciencedirect.com/science/article/pii/S0167299106809079.

Cunha, F.A., Cunha, M. da C.S.O., da Frota, S.M., Mallmann, E.J.J., Freire, T.M., Costa, L.S., Paula, A.J., Menezes, E.A. & Fechine, P.B.A. 2018. Biogenic synthesis of multifunctional silver nanoparticles from Rhodotorula glutinis and Rhodotorula mucilaginosa: antifungal, catalytic and cytotoxicity activities. *World journal of microbiology & biotechnology*, 34(9). https://pubmed.ncbi.nlm.nih.gov/30084085/ 18 April 2022.

Dai, Y., Peng, Q., Liu, K., Tang, X., Zhou, M., Jiang, K. & Zhu, B. 2021. Activation of Peroxymonosulfate by Chrysotile to Degrade Dyes in Water: Performance Enhancement and Activation Mechanism. *Minerals*, 11(4).

Damonte, L.C., Mendoza Zélis, L.A., Marí Soucase, B. & Hernández Fenollosa, M.A. 2004. Nanoparticles of ZnO obtained by mechanical milling. *Powder Technology*, 148(1): 15–19. https://www.sciencedirect.com/science/article/pii/S0032591004003572 5 August 2019.

Daou, T.J., Pourroy, G., Bégin-Colin, S., Grenèche, J.M., Ulhaq-Bouillet, C., Legaré, P., Bernhardt, P., Leuvrey, C. & Rogez, G. 2006. Hydrothermal Synthesis of Monodisperse Magnetite Nanoparticles. *Chemistry of Materials*, 18(18): 4399–4404. https://doi.org/10.1021/cm060805r.

Das, R.K., Pachapur, V.L., Lonappan, L., Naghdi, M., Pulicharla, R., Maiti, S., Cledon, M., Dalila, L.M.A., Sarma, S.J. & Brar, S.K. 2017. Biological synthesis of metallic nanoparticles: plants, animals and microbial aspects. *Nanotechnology for Environmental Engineering*, 2(1): 18. https://doi.org/10.1007/s41204-017-0029-4.

Deljou, A. & Goudarzi, S. 2016. Green extracellular synthesis of the silver nanoparticles using Thermophilic Bacillus Sp. AZ1 and its antimicrobial activity against several human pathogenetic bacteria. *Iranian Journal of Biotechnology*, 14(2): 25–32.

Dewi, N.O.M., Yulizar, Y. & Bagus Apriandanu, D.O. 2019. Green synthesis of Co3O4 nanoparticles using Euphorbia heterophylla L. leaves extract: Characterization and photocatalytic activity. *IOP Conference Series: Materials Science and Engineering*, 509(1).

Dhand, V., Soumya, L., Bharadwaj, S., Chakra, S., Bhatt, D. & Sreedhar, B. 2016. Green synthesis of silver nanoparticles using Coffea arabica seed extract and its antibacterial activity. *Materials Science and Engineering C*, 58(November 2017): 36–43. http://dx.doi.org/10.1016/j.msec.2015.08.018.

Díaz-Hernández, G., Alvarez-Fitz, P., Maldonado-Astudillo, Y., Jiménez-Hernández, J., Parra-Rojas, I., Flores-Alfaro, E., Salazar, R. & Ramírez, M. 2022. Antibacterial, Antiradical and Antiproliferative Potential of Green, Roasted, and Spent Coffee Extracts.

Applied Sciences, 12: 1938.

Dihom, H.R., Al-Shaibani, M.M., Radin Mohamed, R.M.S., Al-Gheethi, A.A., Sharma, A. & Khamidun, M.H. Bin. 2022. Photocatalytic degradation of disperse azo dyes in textile wastewater using green zinc oxide nanoparticles synthesized in plant extract: A critical review. *Journal of Water Process Engineering*, 47: 102705. https://www.sciencedirect.com/science/article/pii/S2214714422001489.

Divekar, P., Narayana, S., Divekar, B., Kumar, R., Gowda G, B., Ray, A., Singh, Achuit, Rani, V., Singh, V., Singh, Akhilesh, Kumar, A., Singh, R., Meena, R. & Behera, T. 2022. Plant Secondary Metabolites as Defense Tools against Herbivores for Sustainable Crop Protection. *International Journal of Molecular Sciences*, 23: 2690.

Diviš, P., Pořízka, J. & Křikala, J. 2019. The effect of coffee beans roasting on its chemical composition. *Potravinarstvo*, 13: 344–350.

Do, Q.D., Angkawijaya, A.E., Tran-Nguyen, P.L., Huynh, L.H., Soetaredjo, F.E., Ismadji, S. & Ju, Y.H. 2014. Effect of extraction solvent on total phenol content, total flavonoid content, and antioxidant activity of Limnophila aromatica. *Journal of Food and Drug Analysis*, 22(3): 296–302. http://dx.doi.org/10.1016/j.jfda.2013.11.001.

Dobrucka, R. 2019. Biofabrication of platinum nanoparticles using Fumariae herba extract and their catalytic properties. *Saudi Journal of Biological Sciences*, 26(1): 31–37. http://dx.doi.org/10.1016/j.sjbs.2016.11.012.

Dobrucka, R. 2016. Synthesis and Structural Characteristic of Platinum Nanoparticles Using Herbal Bidens Tripartitus Extract. *Journal of Inorganic and Organometallic Polymers and Materials*, 26(1): 219–225.

Dobrucka, R. & Długaszewska, J. 2016. Biosynthesis and antibacterial activity of ZnO nanoparticles using Trifolium pratense flower extract. *Saudi Journal of Biological Sciences*, 23(4): 517–523. http://dx.doi.org/10.1016/j.sjbs.2015.05.016.

Dolgaev, S.I., Simakin, A.V., Voronov, V.V., Shafeev, G.A. & Bozon-Verduraz, F. 2002. Nanoparticles produced by laser ablation of solids in liquid environment. *Applied Surface Science*, 186(1–4): 546–551. https://www.sciencedirect.com/science/article/pii/S0169433201006341 6 August 2019.

Dorta, E., Lobo, M.G. & Gonzalez, M. 2012. Reutilization of Mango Byproducts: Study of the Effect of Extraction Solvent and Temperature on Their Antioxidant Properties. *Journal of Food Science*, 77(1): C80–C88. https://doi.org/10.1111/j.1750-3841.2011.02477.x.

Drummer, S., Madzimbamuto, T. & Chowdhury, M. 2021. Green Synthesis of Transition-Metal Nanoparticles and Their Oxides: A Review. *Materials*, 14(11). https://www.mdpi.com/1996-1944/14/11/2700.

Dubey, J. & Singh, A. 2019. Green Synthesis of TiO 2 Nanoparticles Using Extracts of Pomegranate Peels for Pharmaceutical Application. , 9(1): 85–87.

Dubey, S., Kumar, J., Kumar, A. & Sharma, Y.C. 2018. Facile and green synthesis of highly dispersed cobalt oxide (Co3O4) nano powder: Characterization and screening of its eco-toxicity. *Advanced Powder Technology*, 29(11): 2583–2590. https://doi.org/10.1016/j.apt.2018.03.009.

Dung, N.T., Thu, T.V., Van Nguyen, T., Thuy, B.M., Hatsukano, M., Higashimine, K., Maenosono, S. & Zhong, Z. 2020. Catalytic activation of peroxymonosulfate with manganese cobaltite nanoparticles for the degradation of organic dyes. *RSC Advances*, 10(7): 3775–3788. http://dx.doi.org/10.1039/C9RA10169A.

Dutta, A. 2021. The coffee trend in South Africa. *CoffeeBI*. https://coffeebi.com/2021/01/12/the-coffee-trend-in-south-africa/ 30 March 2022.

Ealia, S.A.M. & Saravanakumar, M.P. 2017. A review on the classification, characterisation, synthesis of nanoparticles and their application. , 263: 32019. https://doi.org/10.1088/1757-899x/263/3/032019.

Ebrahimi, K., Shiravand, S. & Mahmoudvand, H. 2017. Biosynthesis of copper nanoparticles using aqueous extract of Capparis spinosa fruit and investigation of its antibacterial activity. *Marmara Pharmaceutical Journal*, 21(4): 866–871.

Ebrahiminezhad, A., Zare-Hoseinabadi, A., Sarmah, A.K., Taghizadeh, S., Ghasemi, Y. & Berenjian, A. 2018. Plant-Mediated Synthesis and Applications of Iron Nanoparticles. *Molecular Biotechnology*, 60(2): 154–168. https://doi.org/10.1007/s12033-017-0053-4.

Ehrampoush, M.H., Miria, M., Salmani, M.H. & Mahvi, A.H. 2015. Cadmium removal from aqueous solution by green synthesis iron oxide nanoparticles with tangerine peel extract. *Journal of environmental health science & engineering*, 13(1). https://pubmed.ncbi.nlm.nih.gov/26682059/ 7 September 2022.

El-Desouky, N., Shoueir, K., El-Mehasseb, I. & El-Kemary, M. 2022. Synthesis of silver nanoparticles using bio valorization coffee waste extract: photocatalytic flow-rate performance, antibacterial activity, and electrochemical investigation. *Biomass Conversion and Biorefinery*. https://doi.org/10.1007/s13399-021-02256-5.

El-Sayyad, G.S., Mosallam, F.M. & El-Batal, A.I. 2018. One-pot green synthesis of magnesium oxide nanoparticles using Penicillium chrysogenum melanin pigment and gamma rays with antimicrobial activity against multidrug-resistant microbes. *Advanced Powder Technology*, 29(11): 2616–2625. https://www.sciencedirect.com/science/article/pii/S0921883118303169.

Elavazhagan, T. & Arunachalam, K.D. 2011. Memecylon edule leaf extract mediated green synthesis of silver and gold nanoparticles. *International journal of nanomedicine*, 6: 1265–1278.

ELEMIKE, E.E., ONWUDIWE, D.C., ARIJEH, O. & NWANKWO, H.U. 2017. Plant-mediated biosynthesis of silver nanoparticles by leaf extracts of Lasienthra africanum and a study of the influence of kinetic parameters. *Bulletin of Materials Science*, 40(1): 129–137. https://doi.org/10.1007/s12034-017-1362-8.

Esmaeili, S., Dehvari, M. & Babaei, A. 2019. Degradation of Acid Orange 7 Dye with PMS and H2O2 Activated by CoFe2O4/PAC Nanocomposite. *Archives of Hygiene Sciences*, 8: 35–45.

Ettadili, F.E., Aghris, S., Laghrib, F., Farahi, A., Saqrane, S., Bakasse, M., Lahrich, S. & El Mhammedi, M.A. 2022. Recent advances in the nanoparticles synthesis using plant extract: Applications and future recommendations. *Journal of Molecular Structure*, 1248: 131538. https://www.sciencedirect.com/science/article/pii/S0022286021016665.

Fahmy, S.A., Fawzy, I.M., Saleh, B.M., Issa, M.Y., Bakowsky, U. & Azzazy, H.M.E.-S. 2021. Green Synthesis of Platinum and Palladium Nanoparticles Using Peganum harmala L. Seed Alkaloids: Biological and Computational Studies. *Nanomaterials*, 11(4). https://www.mdpi.com/2079-4991/11/4/965.

Fan, S., Li, X., Qin, M., Mu, J., Wang, L., Gan, G., Wang, X. & Chen, A. 2019. Rational Design of Peroxymonosulfate Activation and Photoinduced Catalysis Tandem Systems for Artificial Conversion of Solar Light to Chemical Energy. *ACS Omega*, 4: 4113–4128.

Fang, F., Kennedy, J., Manikandan, E., Futter, J. & Markwitz, A. 2012. Morphology and characterization of TiO2 nanoparticles synthesized by arc discharge. *Chemical Physics Letters*, 521: 86–90. https://www.sciencedirect.com/science/article/abs/pii/S0009261411014266 7 August 2019.

Farah, A. & Donangelo, C.M. 2006. Phenolic compounds in coffee. *Brazilian Journal of Plant Physiology*, 18(1): 23–36.

Farida, B., R, D., Cadot, Y. & Seridi, R. 2014. Optimization of extraction parameters of phenolic compounds from Algerian fresh table grapes, (Vitis Vinifera). *International food research journal*, 21 (3): 1025-1029.

Farooq, U., Wang, F., Shahzad, M.K., Carroll, K.C., Lyu, S. & Wang, X. 2022. Study the activation mechanism of peroxymonosulfate in iron copper systems for trichloroethane degradation. *Chemical Engineering Journal Advances*, 11: 100343. https://www.sciencedirect.com/science/article/pii/S266682112200103X.

Farrag, H.M.M., Mostafa, F.A.A.M., Mohamed, M.E. & Huseein, E.A.M. 2020. Green biosynthesis of silver nanoparticles by Aspergillus niger and its antiamoebic effect against Allovahlkampfia spelaea trophozoite and cyst. *Experimental Parasitology*, 219: 108031. https://www.sciencedirect.com/science/article/pii/S0014489420302174.

Fatimah, I., Pradita, R.Y. & Nurfalinda, A. 2016. Plant Extract Mediated of ZnO Nanoparticles by Using Ethanol Extract of Mimosa Pudica Leaves and Coffee Powder. *Procedia Engineering*, 148: 43–48. http://dx.doi.org/10.1016/j.proeng.2016.06.483.

Fernández, J.G., Fernández-Baldo, M.A., Berni, E., Camí, G., Durán, N., Raba, J. & Sanz, M.I. 2016. Production of silver nanoparticles using yeasts and evaluation of their antifungal activity against phytopathogenic fungi. *Process Biochemistry*, 51(9): 1306–1313. https://www.sciencedirect.com/science/article/pii/S1359511316301441.

Fierascu, I.C., Fierascu, I., Fierascu, R.C., Velescu, B.S. & Dinu-Pirvu, C.E. 2022. Natural Sources of Plant Secondary Metabolites and the Role of Plant Polyphenols in the Green Photosynthesis of Metallic Nanoparticles BT - Plant Secondary Metabolites: Physico-Chemical Properties and Therapeutic Applications. In A. K. Sharma & A. Sharma, eds. Singapore: Springer Nature Singapore: 47–75. https://doi.org/10.1007/978-981-16-4779-6_2.

Figgemeier, E., Kylberg, W., Constable, E., Scarisoreanu, M., Alexandrescu, R., Morjan, I., Soare, I., Birjega, R., Popovici, E., Fleaca, C., Gavrila-Florescu, L. & Prodan, G. 2007. Titanium dioxide nanoparticles prepared by laser pyrolysis: Synthesis and photocatalytic properties. *Applied Surface Science*, 254(4): 1037–1041. https://www.sciencedirect.com/science/article/pii/S0169433207012238 13 August 2019.

Firoozi, S., Jamzad, M. & Yari, M. 2016. Biologically synthesized silver nanoparticles by aqueous extract of Satureja intermedia C.A. Mey and the evaluation of total phenolic and flavonoid contents and antioxidant activity. *Journal of Nanostructure in Chemistry*, 6(4): 357–364. https://doi.org/10.1007/s40097-016-0207-0.

Flores-Valdez, M., Meza-Márquez, O.G., Osorio-Revilla, G. & Gallardo-Velázquez, T. 2020. Identification and Quantification of Adulterants in Coffee (Coffea arabica L.) Using FT-MIR Spectroscopy Coupled with Chemometrics. *Foods*, 9(7). /pmc/articles/PMC7404773/ 22 August 2022.

Fujioka, K. & Shibamoto, T. 2008. Chlorogenic acid and caffeine contents in various commercial brewed coffees. *Food Chemistry*, 106(1): 217–221. https://www.sciencedirect.com/science/article/pii/S0308814607005316.

Galvez, A., Herlin-Boime, N., Reynaud, C., Clinard, C. & Rouzaud, J.-N. 2002. Carbon nanoparticles from laser pyrolysis. *Carbon*, 40(15): 2775–2789. https://www.sciencedirect.com/science/article/pii/S0008622302001951 13 August 2019.

Gao, H., Yang, H., Xu, J., Zhang, S. & Li, J. 2018. Strongly Coupled g-C3N4 Nanosheets-Co3O4 Quantum Dots as 2D/0D Heterostructure Composite for Peroxymonosulfate Activation. *Small*, 14(31): 1801353. https://doi.org/10.1002/smll.201801353.

Gao, Q., Wang, G., Chen, Y., Han, B., Xia, K. & Zhou, C. 2021. Utilizing cobalt-doped materials as heterogeneous catalysts to activate peroxymonosulfate for organic pollutant degradation: a critical review. *Environmental Science: Water Research & Technology*, 7(7): 1197–1211. http://dx.doi.org/10.1039/D0EW01042A.

Gardea-Torresdey, J.L., Parsons, J.G., Gomez, E., Peralta-Videa, J., Troiani, H.E., Santiago, P. & Yacaman, M.J. 2002. Formation and Growth of Au Nanoparticles inside Live Alfalfa Plants. *Nano Letters*, 2(4): 397–401. https://doi.org/10.1021/nl015673+.

Garmasheva, I., Kovalenko, N., Voychuk, S., Ostapchuk, A., Livins'ka, O. & Oleschenko, L. 2016. Lactobacillus species mediated synthesis of silver nanoparticles and their antibacterial activity against opportunistic pathogens in vitro. *BioImpacts : BI*, 6(4): 219–223. https://pubmed.ncbi.nlm.nih.gov/28265538.

Genuino, H., Huang, H., Njagi, E., Stafford, L. & Suib, S.L. 2012. A Review of Green Synthesis of Nanophase Inorganic Materials for Green Chemistry Applications. *Handbook of Green Chemistry*: 217–244. https://doi.org/10.1002/9783527628698.hgc092.

Geohegan, D.B., Puretzky, A.A., Duscher, G. & Pennycook, S.J. 1998. Time-resolved imaging of gas phase nanoparticle synthesis by laser ablation. *Applied Physics Letters*, 72(23): 2987–2989. https://doi.org/10.1063/1.121516.

Gerits, N. 2016. *Synthesis of copper nanoparticles using grape stalk and spent coffee extract*. University of Girona.

Ghaem, E.N., Dorranian, D. & Sari, A.H. 2020. Characterization of cobalt oxide nanoparticles produced by laser ablation method: Effects of laser fluence. *Physica E: Low-dimensional Systems and Nanostructures*, 115: 113670. https://www.sciencedirect.com/science/article/pii/S1386947719306800 13 August 2019.

Ghaffari-Moghaddam, M. & Hadi-Dabanlou, R. 2014. Plant mediated green synthesis and antibacterial activity of silver nanoparticles using Crataegus douglasii fruit extract. *Journal of Industrial and Engineering Chemistry*, 20(2): 739–744. https://www.sciencedirect.com/science/article/pii/S1226086X13004231.

Ghanbari, F. & Moradi, M. 2017. Application of peroxymonosulfate and its activation methods for degradation of environmental organic pollutants: Review. *Chemical Engineering Journal*, 310: 41–62. https://www.sciencedirect.com/science/article/pii/S1385894716314759.

Ghashghaei, S. & Emtiazi, G. 2015. The Methods of Nanoparticle Synthesis Using Bacteria as Biological Nanofactories, their Mechanisms and Major Applications. *Current Bionanotechnology (Discontinued)*, 1(1): 3–17. http://www.eurekaselect.com/node/120843/article.

Ghosh, S., Ahmad, R., Banerjee, K., AlAjmi, M.F. & Rahman, S. 2021. Mechanistic Aspects of Microbe-Mediated Nanoparticle Synthesis. *Frontiers in Microbiology*, 12: 867. https://www.frontiersin.org/article/10.3389/fmicb.2021.638068.

Gigliobianco, M.R., Campisi, B., Vargas Peregrina, D., Censi, R., Khamitova, G., Angeloni, S., Caprioli, G., Zannotti, M., Ferraro, S., Giovannetti, R., Angeloni, C., Lupidi, G., Pruccoli, L., Tarozzi, A., Voinovich, D. & Di Martino, P. 2020. Optimization of the Extraction from Spent Coffee Grounds Using the Desirability Approach. *Antioxidants* , 9(5).

Golabiazar, R., Othman, K.I., Khalid, K.M., Maruf, D.H., Aulla, S.M. & Yusif, P.A. 2019. Green Synthesis, Characterization, and Investigation Antibacterial Activity of Silver Nanoparticles Using Pistacia atlantica Leaf Extract. *BioNanoScience*, 9(2): 323–333.

Govender-Ragubeer, Y., Grewar, T., Gericke, M. & Whiteley, C. 2008. Bioreduction of platinum salts into nanoparticles: A mechanistic perspective. *Biotechnology letters*, 31: 95–100.

Govindan, K., Sumanasekara, V. & Jang, A. 2020. Mechanisms for degradation and transformation of β-blocker atenolol: Via electrocoagulation, electro-Fenton, and electro-Fenton-like processes. *Environmental Science: Water Research & Technology*, 6.

Govindasamy, G.A., S.M.N.Mydin, R.B., Harun, N. & Sreekantan, S. 2021. Effect of calcination temperature on physicochemical and antimicrobial properties of green synthesised ZnO/C/Ca nanocomposites using Calotropis gigantea leaves. *Advances in Natural Sciences: Nanoscience and Nanotechnology*, 12.

Grzelczyk, J., Fiurasek, P., Kakkar, A. & Budryn, G. 2022. Evaluation of the thermal stability of bioactive compounds in coffee beans and their fractions modified in the roasting process. *Food Chemistry*, 387: 132888. https://www.sciencedirect.com/science/article/pii/S0308814622008500.

Gu, F., Wang, S.F., Lü, M.K., Zhou, G.J., Xu, D. & Yuan, D.R. 2004. Photoluminescence Properties of SnO2 Nanoparticles Synthesized by Sol−Gel Method. *The Journal of Physical Chemistry B*, 108(24): 8119–8123. https://doi.org/10.1021/jp036741e.

Guerra-Rodríguez, S., Rodríguez, E., Singh, D. & Rodríguez-Chueca, J. 2018. Assessment of Sulfate Radical-Based Advanced Oxidation Processes for Water and Wastewater Treatment: A Review. *Water*, 10: 1828.

Guilger-Casagrande, M. & Lima, R. de. 2019. Synthesis of Silver Nanoparticles Mediated by Fungi: A Review. *Frontiers in Bioengineering and Biotechnology*, 7: 287. https://www.frontiersin.org/article/10.3389/fbioe.2019.00287.

Guillou, F., Bréard, Y. & Hardy, V. 2013. Cobalt spin state above the valence and spin-state transition in (Pr 0.7Sm0.3)0.7Ca0.3CoO3. *Solid State Sciences*, 24: 120–124. http://dx.doi.org/10.1016/j.solidstatesciences.2013.07.013.

Gurunathan, S., Han, J., Park, J. & Kim, J.-H. 2014. Green chemistry approach for synthesizing biocompatible gold nanoparticles. *Nanoscale Research Letters*, 9: 248.

Guzmán, N., Bahamón, A. & Muñoz, L. 2018. ATR-FTIR for disc rimenation of espresso and americano coffee pods. *Coffee Science*, 13: 550.

Haq, S., Abbasi, F., Ben Ali, M., Hedfi, A., Mezni, A., Rehman, W., Waseem, M., Khan, A.R. & Shaheen, H. 2021. Green synthesis of cobalt oxide nanoparticles and the effect of annealing temperature on their physiochemical and biological properties. *Materials Research Express*, 8(7): 75009. http://dx.doi.org/10.1088/2053-1591/ac1187.

Hayashi, H., Hakuta, Y., Hayashi, H. & Hakuta, Y. 2010. Hydrothermal Synthesis of Metal Oxide Nanoparticles in Supercritical Water. *Materials*, 3(7): 3794–3817. http://www.mdpi.com/1996-1944/3/7/3794 12 August 2019.

Hečimović, I., Belščak-Cvitanović, A., Horžić, D. & Komes, D. 2011. Comparative study of polyphenols and caffeine in different coffee varieties affected by the degree of roasting. *Food Chemistry*, 129(3): 991–1000.

Heiligtag, F.J. & Niederberger, M. 2013. The fascinating world of nanoparticle research. *Materials Today*, 16(7): 262–271. https://www.sciencedirect.com/science/article/pii/S1369702113002253.

Hemalatha, S., p ramadas, L. & Arulpriya, P. 2010. Antioxidant activities of the extracts of the aerial roots of Pothos aurea. *Der Chem. Sin.*, 2: 84–89.

Hench, L.L. & West, J.K. 1990. The Sol-Gel Process. *Chemical Reviews*, 90(1): 33–72.

Herawati, D., Loisanjaya, M.O., Kamal, R.H., Adawiyah, D.R. & Andarwulan, N. 2022. Profile of Bioactive Compounds, Aromas, and Cup Quality of Excelsa Coffee (*Coffea liberica* var. *dewevrei*) Prepared from Diverse Postharvest Processes C. Monton, ed. *International Journal of Food Science*, 2022: 2365603. https://doi.org/10.1155/2022/2365603.

Hingorani, S., Pillai, V., Kumar, P., Multani, M.S. & Shah, D.O. 1993. Microemulsion mediated synthesis of zinc-oxide nanoparticles for varistor studies. *Materials Research Bulletin*, 28(12): 1303–1310. https://www.sciencedirect.com/science/article/pii/002554089390178G 12 August 2019.

Hoseinpour, V., Souri, M., Ghaemi, N. & Shakeri, A. 2017. *Green Synthesis of Manganese Nanoparticles by Yucca gloriosa Aqueous Extract, Optimization and Characterization*.

Hou, W., Zhang, W., Chen, G. & Luo, Y.-P. 2016. Optimization of Extraction Conditions for Maximal Phenolic, Flavonoid and Antioxidant Activity from Melaleuca bracteata Leaves Using the Response Surface Methodology. *PloS one*, 11: e0162139.

Huang, H., Wang, J., Zhang, J., Cai, J., Pi, J. & Xu, J.-F. 2021. Inspirations of Cobalt Oxide Nanoparticle Based Anticancer Therapeutics. *Pharmaceutics*, 13(10).

Huang, Y., Wang, Z., Liu, Q., Wang, X., Yuan, Z. & Liu, J. 2017. Effects of chloride on PMS-based pollutant degradation: A substantial discrepancy between dyes and their common decomposition intermediate (phthalic acid). *Chemosphere*, 187: 338–346. https://www.sciencedirect.com/science/article/pii/S0045653517313449.

Hulla, J.E., Sahu, S.C. & Hayes, A.W. 2015. Nanotechnology: History and future. *Human \& Experimental Toxicology*, 34(12): 1318–1321. https://doi.org/10.1177/0960327115603588.

Huq, M.A. 2020. Biogenic Silver Nanoparticles Synthesized by Lysinibacillus xylanilyticus MAHUQ-40 to Control Antibiotic-Resistant Human Pathogens Vibrio parahaemolyticus and Salmonella Typhimurium. *Frontiers in Bioengineering and Biotechnology*, 8. https://www.frontiersin.org/article/10.3389/fbioe.2020.597502.

Hussain, I., Singh, N.B., Singh, A., Singh, H. & Singh, S.C. 2016. Green synthesis of nanoparticles and its potential application. *Biotechnology Letters*, 38(4): 545–560.

Hussein, R. & El-Anssary, A.A. 2019. Plants Secondary Metabolites: The Key Drivers of the Pharmacological Actions of Medicinal Plants. In *Herbal Medicine*. IntechOpen. http://dx.doi.org/10.1039/C7RA00172J%0Ahttps://www.intechopen.com/books/advanced-biometric-technologies/liveness-detection-in-biometrics%0Ahttp://dx.doi.org/10.1016/j.colsurfa.2011.12.014.

Ibañez, E., Kubátová, A., Señoráns, F.J., Cavero, S., Reglero, U. & Hawthorne, S.B. 2003. Subcritical water extraction of antioxidant compounds from rosemary plants. *Journal of agricultural and food chemistry*, 51(2): 375–382. https://pubmed.ncbi.nlm.nih.gov/12517098/ 26 August 2022.

Ibrahim, H.M.M. 2015. Green synthesis and characterization of silver nanoparticles using banana peel extract and their antimicrobial activity against representative microorganisms. *Journal of Radiation Research and Applied Sciences*, 8(3): 265–275. http://dx.doi.org/10.1016/j.jrras.2015.01.007.

Ijaz, F., Shahid, S., Khan, S.A., Ahmad, W. & Zaman, S. 2017. Green synthesis of copper oxide nanoparticles using abutilon indicum leaf extract: Antimicrobial, antioxidant and photocatalytic dye degradation activities. *Tropical Journal of Pharmaceutical Research*, 16(4): 743–753.

Iravani, S. 2014. Bacteria in Nanoparticle Synthesis: Current Status and Future Prospects M.

Labrenz, ed. *International Scholarly Research Notices*, 2014: 359316. https://doi.org/10.1155/2014/359316.

Iravani, S. & Varma, R.S. 2020. Sustainable synthesis of cobalt and cobalt oxide nanoparticles and their catalytic and biomedical applications. *Green Chemistry*, 22(9): 2643–2661. http://dx.doi.org/10.1039/D0GC00885K.

Iravani, S. & Zolfaghari, B. 2013. Green Synthesis of Silver Nanoparticles Using *Pinus eldarica* Bark Extract M. A. Z. Coelho, ed. *BioMed Research International*, 2013: 639725. https://doi.org/10.1155/2013/639725.

Ismail, M., Gul, S., Khan, M.I., Khan, M.A., Asiri, A.M. & Khan, S.B. 2019. Green synthesis of zerovalent copper nanoparticles for efficient reduction of toxic azo dyes congo red and methyl orange. *Green Processing and Synthesis*, 8(1): 135–143.

Iwuozor, K.O., Ogunfowora, L.A. & Oyekunle, I.P. 2022. Review on Sugarcane-Mediated Nanoparticle Synthesis: A Green Approach. *Sugar Tech*, 24(4): 1186–1197. https://doi.org/10.1007/s12355-021-01038-7.

Izawa, K., Amino, Y., Kohmura, M., Ueda, Y. & Kuroda, M. 2010. Human–Environment Interactions – Taste. *Comprehensive Natural Products II*: 631–671. https://www.sciencedirect.com/science/article/pii/B9780080453828001088 26 May 2019.

Jadoun, S., Arif, R., Jangid, N.K. & Meena, R.K. 2021. Green synthesis of nanoparticles using plant extracts: a review. *Environmental Chemistry Letters*, 19(1): 355–374. https://doi.org/10.1007/s10311-020-01074-x.

Jagadale, T.C., Takale, S.P., Sonawane, R.S., Joshi, H.M., Patil, S.I., Kale, B.B. & Ogale, S.B. 2008. N-Doped TiO2 Nanoparticle Based Visible Light Photocatalyst by Modified Peroxide Sol−Gel Method. *The Journal of Physical Chemistry C*, 112(37): 14595–14602. https://doi.org/10.1021/jp803567f.

Jain, S. & Mehata, M.S. 2017. Medicinal Plant Leaf Extract and Pure Flavonoid Mediated Green Synthesis of Silver Nanoparticles and their Enhanced Antibacterial Property. *Scientific Reports*, 7(1): 1–13. http://dx.doi.org/10.1038/s41598-017-15724-8.

Jamkhande, P.G., Ghule, N.W., Bamer, A.H. & Kalaskar, M.G. 2019. Metal nanoparticles synthesis: An overview on methods of preparation, advantages and disadvantages, and applications. *Journal of Drug Delivery Science and Technology*, 53: 101174.

Jeevanandam, J., Chan, Y.S. & Danquah, M.K. 2016. Biosynthesis of Metal and Metal Oxide Nanoparticles. *ChemBioEng Reviews*, 3(2): 55–67.

Jeevanandam, J., Kiew, S.F., Boakye-Ansah, S., Lau, S.Y., Barhoum, A., Danquah, M.K. & Rodrigues, J. 2022. Green approaches for the synthesis of metal and metal oxide nanoparticles using microbial and plant extracts. *Nanoscale*, 14(7): 2534–2571. http://dx.doi.org/10.1039/D1NR08144F.

Jeong, J., Han, Y., Poland, C. & Cho, W.-S. 2015. Response-metrics for acute lung inflammation pattern by cobalt-based nanoparticles. *Particle and fibre toxicology*, 12: 13.

Jeszka-Skowron, M., Zgoła-Grześkowiak, A. & Grześkowiak, T. 2015. Analytical methods applied for the characterization and the determination of bioactive compounds in coffee. *European Food Research and Technology*, 240(1): 19–31. https://doi.org/10.1007/s00217-014-2356-z.

Jiménez-Moreno, N., Volpe, F., Moler, J.A., Esparza, I. & Ancín-Azpilicueta, C. 2019. Impact of Extraction Conditions on the Phenolic Composition and Antioxidant Capacity of Grape Stem Extracts. *Antioxidants*, 8(12). /pmc/articles/PMC6943662/ 25 August 2022.

Kandpal, N.D., Sah, N., Loshali, R., Joshi, R. & Prasad, J. 2014. Co-precipitation method of synthesis and characterization of iron oxide nanoparticles. *Journal of Scientific and Industrial Research*, 73(2): 87–90.

Kaningini, A.G., Azizi, S., Sintwa, N., Mokalane, K., Mohale, K.C., Mudau, F.N. & Maaza, M. 2022. Effect of Optimized Precursor Concentration, Temperature, and Doping on Optical Properties of ZnO Nanoparticles Synthesized via a Green Route Using Bush Tea (Athrixia phylicoides DC.) Leaf Extracts. *ACS Omega*, 7(36): 31658–31666. https://doi.org/10.1021/acsomega.2c00530.

Karade, V.C., Dongale, T.D., Sahoo, S.C., Kollu, P., Chougale, A.D., Patil, P.S. & Patil, P.B. 2018. Effect of reaction time on structural and magnetic properties of green-synthesized magnetic nanoparticles. *Journal of Physics and Chemistry of Solids*, 120: 161–166. https://www.sciencedirect.com/science/article/pii/S0022369717312623.

Karam, S.T. & Abdulrahman, A.F. 2022. Green Synthesis and Characterization of ZnO Nanoparticles by Using Thyme Plant Leaf Extract. *Photonics*, 9(8).

Karuppiah, C., Palanisamy, S., Chen, S.-M., Veeramani, V. & Periakaruppan, P. 2014. A novel enzymatic glucose biosensor and sensitive non-enzymatic hydrogen peroxide sensor based on graphene and cobalt oxide nanoparticles composite modified glassy carbon electrode. *Sensors and Actuators B: Chemical*, 196: 450–456. https://www.sciencedirect.com/science/article/pii/S0925400514001828.

Kassaee, M.Z., Motamedi, E., Mikhak, A. & Rahnemaie, R. 2011. Nitrate removal from water using iron nanoparticles produced by arc discharge vs. reduction. *Chemical Engineering Journal*, 166(2): 490–495. https://www.sciencedirect.com/science/article/pii/S1385894710010508 7 August 2019.

Kathiraven, T., Sundaramanickam, A., Shanmugam, N. & Balasubramanian, T. 2015. Green synthesis of silver nanoparticles using marine algae Caulerpa racemosa and their antibacterial activity against some human pathogens. *Applied Nanoscience (Switzerland)*, 5(4): 499–504.

Kavitha, S., Dhamodaran, M., Prasad, R. & Ganesan, M. 2017. Synthesis and characterisation of zinc oxide nanoparticles using terpenoid fractions of Andrographis paniculata leaves. *International Nano Letters*, 7(2): 141–147. https://doi.org/10.1007/s40089-017-0207-1.

Keshta, B.E., Gemeay, A.H. & Khamis, A.A. 2022. Impacts of horseradish peroxidase immobilization onto functionalized superparamagnetic iron oxide nanoparticles as a biocatalyst for dye degradation. *Environmental Science and Pollution Research*, 29(5): 6633–6645. https://doi.org/10.1007/s11356-021-16119-z.

Khalil, A.T., Ovais, M., Ullah, I., Ali, M., Shinwari, Z.K. & Maaza, M. 2017. Physical properties, biological applications and biocompatibility studies on biosynthesized single phase cobalt oxide (Co3O4) nanoparticles via Sageretia thea (Osbeck.). *Arabian Journal of Chemistry*. https://www.sciencedirect.com/science/article/pii/S187853521730134X 17 April 2019.

Khalil, M.M.H., Ismail, E.H., El-Baghdady, K.Z. & Mohamed, D. 2014. Green synthesis of silver nanoparticles using olive leaf extract and its antibacterial activity. *Arabian Journal of Chemistry*, 7(6): 1131–1139. https://www.sciencedirect.com/science/article/pii/S1878535213000968.

Khan, F., Shariq, M., Asif, M., Siddiqui, M., Malan, P. & Ahmad, F. 2022. Green Nanotechnology: Plant-Mediated Nanoparticle Synthesis and Application. *Nanomaterials*, 12: 673.

Khan, Mujeeb, Khan, Merajuddin, Kuniyil, M., Adil, S.F., Al-Warthan, A., Alkhathlan, H.Z.,

Tremel, W., Tahir, M.N. & Siddiqui, M.R.H. 2014. Biogenic synthesis of palladium nanoparticles using Pulicaria glutinosa extract and their catalytic activity towards the Suzuki coupling reaction. *Dalton Transactions*, 43(24): 9026–9031.

Khandelwal, G., Sharma, K. & Kumar, V. 2019. Graphene–Metal Modified Electrochemical Sensors. In A. Pandikumar & P. B. T.-G.-B. E. S. for B. Rameshkumar, eds. *Micro and Nano Technologies*. Elsevier: 89–111. https://www.sciencedirect.com/science/article/pii/B9780128153949000042.

Kharissova, O. V., Dias, H.V.R., Kharisov, B.I., Pérez, B.O. & Pérez, V.M.J. 2013. The greener synthesis of nanoparticles. *Trends in Biotechnology*, 31(4): 240–248.

Kieu Tran, T.M., Kirkman, T., Nguyen, M. & Van Vuong, Q. 2020. Effects of drying on physical properties, phenolic compounds and antioxidant capacity of Robusta wet coffee pulp (Coffea canephora). *Heliyon*, 6(7): e04498. https://www.sciencedirect.com/science/article/pii/S2405844020313426.

Kim, Y. Il, Kim, D. & Lee, C.S. 2003. Synthesis and characterization of CoFe2O4 magnetic nanoparticles prepared by temperature-controlled coprecipitation method. *Physica B: Condensed Matter*, 337(1): 42–51. https://www.sciencedirect.com/science/article/pii/S0921452603003223.

Kohantorabi, M., Moussavi, G. & Giannakis, S. 2021. A review of the innovations in metal- and carbon-based catalysts explored for heterogeneous peroxymonosulfate (PMS) activation, with focus on radical vs. non-radical degradation pathways of organic contaminants. *Chemical Engineering Journal*, 411: 127957. https://www.sciencedirect.com/science/article/pii/S1385894720340766.

Kohantorabi, M., Moussavi, G., Mohammadi, S., Oulego, P. & Giannakis, S. 2021. Photocatalytic activation of peroxymonosulfate (PMS) by novel mesoporous Ag/ZnO@NiFe2O4 nanorods, inducing radical-mediated acetaminophen degradation under UVA irradiation. *Chemosphere*, 277. https://pubmed.ncbi.nlm.nih.gov/33770697/ 7 October 2022.

Kolthoff, I.M. 1932. 'Theory of Coprecipitation.' The formation and properties of crystalline precipitates. *Journal of Physical Chemistry*, 36(3): 860–881.

Kombaiah, K., Vijaya, J.J., Kennedy, L.J., Kaviyarasu, K., Ramalingam, R.J. & Al-Lohedan, H.A. 2018. Green Synthesis of Co3O4 Nanorods for Highly Efficient Catalytic, Photocatalytic, and Antibacterial Activities. *Journal of Nanoscience and Nanotechnology*, 19(5): 2590–2598.

Konig, E., Ritter, G. & Kulshreshtha, S.K. 1985. The nature of spin-state transitions in solid complexes of iron(II) and the interpretation of some associated phenomena. *Chemical Reviews*, 85(3): 219–234. https://pubs.acs.org/doi/abs/10.1021/cr00067a003.

Kornei, K. 2016. The Beginning of Nanotechnology at the 1959 APS Meeting. *APS*. https://www.aps.org/publications/apsnews/201611/nanotechnology.cfm 20 September 2021.

Köseoğlu, Y., Alan, F., Tan, M., Yilgin, R. & Öztürk, M. 2012. Low temperature hydrothermal synthesis and characterization of Mn doped cobalt ferrite nanoparticles. *Ceramics International*, 38(5): 3625–3634. https://www.sciencedirect.com/science/article/pii/S027288421200003X 12 August 2019.

Kowshik, M., Ashtaputre, S., Kharrazi, S., Vogel, W., Urban, J., Kulkarni, S.K. & Paknikar, K.M. 2002. Extracellular synthesis of silver nanoparticles by a silver-tolerant yeast strain MKY3. *Nanotechnology*, 14(1): 95–100. http://dx.doi.org/10.1088/0957-4484/14/1/321.

Kozma, G., Rónavári, A., Kónya, Z. & Kukovecz, Á. 2016. Environmentally Benign Synthesis

Methods of Zero-Valent Iron Nanoparticles. *ACS Sustainable Chemistry and Engineering*, 4(1): 291–297.

Kredy, H.M. 2018. The effect of pH, temperature on the green synthesis and biochemical activities of silver nanoparticles from Lawsonia inermis extract. *Journal of Pharmaceutical Sciences and Research*, 10(8): 2022–2026.

Kulasooriya, T.P.K., Priyantha, N. & Navaratne, A.N. 2020. Removal of textile dyes from industrial effluents using burnt brick pieces: adsorption isotherms, kinetics and desorption. *SN Applied Sciences*, 2(11): 1789. https://doi.org/10.1007/s42452-020-03533-0.

Kumar, P.V., Jelastin Kala, S.M. & Prakash, K.S. 2019. Green synthesis derived Pt-nanoparticles using Xanthium strumarium leaf extract and their biological studies. *Journal of Environmental Chemical Engineering*, 7(3): 103146. https://doi.org/10.1016/j.jece.2019.103146.

Kumar, S., Sandhir, R. & Ojha, S. 2014. Evaluation of antioxidant activity and total phenol in different varieties of Lantana camara leaves. *BMC Research Notes*, 7(1): 560. https://doi.org/10.1186/1756-0500-7-560.

Kurian, M. 2021. Advanced oxidation processes and nanomaterials -a review. *Cleaner Engineering and Technology*, 2: 100090. https://www.sciencedirect.com/science/article/pii/S2666790821000501.

Kuriechen, S.K. & Murugesan, S. 2013. Carbon-Doped Titanium Dioxide Nanoparticles Mediated Photocatalytic Degradation of Azo Dyes Under Visible Light. *Water, Air, & Soil Pollution*, 224(9): 1671. https://doi.org/10.1007/s11270-013-1671-5.

Lacour, F., Guillois, O., Portier, X., Perez, H., Herlin, N. & Reynaud, C. 2007. Laser pyrolysis synthesis and characterization of luminescent silicon nanocrystals. *Physica E: Low-dimensional Systems and Nanostructures*, 38(1–2): 11–15. https://www.sciencedirect.com/science/article/pii/S1386947706005856 13 August 2019.

Lahiri, D., Nag, M., Sheikh, H.I., Sarkar, T., Edinur, H.A., Pati, S. & Ray, R.R. 2021. Microbiologically-Synthesized Nanoparticles and Their Role in Silencing the Biofilm Signaling Cascade. *Frontiers in Microbiology*, 12: 180. https://www.frontiersin.org/article/10.3389/fmicb.2021.636588.

Lee, H., Purdon, A.M., Chu, V. & Westervelt, R.M. 2004. Controlled Assembly of Magnetic Nanoparticles from Magnetotactic Bacteria Using Microelectromagnets Arrays. *Nano Letters*, 4(5): 995–998. https://doi.org/10.1021/nl049562x.

Li, F., Kang, Y., Chen, M., Liu, G., Lv, W., Yao, K., Chen, P. & Huang, H. 2016. Photocatalytic degradation and removal mechanism of ibuprofen via monoclinic BiVO4 under simulated solar light. *Chemosphere*, 150: 139–144. https://www.sciencedirect.com/science/article/pii/S0045653516301977.

Li, X., Xu, H., Chen, Z.-S. & Chen, G. 2011. Biosynthesis of Nanoparticles by Microorganisms and Their Applications X. J. Liang, ed. *Journal of Nanomaterials*, 2011: 270974. https://doi.org/10.1155/2011/270974.

Lin, K.-Y.A. & Lin, T.-Y. 2017. Degradation of Acid Azo Dyes Using Oxone Activated by Cobalt Titanate Perovskite. *Water, Air, & Soil Pollution*, 229(1): 10. https://doi.org/10.1007/s11270-017-3648-2.

Linlin, H., Wang, P. & Valiyaveettil, S. 2017. Successive extraction of As(V), Cu(II) and P(V) ions from water using spent coffee powder as renewable bioadsorbents. *Scientific Reports*, 7: 42881.

Liu, H., Zhang, H., Wang, J. & Wei, J. 2020. Effect of temperature on the size of

biosynthesized silver nanoparticle: Deep insight into microscopic kinetics analysis. *Arabian Journal of Chemistry*, 13(1): 1011–1019. https://www.sciencedirect.com/science/article/pii/S1878535217301727.

Liu, J., Zhou, J., Ding, Z., Zhao, Z., Xu, X. & Fang, Z. 2017. Ultrasound irritation enhanced heterogeneous activation of peroxymonosulfate with Fe3O4 for degradation of azo dye. *Ultrasonics Sonochemistry*, 34: 953–959. https://www.sciencedirect.com/science/article/pii/S1350417716302759.

Liyana-Pathirana, C. & Shahidi, F. 2005. Optimization of extraction of phenolic compounds from wheat using response surface methodology. *Food Chemistry*, 93(1): 47–56. https://www.sciencedirect.com/science/article/pii/S0308814604006910.

Lou, X., Wu, L., Guo, Y., Chen, C., Wang, Z., Xiao, D., Fang, C., Liu, J., Zhao, J. & Lu, S. 2014. Peroxymonosulfate activation by phosphate anion for organics degradation in water. *Chemosphere*, 117: 582–585. https://www.sciencedirect.com/science/article/pii/S0045653514011217.

Lu, W., Liao, F., Luo, Y., Chang, G. & Sun, X. 2011. Hydrothermal synthesis of well-stable silver nanoparticles and their application for enzymeless hydrogen peroxide detection. *Electrochimica Acta*, 56(5): 2295–2298. https://www.sciencedirect.com/science/article/pii/S0013468610015653 12 August 2019.

Lu, Y., Yin, Y., Mayers, B.T. & Xia, Y. 2002. Modifying the Surface Properties of Superparamagnetic Iron Oxide Nanoparticles through A Sol−Gel Approach. *Nano Letters*, 2(3): 183–186. https://doi.org/10.1021/nl015681q.

Lung, J.-K., Huang, J.-C., Tien, D.-C., Liao, C.-Y., Tseng, K.-H., Tsung, T.-T., Kao, W.-S., Tsai, T.-H., Jwo, C.-S., Lin, H.-M. & Stobinski, L. 2007. Preparation of gold nanoparticles by arc discharge in water. *Journal of Alloys and Compounds*, 434–435: 655–658. https://www.sciencedirect.com/science/article/abs/pii/S0925838806013028 7 August 2019.

Lyman, D.J., Benck, R., Dell, S., Merle, S. & Murray-Wijelath, J. 2003. FTIR-ATR Analysis of Brewed Coffee: Effect of Roasting Conditions. *Journal of Agricultural and Food Chemistry*, 51(11): 3268–3272. https://doi.org/10.1021/jf0209793.

Ma, W., Wang, N., Fan, Y., Tong, T., Han, X. & Du, Y. 2018. Non-radical-dominated catalytic degradation of bisphenol A by ZIF-67 derived nitrogen-doped carbon nanotubes frameworks in the presence of peroxymonosulfate. *Chemical Engineering Journal*, 336: 721–731. https://www.sciencedirect.com/science/article/pii/S1385894717320879.

Madhavan, J., Muthuraaman, B., Murugesan, S., Anandan, S. & Maruthamuthu, P. 2006. Peroxomonosulphate, an efficient oxidant for the photocatalysed degradation of a textile dye, acid red 88. *Solar Energy Materials and Solar Cells*, 90(13): 1875–1887. https://www.sciencedirect.com/science/article/pii/S0927024805003594.

Madhuri, K. V. 2020. Thermal protection coatings of metal oxide powders. In Y. B. T.-M. O. P. T. Al-Douri, ed. *Metal Oxides*. Elsevier: 209–231. https://www.sciencedirect.com/science/article/pii/B9780128175057000105.

Mafuné, F., Kohno, J., Takeda, Y. & Kondow, T. 2003. Formation of Stable Platinum Nanoparticles by Laser Ablation in Water. *The Journal of Physical Chemistry B*, 107(18): 4218–4223. https://doi.org/10.1021/jp021580k.

Mafuné, F., Kohno, J., Takeda, Y., Kondow, T. & Sawabe, H. 2001. Formation of Gold Nanoparticles by Laser Ablation in Aqueous Solution of Surfactant. *The Journal of Physical Chemistry B*, 105(22): 5114–5120. https://doi.org/10.1021/jp0037091.

Mafuné, F., Kohno, J., Takeda, Y., Kondow, T. & Sawabe, H. 2000. Structure and Stability of

Silver Nanoparticles in Aqueous Solution Produced by Laser Ablation. *The Journal of Physical Chemistry B*, 104(35): 8333–8337. https://doi.org/10.1021/jp001803b.

Mahmood, T. 2022. Technologies for Removal of Emerging Contaminants from Wastewater. In S. Momin, ed. Rijeka: IntechOpen: Ch. 12. https://doi.org/10.5772/intechopen.104466.

Mahmoud, M.A., Poncheri, A., Badr, Y. & Abd El Wahed, M.G. 2009. Photocatalytic degradation of methyl red dye. *South African Journal of Science*, 105: 299–303. http://www.scielo.org.za/scielo.php?script=sci_arttext&pid=S0038-23532009000400019&nrm=iso.

Mahmoud, R., Kotp, A.A., Abo El-Ela, F.I., Farghali, A.A., Moaty, S.A.A., Zahran, H.Y. & Amin, R. 2021. Green synthesis of iron nanoparticles of clove and green coffee origin with an in vivo hepatoprotective investigation. *Journal of Environmental Chemical Engineering*, 9(6): 106320. https://www.sciencedirect.com/science/article/pii/S2213343721012975.

Makarov, V. V, Love, A.J., Sinitsyna, O. V, Makarova, S.S., Yaminsky, I. V, Taliansky, M.E. & Kalinina, N.O. 2014. 'Green' nanotechnologies: synthesis of metal nanoparticles using plants. *Acta naturae*, 6(1): 35–44. https://pubmed.ncbi.nlm.nih.gov/24772325.

Makhlouf, S.A., Bakr, Z.H., Aly, K.I. & Moustafa, M.S. 2013. Structural, electrical and optical properties of Co3O4 nanoparticles. *Superlattices and Microstructures*, 64: 107–117. https://www.sciencedirect.com/science/article/pii/S0749603613003042 5 April 2019.

Makuła, P., Pacia, M. & Macyk, W. 2018. How To Correctly Determine the Band Gap Energy of Modified Semiconductor Photocatalysts Based on UV–Vis Spectra. *The Journal of Physical Chemistry Letters*, 9(23): 6814–6817. https://doi.org/10.1021/acs.jpclett.8b02892.

Malarkodi, C., Rajeshkumar, S., Vanaja, M., Paulkumar, K., Gnanajobitha, G. & Annadurai, G. 2013. Eco-friendly synthesis and characterization of gold nanoparticles using Klebsiella pneumoniae. *Journal of Nanostructure in Chemistry*, 3(1): 30. https://doi.org/10.1186/2193-8865-3-30.

Malik, M.A., Wani, M.Y. & Hashim, M.A. 2012. Microemulsion method: A novel route to synthesize organic and inorganic nanomaterials: 1st Nano Update. *Arabian Journal of Chemistry*, 5(4): 397–417. https://www.sciencedirect.com/science/article/pii/S1878535210002005 17 August 2019.

Malik, P., Shankar, R., Malik, V., Sharma, N. & Mukherjee, T. 2014. Green Chemistry Based Benign Routes for Nanoparticle Synthesis. *Journal of nanoparticle*, 2014.

Mamdooh, N.W. & Naeem, G.A. 2022. The effect of temperature on green synthesis of silver nanoparticles. *AIP Conference Proceedings*, 2450(1): 20045. https://aip.scitation.org/doi/abs/10.1063/5.0094029.

Martin, P. 2010. Deposition Technologies: An Overview. In P. M. B. T.-H. of D. T. for F. and C. (Third E. Martin, ed. Boston: William Andrew Publishing: 1–31. https://www.sciencedirect.com/science/article/pii/B9780815520313000016.

Martínez-Abad, A. 2011. Silver-based antimicrobial polymers for food packaging. In J.-M. B. T.-M. and N. P. for F. P. Lagarón, ed. Woodhead Publishing: 347–367. https://www.sciencedirect.com/science/article/pii/B9781845697389500136.

Martinez, E. 2019. The Drying of Spent Coffee Grounds in a Tray Drier. *American Journal of Biomedical Science & Research*, 6: 416–425.

Martín, M.., Pablos, F. & González, A.. 1999. Characterization of arabica and robusta roasted coffee varieties and mixture resolution according to their metal content. *Food*

Chemistry, 66(3): 365–370.
https://www.sciencedirect.com/science/article/pii/S0308814699000928 27 May 2019.

Mary, A.P.A., Ansari, A.T. & Subramanian, R. 2021. Caffeine-mediated synthesis of CuO nanoparticles: characterization, morphology changes, and bactericidal activity. *Inorganic and Nano-Metal Chemistry*, 51(2): 174–181. https://doi.org/10.1080/24701556.2020.1769667.

Mascolo, M.C., Pei, Y. & Ring, T.A. 2013. Room Temperature Co-Precipitation Synthesis of Magnetite Nanoparticles in a Large ph Window with Different Bases. *Materials*, 6(12): 5549–5567.

Matinise, N, Mayedwa, N., Fuku, X.G., Mongwaketsi, N. & Maaza, M. 2018. Green synthesis of cobalt (II, III) oxide nanoparticles using Moringa Oleifera natural extract as high electrochemical electrode for supercapacitors. *AIP Conference Proceedings*, 1962(1): 40005. https://aip.scitation.org/doi/abs/10.1063/1.5035543.

Matinise, N., Mayedwa, N., Fuku, X.G., Mongwaketsi, N. & Maaza, M. 2018. Green synthesis of cobalt (II, III) oxide nanoparticles using Moringa Oleifera natural extract as high electrochemical electrode for supercapacitors. *AIP Conference Proceedings*, 1962.

Mei, J., Liao, T., Ayoko, G.A., Bell, J. & Sun, Z. 2019. Cobalt oxide-based nanoarchitectures for electrochemical energy applications. *Progress in Materials Science*, 103: 596–677. https://www.sciencedirect.com/science/article/pii/S0079642519300246.

Meng, W., Wang, Y., Zhang, Y., Liu, C., Wang, Z., Song, Z., Xu, B., Qi, F. & Ikhlaq, A. 2020. Degradation Rhodamine B dye wastewater by sulfate radical-based visible light-fenton mediated by LaFeO3: Reaction mechanism and empirical modeling. *Journal of the Taiwan Institute of Chemical Engineers*, 111: 162–169. https://www.sciencedirect.com/science/article/pii/S1876107020300894.

Metz, K.M., Sanders, S.E., Pender, J.P., Dix, M.R., Hinds, D.T., Quinn, S.J., Ward, A.D., Duffy, P., Cullen, R.J. & Colavita, P.E. 2015. Green Synthesis of Metal Nanoparticles via Natural Extracts: The Biogenic Nanoparticle Corona and Its Effects on Reactivity. *ACS Sustainable Chemistry and Engineering*, 3(7): 1610–1617.

Mills, C.E., Oruna-Concha, M.J., Mottram, D.S., Gibson, G.R. & Spencer, J.P.E. 2013. The effect of processing on chlorogenic acid content of commercially available coffee. *Food Chemistry*, 141(4): 3335–3340. https://www.sciencedirect.com/science/article/pii/S0308814613007802.

Mishra, A.N., Bhadauria, S., Gaur, M.S. & Pasricha, R. 2010. Extracellular microbial synthesis of gold nanoparticles using fungus Hormoconis resinae. *JOM*, 62(11): 45–48. https://doi.org/10.1007/s11837-010-0168-6.

Mittal, A.K., Chisti, Y. & Banerjee, U.C. 2013. Synthesis of metallic nanoparticles using plant extracts. *Biotechnology Advances*, 31(2): 346–356. https://www.sciencedirect.com/science/article/pii/S0734975013000050 26 May 2019.

Mo, Y., Xu, W., Zhang, X. & Zhou, S. 2022. Enhanced Degradation of Rhodamine B through Peroxymonosulfate Activated by a Metal Oxide/Carbon Nitride Composite. *Water*, 14: 2054.

Moghadam, N.C.Z., Jasim, S.A., Ameen, F., Alotaibi, D.H., Nobre, M.A.L., Sellami, H. & Khatami, M. 2022. Nickel oxide nanoparticles synthesis using plant extract and evaluation of their antibacterial effects on Streptococcus mutans. *Bioprocess and Biosystems Engineering*, 45(7): 1201–1210. https://doi.org/10.1007/s00449-022-02736-6.

Mohamed Reda, G., Fan, H. & Tian, H. 2017. Room-temperature solid state synthesis of

Co3O4/ZnO p–n heterostructure and its photocatalytic activity. *Advanced Powder Technology*, 28(3): 953–963. https://www.sciencedirect.com/science/article/pii/S0921883116303971.

Mohammadi, F.M. & Ghasemi, N. 2018. Influence of temperature and concentration on biosynthesis and characterization of zinc oxide nanoparticles using cherry extract. *Journal of Nanostructure in Chemistry*, 8(1): 93–102. https://doi.org/10.1007/s40097-018-0257-6.

Mokrani, A. & Madani, K. 2016. Effect of solvent, time and temperature on the extraction of phenolic compounds and antioxidant capacity of peach (Prunus persica L.) fruit. *Separation and Purification Technology*, 162.

Molnár, Z., Bódai, V., Szakacs, G., Erdélyi, B., Fogarassy, Z., Sáfrán, G., Varga, T., Kónya, Z., Tóth-Szeles, E., Szucs, R. & Lagzi, I. 2018. Green synthesis of gold nanoparticles by thermophilic filamentous fungi. *Scientific Reports*, 8(1): 1–12.

Moon, J.-K. & Shibamoto, T. 2010. Formation of volatile chemicals from thermal degradation of less volatile coffee components: quinic acid, caffeic acid, and chlorogenic acid. *Journal of agricultural and food chemistry*, 58(9): 5465–5470.

Moorthy, S.K., Ashok, C.H., Rao, K.V. & Viswanathan, C. 2015. Synthesis and Characterization of Mgo Nanoparticles by Neem Leaves through Green Method. *Materials Today: Proceedings*, 2(9, Part A): 4360–4368. https://www.sciencedirect.com/science/article/pii/S2214785315008482.

Muhammad, H., Shaheen, R., Akram, B., Abdin, Z., Haq, S., Mahsud, S. & Ali, S. 2020. Green Synthesis of cobalt oxide nanoparticles for potential biological applications. *Materials Research Express*, 7.

Mukherjee, P., Senapati, S., Mandal, D., Ahmad, A., Khan, M.I., Kumar, R. & Sastry, M. 2002. Extracellular Synthesis of Gold Nanoparticles by the Fungus Fusarium oxysporum. *ChemBioChem*, 3(5): 461–463. https://doi.org/10.1002/1439-7633(20020503)3:5%3C461::AID-CBIC461%3E3.0.CO.

Mustapha, T., Misni, N., Ithnin, R., Daskum, A. & Unyah, Z. 2022. A Review on Plants and Microorganisms Mediated Synthesis of Silver Nanoparticles, Role of Plants Metabolites and Applications. *International Journal of Environmental Research and Public Health*, 19: 674.

Myo, H. & Khat-udomkiri, N. 2022. Optimization of ultrasound-assisted extraction of bioactive compounds from coffee pulp using propylene glycol as a solvent and their antioxidant activities. *Ultrasonics Sonochemistry*, 89: 106127. https://www.sciencedirect.com/science/article/pii/S1350417722002231.

Nadagouda, M.N. & Varma, R.S. 2008. Green synthesis of silver and palladium nanoparticles at room temperature using coffee and tea extract. *Green Chemistry*, 10(8): 859–862.

Nagajyothi, P.C., Prabhakar Vattikuti, S. V, Devarayapalli, K.C., Yoo, K., Shim, J. & Sreekanth, T.V.M. 2020. Green synthesis: Photocatalytic degradation of textile dyes using metal and metal oxide nanoparticles-latest trends and advancements. *Critical Reviews in Environmental Science and Technology*, 50(24): 2617–2723. https://doi.org/10.1080/10643389.2019.1705103.

Nagar, N. 2018. *Synthesis of Metal Nanoparticles and Their Application in Degradation of Textile Dyes by Advanced Oxidation Process*. University of Kota.

Nagar, N. & Devra, V. 2018. Green synthesis and characterization of copper nanoparticles using Azadirachta indica leaves. *Materials Chemistry and Physics*, 213: 44–51.

https://www.sciencedirect.com/science/article/pii/S0254058418302694.

Nagar, N. & Devra, V. 2019. Textile Dyes Degradation from Activated Peroxomonosulphate by Green synthesize Silver Nanoparticles: A Kinetic Study. *Journal of Inorganic and Organometallic Polymers and Materials*.

Naito, M., Yokoyama, T., Hosokawa, K. & Nogi, K. 2018. *Nanoparticle Technology Handbook*. Elsevier Science.

Nam, N.H. & Luong, N.H. 2019. Nanoparticles: synthesis and applications V. Grumezescu & A. M. Grumezescu, eds. *Materials for Biomedical Engineering*: 211–240. https://www.ncbi.nlm.nih.gov/pmc/articles/PMC7151836/.

Nanda, A. & Saravanan, M. 2009. Biosynthesis of silver nanoparticles from Staphylococcus aureus and its antimicrobial activity against MRSA and MRSE. *Nanomedicine: Nanotechnology, Biology and Medicine*, 5(4): 452–456. https://www.sciencedirect.com/science/article/pii/S1549963409000501.

Narayanan, R., Tabor, C. & El-Sayed, M.A. 2008. Can the Observed Changes in the Size or Shape of a Colloidal Nanocatalyst Reveal the Nanocatalysis Mechanism Type: Homogeneous or Heterogeneous? *Topics in Catalysis*, 48(1): 60. https://doi.org/10.1007/s11244-008-9057-4.

Nasrollahzadeh, M. & Mohammad Sajadi, S. 2016. Pd nanoparticles synthesized in situ with the use of Euphorbia granulate leaf extract: Catalytic properties of the resulting particles. *Journal of Colloid and Interface Science*, 462: 243–251. http://dx.doi.org/10.1016/j.jcis.2015.09.065.

Nasrollahzadeh, M., Sajadi, S.M. & Khalaj, M. 2014. Green synthesis of copper nanoparticles using aqueous extract of the leaves of Euphorbia esula L and their catalytic activity for ligand-free Ullmann-coupling reaction and reduction of 4-nitrophenol. *RSC Advances*, 4(88): 47313–47318. http://dx.doi.org/10.1039/C4RA08863H.

Nebesny, E. & Budryn, G. 2003. Antioxidative activity of green and roasted coffee beans as influenced by convection and microwave roasting methods and content of certain compounds. *European Food Research and Technology*, 217(2): 157–163. https://doi.org/10.1007/s00217-003-0705-4.

Niederberger, M. 2007. Nonaqueous Sol–Gel Routes to Metal Oxide Nanoparticles. *Accounts of Chemical Research*, 40(9): 793–800. https://doi.org/10.1021/ar600035e.

Niknejad, F., Nabili, M., Daie Ghazvini, R. & Moazeni, M. 2015. Green synthesis of silver nanoparticles: Another honor for the yeast model Saccharomyces cerevisiae. *Current Medical Mycology*, 1(3): 17–24.

Niroula, A., Khatri, S., Khadka, D. & Timilsina, R. 2019. Total phenolic contents and antioxidant activity profile of selected cereal sprouts and grasses. *International Journal of Food Properties*, 22(1): 427–437. https://doi.org/10.1080/10942912.2019.1588297.

Nosal, B.M., Sakaki, J.R., Kim, D.-O. & Chun, O.K. 2022. Impact of coffee preparation on total phenolic content in brewed coffee extracts and their contribution to the body's antioxidant status. *Food Science and Biotechnology*, 31(8): 1081–1088. https://doi.org/10.1007/s10068-022-01100-4.

Ohde, H., Hunt, F. & Wai, C.M. 2001. Synthesis of Silver and Copper Nanoparticles in a Water-in-Supercritical-Carbon Dioxide Microemulsion. *Chemistry of Materials*, 13(11): 4130–4135. https://doi.org/10.1021/cm010030g.

Ovais, M., Khalil, A.T., Islam, N.U., Ahmad, I., Ayaz, M., Saravanan, M., Shinwari, Z.K. & Mukherjee, S. 2018. Role of plant phytochemicals and microbial enzymes in biosynthesis of metallic nanoparticles. *Applied Microbiology and Biotechnology,*

102(16): 6799–6814.

Paixão, N., Perestrelo, R., Marques, J.C. & Câmara, J.S. 2007. Relationship between antioxidant capacity and total phenolic content of red, rosé and white wines. *Food Chemistry*, 105(1): 204–214. https://www.sciencedirect.com/science/article/pii/S0308814607003317 25 April 2019.

Pal, G., Rai, P. & Pandey, A. 2019. Green synthesis of nanoparticles: A greener approach for a cleaner future. In A. K. Shukla & S. B. T.-G. S. Iravani Characterization and Applications of Nanoparticles, eds. *Micro and Nano Technologies*. Elsevier: 1–26. https://www.sciencedirect.com/science/article/pii/B9780081025796000010.

Pal, S., Jana, U., Manna, P., Mohanta, G. & Manavalan, R. 2011. Nanoparticle: An overview of preparation and characterization. *Journal of Applied Pharmaceutical Science*, 1: 228–234.

Pandit, C., Roy, A., Ghotekar, S., Khusro, A., Islam, M.N., Emran, T. Bin, Lam, S.E., Khandaker, M.U. & Bradley, D.A. 2022. Biological agents for synthesis of nanoparticles and their applications. *Journal of King Saud University - Science*, 34(3): 101869. https://www.sciencedirect.com/science/article/pii/S1018364722000507.

Panzella, L., Cerruti, P., Aprea, P., Paolillo, R., Pellegrino, G., Moccia, F., Condorelli, G.G., Vollaro, A., Ambrogi, V., Catania, M.R., d'Ischia, M. & Napolitano, A. 2020. Silver nanoparticles on hydrolyzed spent coffee grounds (HSCG) for green antibacterial devices. *Journal of Cleaner Production*, 268: 122352.

Parveen, K., Banse, V. & Ledwani, L. 2016. Green synthesis of nanoparticles: Their advantages and disadvantages. *AIP Conference Proceedings*, 1724(1): 20048. https://aip.scitation.org/doi/abs/10.1063/1.4945168.

Peng, W., Liu, J., Li, C., Zong, F., Xu, W., Zhang, X. & Fang, Z. 2018. A multipath peroxymonosulfate activation process over supported by magnetic CuO-Fe3O4 nanoparticles for efficient degradation of 4-chlorophenol. *Korean Journal of Chemical Engineering*, 35(8): 1662–1672. https://doi.org/10.1007/s11814-018-0074-0.

Petcharoen, K. & Sirivat, A. 2012. Synthesis and characterization of magnetite nanoparticles via the chemical co-precipitation method. *Materials Science and Engineering: B*, 177(5): 421–427. https://www.sciencedirect.com/science/article/pii/S0921510712000499.

Pichersky, E. & Gang, D.R. 2000. Genetics and biochemistry of secondary metabolites in plants: an evolutionary perspective. *Trends in Plant Science*, 5(10): 439–445. https://www.sciencedirect.com/science/article/pii/S1360138500017416.

Pimpin, A. & Srituravanich, W. 2012. Review on Micro- and Nanolithography Techniques and Their Applications. *Engineering Journal*, 16: 37–56.

Prakash, S., Elavarasan, N., Venkatesan, A., Subashini, K., Sowndharya, M. & Sujatha, V. 2018. Green synthesis of copper oxide nanoparticles and its effective applications in Biginelli reaction, BTB photodegradation and antibacterial activity. *Advanced Powder Technology*, 29(12): 3315–3326. https://doi.org/10.1016/j.apt.2018.09.009.

Prasad Yadav, T., Manohar Yadav, R. & Pratap Singh, D. 2012. Mechanical Milling: a Top Down Approach for the Synthesis of Nanomaterials and Nanocomposites. *Nanoscience and Nanotechnology*, 2(3): 22–48.

Pulit, J., Banach, M. & Kowalski, Z. 2013. Chemical Reduction as the Main Method for Obtaining Nanosilver. *Journal of Computational and Theoretical Nanoscience, vol. 10, issue 2, pp. 276-284*, 10: 276–284.

Pushparaj, K., Liu, W.-C., Meyyazhagan, A., Orlacchio, A., Pappusamy, M., Vadivalagan, C., Robert, A.A., Arumugam, V.A., Kamyab, H., Klemeš, J.J., Khademi, T., Mesbah, M.,

Chelliapan, S. & Balasubramanian, B. 2022. Nano- from nature to nurture: A comprehensive review on facets, trends, perspectives and sustainability of nanotechnology in the food sector. *Energy*, 240: 122732. https://www.sciencedirect.com/science/article/pii/S0360544221029819.

Puvaneswari, N., Muthukrishnan, J. & Gunasekaran, P. 2006. Toxicity assessment and microbial degradation of azo dyes. *IJEB Vol.44(08) [August 2006]*, 44: 618–626. http://nopr.niscpr.res.in/handle/123456789/6554 13 August 2022.

Qiao, L., Xiao, H.Y., Meyer, H.M., Sun, J.N., Rouleau, C.M., Puretzky, A.A., Geohegan, D.B., Ivanov, I.N., Yoon, M., Weber, W.J. & Biegalski, M.D. 2013. Nature of the band gap and origin of the electro-/photo-activity of Co3O4. *Journal of Materials Chemistry C*, 1(31): 4628–4633. http://dx.doi.org/10.1039/C3TC30861H.

Rafique, M., Tahir, R., Gillani, S., Tahir, M., Shakil, M., Iqbal, T. & Abdellahi, M. 2019. Plant mediated green synthesis of zinc oxide nanoparticles from Syzygium Cumini for seed germination and wastewater purification. *International Journal of Environmental Analytical Chemistry*, 102.

Rahimi, G., Alizadeh, F. & Khodavandi, A. 2016. Mycosynthesis of Silver Nanoparticles from Candida albicans and its Antibacterial Activity against Escherichia coli and Staphylococcus aureus. *Tropical Journal of Pharmaceutical Research*, 15.

Rajaeiyan, A. & Bagheri-Mohagheghi, M.M. 2013. Comparison of sol-gel and co-precipitation methods on the structural properties and phase transformation of γ and α-Al2O3 nanoparticles. *Advances in Manufacturing*, 1(2): 176–182.

Rajendran, A., Siva, E., Dhanraj, C. & Senthilkumar, S. 2018. A Green and Facile Approach for the Synthesis Copper Oxide Nanoparticles Using Hibiscus rosa-sinensis Flower Extracts and It's Antibacterial Activities. *Journal of Bioprocessing & Biotechniques*, 08(03): 8–11.

Rajha, H.N., Darra, N. El, Hobaika, Z., Boussetta, N., Vorobiev, E., Maroun, R.G. & Louka, N. 2014. Extraction of Total Phenolic Compounds, Flavonoids, Anthocyanins and Tannins from Grape Byproducts by Response Surface Methodology. Influence of Solid-Liquid Ratio, Particle Size, Time, Temperature and Solvent Mixtures on the Optimization Process. *Food and Nutrition Sciences*, 2014(04): 397–409. http://www.scirp.org/journal/PaperInformation.aspx?PaperID=42786 25 August 2022.

Rameli, N., Jumbri, K., Wahab, R., Ramli, A. & Huyop, F. 2018. Synthesis and characterization of mesoporous silica nanoparticles using ionic liquids as a template. *Journal of Physics: Conference Series*, 1123: 12068.

Ramesh, P.S., Kokila, T. & Geetha, D. 2015. Plant mediated green synthesis and antibacterial activity of silver nanoparticles using Emblica officinalis fruit extract. *Spectrochimica Acta Part A: Molecular and Biomolecular Spectroscopy*, 142: 339–343. https://www.sciencedirect.com/science/article/pii/S1386142515000839.

Rana, A., Yadav, K. & Jagadevan, S. 2020. A comprehensive review on green synthesis of nature-inspired metal nanoparticles: Mechanism, application and toxicity. *Journal of Cleaner Production*, 272: 122880.

Rao, Y.F., Qu, L., Yang, H. & Chu, W. 2014. Degradation of carbamazepine by Fe(II)-activated persulfate process. *Journal of Hazardous Materials*, 268: 23–32. https://www.sciencedirect.com/science/article/pii/S0304389414000235.

Rastogi, A., Singh, P. & Haraz, F.A. 2018. Biological synthesis of nanoparticles: an environmentally benign approach. *Fundamentals of Nanoparticles*: 571–604. https://www.sciencedirect.com/science/article/pii/B9780323512558000239 22 April 2020.

Ratautas, D. & Dagys, M. 2020. Nanocatalysts Containing Direct Electron Transfer-Capable Oxidoreductases: Recent Advances and Applications. *Catalysts*, 10(1). https://www.mdpi.com/2073-4344/10/1/9.

Raveau, B. & Seikh, M. 2012. *Bernard Raveau and Md. Motin Seikh Cobalt Oxides*. Weinheim, Germany: Wiley-VCH.

Reis, N., Botelho, B.G., Franca, A.S. & Oliveira, L.S. 2017. Simultaneous Detection of Multiple Adulterants in Ground Roasted Coffee by ATR-FTIR Spectroscopy and Data Fusion. *Food Analytical Methods*, 10(8): 2700–2709. https://doi.org/10.1007/s12161-017-0832-3.

de Rigal, D., Gauillard, F. & Richard-Forget, F. 2000. Changes in the carotenoid content of apricot (Prunus armeniaca, var Bergeron) during enzymatic browning: β-carotene inhibition of chlorogenic acid degradation. *Journal of the Science of Food and Agriculture*, 80(6): 763–768. https://doi.org/10.1002/(SICI)1097-0010(20000501)80:6%3C763::AID-JSFA623%3E3.0.CO.

Roco, M.C. 1999. Nanoparticles and Nanotechnology Research. *Journal of Nanoparticle Research*, 1(1): 1–6. https://doi.org/10.1023/A:1010093308079.

Roduner, E. 2014. Understanding catalysis. *Chemical Society Reviews*, 43(24): 8226–8239. http://dx.doi.org/10.1039/C4CS00210E.

Rónavári, A., Kovács, D., Igaz, N., Vágvölgyi, C., Boros, I.M., Kónya, Z., Pfeiffer, I. & Kiricsi, M. 2017. Biological activity of green-synthesized silver nanoparticles depends on the applied natural extracts: A comprehensive study. *International Journal of Nanomedicine*, 12: 871–883.

Roque-Malherbe, R. 2019. Heterogeneous Catalysis Review. , 19: 70.

Roy, A. & Bharadvaja, N. 2017. Centella Asiatica: A Pharmaceutically Important Medicinal Plant. *Current Trends in Biomedical Engineering and Bioscience*, 5: 555661.

Ruchita, Srivastava, R. & Yadav, B.C. 2016. Nanolithography: Processing Methods for Nanofabrication Development. *Imperial journal of interdisciplinary research*, 2.

Ryaidh, A.-H. & Al-Qayim, M.A.J. 2017. Bio-Synthesis and Characterizations of Magnetic Iron Oxide Nanoparticles Mediated By Iraq Propolis Extract. *IOSR Journal of Pharmacy and Biological Sciences (IOSR-JPBS*, 12(6): 65–73. www.iosrjournals.org.

Sabzoi, N., Siddiqui, M.T.H., Mujawar, M., Baloch, H., Abdullah, E., Mazari, S., Griffin, G., Srinivasan, M. & Tanksale, A. 2018. Iron Oxide Nanomaterials for the Removal of Heavy Metals and Dyes From Wastewater. In *Nanoscale Materials in Water Purification*. Elsevier: 447–472.

Sadowski, Z., Maliszewska, I., Grochowalska, B., Polowczyk, I. & Koźlecki, T. 2008. Synthesis of silver nanoparticles using microorganisms. *Materials Science-Poland*, 26.

Saeed, N., Khan, M.R. & Shabbir, M. 2012. Antioxidant activity, total phenolic and total flavonoid contents of whole plant extracts Torilis leptophylla L. *BMC Complementary and Alternative Medicine*, 12(1): 221. https://doi.org/10.1186/1472-6882-12-221.

Salama, A., Mohamed, A., Aboamera, N.M., Osman, T.A. & Khattab, A. 2018. Photocatalytic degradation of organic dyes using composite nanofibers under UV irradiation. *Applied Nanoscience*, 8(1): 155–161. https://doi.org/10.1007/s13204-018-0660-9.

Salgado, P., Márquez, K., Rubilar, O., Contreras, D. & Vidal, G. 2019. The effect of phenolic compounds on the green synthesis of iron nanoparticles (FexOy-NPs) with photocatalytic activity. *Applied Nanoscience*, 9(3): 371–385. https://doi.org/10.1007/s13204-018-0931-5.

van Santen, R.A. 2012. Catalysis in perspective : historic review. *Catalysis : from principles to applications*: 1–19.

Saragih, B., Rahmawati, M., Ismanto, A. & Saragih, F.M. 2022. Profile of FTIR (Fourier Transform Infra Red) and Comparison of Antioxidant Activity of Coffee with Tiwai (Eleutherine americana Merr) BT - Proceedings of the 6th International Conference of Food, Agriculture, and Natural Resource (IC-FANRES 2021). In Atlantis Press: 27–31. https://doi.org/10.2991/absr.k.220101.005.

Saratale, R., Saratale, G., Chang, J.-S. & Govindwar, S. 2011. *Bacterial Decolorization and Degradation of Azo Dyes: A Review*.

Sarfraz, A. & Hasanain, K. 2014. Size Dependence of Magnetic and Optical Properties of Co 3 O 4 Nanoparticles. *Acta Physica Polonica A*, 125: 139–144.

Sari, A.Y., Eko, A.S., Candra, K., Hasibuan, D.P., Ginting, M., Sebayang, P. & Simamora, P. 2017. Synthesis, Properties and Application of Glucose Coated Fe3O4 Nanoparticles Prepared by Co-precipitation Method. *IOP Conference Series: Materials Science and Engineering*, 214(1).

Sastry, M., Ahmad, A., Khan, M. & Kumar, R. 2003. Biosynthesis of metal nanoparticles using fungi and actinomycete. *Current Science*, 85.

Schlögl, R. 2015. Heterogeneous Catalysis. *Angewandte Chemie International Edition*, 54(11): 3465–3520. https://doi.org/10.1002/anie.201410738.

Schlögl, R. & Abd Hamid, S.B. 2004. Nanocatalysis: Mature Science Revisited or Something Really New? *Angewandte Chemie International Edition*, 43(13): 1628–1637. https://doi.org/10.1002/anie.200301684.

Senapati, S. & Maiti, P. 2020. Emerging bio-applications of two-dimensional nanoheterostructure materials. In S. Jit & S. B. T.-2D N. H. M. Das, eds. *Micro and Nano Technologies*. Elsevier: 243–255. https://www.sciencedirect.com/science/article/pii/B9780128176788000099.

Shan, A., Idrees, A., Zaman, W.Q., Abbas, Z., Ali, M., Rehman, M.S.U., Hussain, S., Danish, M., Gu, X. & Lyu, S. 2021. Synthesis of nZVI-Ni@BC composite as a stable catalyst to activate persulfate: Trichloroethylene degradation and insight mechanism. *Journal of Environmental Chemical Engineering*, 9(1): 104808. https://www.sciencedirect.com/science/article/pii/S221334372031157X.

Sharifi, S.L., Shakur, H.R., Mirzaei, A., Salmani, A. & Hosseini, M.H. 2013. Characterization of Cobalt Oxide Co 3 O 4 Nanoparticles Prepared by Various Methods: Effect of Calcination Temperatures on Size, Dimension and Catalytic Decomposition of Hydrogen Peroxide. *Int. J. Nanosci. Nanotechnol*, 9(1): 51–58.

Sharma, R. & Tripathi, A. 2022. Green synthesis of nanoparticles and its key applications in various sectors. *Materials Today: Proceedings*, 48: 1626–1632. https://www.sciencedirect.com/science/article/pii/S2214785321064324.

Shen, C., Song, S., Zang, L., Kang, X., Wen, Y., Liu, W. & Fu, L. 2010. Efficient removal of dyes in water using chitosan microsphere supported cobalt (II) tetrasulfophthalocyanine with H2O2. *Journal of Hazardous Materials*, 177(1): 560–566. https://www.sciencedirect.com/science/article/pii/S0304389409020585.

Shi, P., Su, R., Zhu, S., Zhu, M., Li, D. & Xu, S. 2012. Supported cobalt oxide on graphene oxide: Highly efficient catalysts for the removal of Orange II from water. *Journal of Hazardous Materials*, 229–230: 331–339. https://www.sciencedirect.com/science/article/pii/S0304389412006279?via%3Dihub 5 April 2019.

Shi, Y., Ding, J. & Yin, H. 2000. CoFe2O4 nanoparticles prepared by the mechanochemical method. *Journal of Alloys and Compounds*, 308(1–2): 290–295.

Shi, Y., Wang, H., Song, G., Zhang, Y., Tong, L., Sun, Y. & Ding, G. 2022. Efficient degradation of organic dyes using peroxymonosulfate activated by magnetic graphene oxide. *RSC Advances*, 12(33): 21026–21040. http://dx.doi.org/10.1039/D2RA03511A.

Shukla, P., Sun, H., Wang, S., Ang, H.M. & Tadé, M.O. 2011. Nanosized Co3O4/SiO2 for heterogeneous oxidation of phenolic contaminants in waste water. *Separation and Purification Technology*, 77(2): 230–236. https://www.sciencedirect.com/science/article/pii/S1383586610005095.

Siddique, M., Khan, N. & Saeed, M. 2018. Photocatalytic Activity of Bismuth Ferrite Nanoparticles Synthesized via Sol-Gel Route. *Zeitschrift für Physikalische Chemie*, 233.

Siddique, M., Khan, N.M., Saeed, M., Ali, S. & Shah, Z. 2021. Green synthesis of cobalt oxide nanoparticles using Citrus medica leaves extract: characterization and photo-catalytic activity. *Zeitschrift für Physikalische Chemie*, 235(6): 663–681. https://doi.org/10.1515/zpch-2019-1583.

da Silva, A.F.V., Fagundes, A.P., Macuvele, D.L.P., de Carvalho, E.F.U., Durazzo, M., Padoin, N., Soares, C. & Riella, H.G. 2019. Green synthesis of zirconia nanoparticles based on Euclea natalensis plant extract: Optimization of reaction conditions and evaluation of adsorptive properties. *Colloids and Surfaces A: Physicochemical and Engineering Aspects*, 583: 123915. https://www.sciencedirect.com/science/article/pii/S0927775719309033.

Singaravelu, G., Arockiamary, J.S., Kumar, V.G. & Govindaraju, K. 2007. A novel extracellular synthesis of monodisperse gold nanoparticles using marine alga, Sargassum wightii Greville. *Colloids and Surfaces B: Biointerfaces*, 57(1): 97–101. https://www.sciencedirect.com/science/article/pii/S0927776507000252.

Singh, A.K. & Srivastava, O.N. 2015. One-Step Green Synthesis of Gold Nanoparticles Using Black Cardamom and Effect of pH on Its Synthesis. *Nanoscale Research Letters*, 10(1): 353. https://doi.org/10.1186/s11671-015-1055-4.

Singh, B.R., Wechter, M.A., Hu, Y. & Lafontaine, C. 1998. Determination of caffeine content in coffee using Fourier transform infra-red spectroscopy in combination with attenuated total reflectance technique: a bioanalytical chemistry experiment for biochemists. *Biochemical Education*, 26: 243–247.

Singh, J., Dutta, T., Kim, K.-H., Rawat, M., Samddar, P. & Kumar, P. 2018. 'Green' synthesis of metals and their oxide nanoparticles: applications for environmental remediation. *Journal of Nanobiotechnology*, 16(1): 84. https://doi.org/10.1186/s12951-018-0408-4.

Singh, M., Goyal, M. & Devlal, K. 2018. Size and shape effects on the band gap of semiconductor compound nanomaterials. *Journal of Taibah University for Science*, 12(4): 470–475. https://doi.org/10.1080/16583655.2018.1473946.

Singh, P., Kim, Y.-J., Zhang, D. & Yang, D.-C. 2016. Biological Synthesis of Nanoparticles from Plants and Microorganisms. *Trends in Biotechnology*, 34(7): 588–599. https://www.sciencedirect.com/science/article/abs/pii/S0167779916000408 22 April 2020.

Singhai, M., Chhabra, V., Kang, P. & Shah, D.O. 1997. Synthesis of ZnO nanoparticles for varistor application using Zn-substituted aerosol ot microemulsion. *Materials Research Bulletin*, 32(2): 239–247. https://www.sciencedirect.com/science/article/pii/S0025540896001754 12 August 2019.

Singleton, V.L. & Rossi, J.A. 1965. Colorimetry of Total Phenolics with Phosphomolybdic-

Phosphotungstic Acid Reagents. *American Journal of Enology and Viticulture*, 16(3): 144–158. https://www.ajevonline.org/content/16/3/144.

Somwanshi, S.B., Somvanshi, S.B. & Kharat, P.B. 2020. Nanocatalyst: A Brief Review on Synthesis to Applications. *Journal of Physics: Conference Series*, 1644(1): 12046. https://dx.doi.org/10.1088/1742-6596/1644/1/012046.

Soobrattee, M.A., Neergheen, V.S., Luximon-Ramma, A., Aruoma, O.I. & Bahorun, T. 2005. Phenolics as potential antioxidant therapeutic agents: mechanism and actions. *Mutation research*, 579(1–2): 200–213.

Spreafico, C., Russo, D. & Degl'Innocenti, R. 2022. Laser pyrolysis in papers and patents. *Journal of Intelligent Manufacturing*, 33(2): 353–385. https://doi.org/10.1007/s10845-021-01809-9.

Sudhasree, S., Doss, V.K., Shakila Banu, A. & Kurian, G.A. 2015. Desmodium gangeticum root aqueous extract mediated synthesis of Ni nanoparticle and its biological evaluation. *International Journal of Pharmacy and Pharmaceutical Sciences*, 7: 141–146.

Sun, L., Cao, G., Xu, M., Cheng, G., Xia, D., Yuan, X. & Liu, J. 2021. Visible-light-induced peroxymonosulfate activation over ZnFe2O4 fine nanoparticles for ofloxacin degradation. *Elementa: Science of the Anthropocene*, 9(1): 96. https://doi.org/10.1525/elementa.2020.00096.

Sun, Q., Cai, X., Li, J., Zheng, M., Chen, Z. & Yu, C.-P. 2014. Green synthesis of silver nanoparticles using tea leaf extract and evaluation of their stability and antibacterial activity. *Colloids and Surfaces A: Physicochemical and Engineering Aspects*, 444: 226–231. https://www.sciencedirect.com/science/article/pii/S0927775714000065.

Sutradhar, P., Debbarma, M. & Saha, M. 2016. Microwave Synthesis of Zinc Oxide Nanoparticles Using Coffee Powder Extract and Its Application for Solar Cell. *Synthesis and Reactivity in Inorganic, Metal-Organic and Nano-Metal Chemistry*, 46(11): 1622–1627.

Sutradhar, P., Debnath, N. & Saha, M. 2013. Microwave-assisted rapid synthesis of alumina nanoparticles using tea, coffee and triphala extracts. *Advances in Manufacturing*, 1(4): 357–361.

Sutradhar, P., Saha, M. & Maiti, D. 2014. Microwave synthesis of copper oxide nanoparticles using tea leaf and coffee powder extracts and its antibacterial activity. *Journal of Nanostructure in Chemistry*, 4(1): 4–9.

Syahirah Kamarudin, N., Jusoh, R., Dina Setiabudi, H. & Fateha Sukor, N. 2018. Photodegradation of methylene blue using phyto-mediated synthesis of silver nanoparticles: effect of calcination treatment. *Materials Today: Proceedings*, 5(10, Part 2): 21981–21989. https://www.sciencedirect.com/science/article/pii/S2214785318318583.

Tahir, M.B., Rafique, M., Rafique, M.S., Nawaz, T., Rizwan, M. & Tanveer, M. 2020. Photocatalytic nanomaterials for degradation of organic pollutants and heavy metals. In M. B. Tahir, M. Rafique, & M. S. B. T.-N. and P. for E. A. Rafique, eds. *Micro and Nano Technologies*. Elsevier: 119–138. https://www.sciencedirect.com/science/article/pii/B9780128211922000085.

Tan, J., Xu, C., Zhang, X. & Huang, Y. 2022. MOFs-derived defect carbon encapsulated magnetic metallic Co nanoparticles capable of efficiently activating PMS to rapidly degrade dyes. *Separation and Purification Technology*, 289: 120812. https://www.sciencedirect.com/science/article/pii/S1383586622003707.

Tan, M.C., Tan, C.P. & Ho, C.W. 2013. Effects of extraction solvent system, time and

temperature on total phenolic content of henna (Lawsonia inermis) stems. *International Food Research Journal*, 20(6): 3117–3123. https://www.proquest.com/scholarly-journals/effects-extraction-solvent-system-time/docview/1491100557/se-2?accountid=26862.

Tao, H., Wu, T., Aldeghi, M., Wu, T.C., Aspuru-Guzik, A. & Kumacheva, E. 2021. Nanoparticle synthesis assisted by machine learning. *Nature Reviews Materials*, 6(8): 701–716. https://doi.org/10.1038/s41578-021-00337-5.

Tarigan, E., Wardiana, E., Hilmi, Y. & Komarudin, N. 2022. The changes in chemical properties of coffee during roasting: A review. *IOP Conference Series: Earth and Environmental Science*, 974: 12115.

Thakur, B.K., Kumar, A. & Kumar, D. 2019. Green synthesis of titanium dioxide nanoparticles using Azadirachta indica leaf extract and evaluation of their antibacterial activity. *South African Journal of Botany*, 124: 223–227. https://doi.org/10.1016/j.sajb.2019.05.024.

Thoo, Y.Y., Ho, S.K., Liang, J.Y., Ho, C.W. & Tan, C.P. 2010. Effects of binary solvent extraction system, extraction time and extraction temperature on phenolic antioxidants and antioxidant capacity from mengkudu (Morinda citrifolia). *Food Chemistry*, 120(1): 290–295. https://www.sciencedirect.com/science/article/pii/S0308814609011248.

Tian, L., He, G., Cai, Y., Wu, S., Su, Y., Yan, H., Yang, C., Chen, Y. & Li, L. 2018. Co3O4 based non-enzymatic glucose sensor with high sensitivity and reliable stability derived from hollow hierarchical architecture. *Nanotechnology*, 29(7): 75502–75532.

Tijani, J.O., Ugochukwu, O., Fadipe, L.A., Bankole, M.T., Abdulkareem, A.S. & Roos, W.D. 2019. One-step green synthesis of WO3 nanoparticles using Spondias mombin aqueous extract: effect of solution pH and calcination temperature. *Applied Physics A*, 125(3): 162. https://doi.org/10.1007/s00339-019-2450-y.

Torres-Martínez, L., Kharissova, O. & Kharisov, B. 2019. *Handbook of Ecomaterials, Volumes 1-5*.

Traiwatcharanon, P., Timsorn, K. & Wongchoosuk, C. 2016. Effect of pH on the Green Synthesis of Silver Nanoparticles through Reduction with Pistiastratiotes L. Extract. *Advanced Materials Research*, 1131: 223–226. https://www.scientific.net/AMR.1131.223 12 September 2022.

Trewyn, B.G., Slowing, I.I., Giri, S., Chen, H.-T. & Lin, V.S.-Y. 2007. Synthesis and Functionalization of a Mesoporous Silica Nanoparticle Based on the Sol–Gel Process and Applications in Controlled Release. *Accounts of Chemical Research*, 40(9): 846–853. https://doi.org/10.1021/ar600032u.

Trugo, L.C. & Macrae, R. 1984. A study of the effect of roasting on the chlorogenic acid composition of coffee using HPLC. *Food Chemistry*, 15(3): 219–227. https://www.sciencedirect.com/science/article/pii/0308814684900062.

Twaij, B.M. & Hasan, M.N. 2022. Bioactive Secondary Metabolites from Plant Sources: Types, Synthesis, and Their Therapeutic Uses. *International Journal of Plant Biology*, 13(1): 4–14.

Upadhyay, R. & Mohan Rao, L.J. 2013. An Outlook on Chlorogenic Acids—Occurrence, Chemistry, Technology, and Biological Activities. *Critical Reviews in Food Science and Nutrition*, 53(9): 968–984. https://doi.org/10.1080/10408398.2011.576319.

Vafaee, M. & Ghamsari, M.S. 2007. Preparation and characterization of ZnO nanoparticles by a novel sol–gel route. *Materials Letters*, 61(14–15): 3265–3268. https://www.sciencedirect.com/science/article/abs/pii/S0167577X06013644 12 August 2019.

Vanaja, M., Shanmugam, R., Paulkumar, K., Gnanajobitha, G., Chelladurai, M. & Gurusamy, A. 2013. Kinetic study on green synthesis of silver nanoparticles using Coleus aromaticus leaf extract. *Advances in Applied Science Research*, 4: 50–55.

Vanlalveni, C., Lallianrawna, S., Biswas, A., Selvaraj, M., Changmai, B. & Rokhum, S.L. 2021. Green synthesis of silver nanoparticles using plant extracts and their antimicrobial activities: a review of recent literature. *RSC Adv.*, 11(5): 2804–2837. http://dx.doi.org/10.1039/D0RA09941D.

Vatai, T., Škerget, M. & Knez, Ž. 2009. Extraction of phenolic compounds from elder berry and different grape marc varieties using organic solvents and/or supercritical carbon dioxide. *Journal of Food Engineering*, 90(2): 246–254. https://www.sciencedirect.com/science/article/pii/S0260877408003178.

Venkat Kumar, S. & Rajeshkumar, S. 2018. Plant-Based Synthesis of Nanoparticles and Their Impact. In D. K. Tripathi, P. Ahmad, S. Sharma, D. K. Chauhan, & N. K. B. T.-N. in P. Dubey Algae, and Microorganisms, eds. *Nanomaterial in Plants, Algae, and Microorganisms*. Academic Press: 33–57. https://www.sciencedirect.com/science/article/pii/B9780128114872000025.

Vennela, A. 2019. Structural and Optical Properties of Co3O4 Nanoparticles Prepared by Sol-gel Technique for Photocatalytic Application. *International Journal of Electrochemical Science*, 14: 3535–3552.

Ventura-camargo, B.D.C. & Marin-morales, M.A. 2013. Azo Dyes: Characterization and Toxicity– A Review. *Textiles and Light Industrial Science and Technology*, (October).

Venugopal, G. & Kim, S.-J. 2013. Nanolithography. In 187–206.

Vidal-Vidal, J., Rivas, J. & López-Quintela, M.A. 2006. Synthesis of monodisperse maghemite nanoparticles by the microemulsion method. *Colloids and Surfaces A: Physicochemical and Engineering Aspects*, 288(1–3): 44–51. https://www.sciencedirect.com/science/article/pii/S0927775706003128 12 August 2019.

Vieira, A.J.S.C., Gaspar, E.M. & Santos, P.M.P. 2020. Mechanisms of potential antioxidant activity of caffeine. *Radiation Physics and Chemistry*, 174: 108968. https://www.sciencedirect.com/science/article/pii/S0969806X20302899.

Vigneshwaran, N., Ashtaputre, N.M., Varadarajan, P. V, Nachane, R.P., Paralikar, K.M. & Balasubramanya, R.H. 2007. Biological synthesis of silver nanoparticles using the fungus Aspergillus flavus. *Materials Letters*, 61(6): 1413–1418. https://www.sciencedirect.com/science/article/pii/S0167577X06008512.

Vignoli, J.A., Bassoli, D.G. & Benassi, M.T. 2011. Antioxidant activity, polyphenols, caffeine and melanoidins in soluble coffee: The influence of processing conditions and raw material. *Food Chemistry*, 124(3): 863–868. https://www.sciencedirect.com/science/article/pii/S0308814610008319.

Vijayaraghavan, K. & Ashokkumar, T. 2017. Plant-mediated biosynthesis of metallic nanoparticles: A review of literature, factors affecting synthesis, characterization techniques and applications. *Journal of Environmental Chemical Engineering*, 5(5): 4866–4883. https://www.sciencedirect.com/science/article/pii/S2213343717304645.

Wadekar, K.F., Nemade K.R. & Waghuley S.A. 2017. Chemical synthesis of cobalt oxide (Co3O4) nanoparticles using Co-precipitation method. *Research Journal of Chemical International Science Community Association Research Journal of Chemical Sciences Res. J. Chem. Sci*, 7(71): 53–55. http://www.isca.in/rjcs/Archives/v7/i1/9.ISCA-RJCS-2016-055.pdf.

Wadhwani, S.A., Gorain, M., Banerjee, P.P., Shedbalkar, U.U., Singh, R., Kundu, G.C. &

Chopade, B.A. 2017. Green synthesis of selenium nanoparticles using Acinetobacter sp. SW30: optimization, characterization and its anticancer activity in breast cancer cells. *International Journal of Nanomedicine*, 12: 6841–6855.

Wang, D., Liu, L., Jiang, X., Yu, J. & Chen, X. 2015. Adsorption and removal of malachite green from aqueous solution using magnetic β-cyclodextrin-graphene oxide nanocomposites as adsorbents. *Colloids and Surfaces A: Physicochemical and Engineering Aspects*, 466: 166–173. http://dx.doi.org/10.1016/j.colsurfa.2014.11.021.

Wang, G., Zhao, K., Gao, C., Wang, J., Mei, Y., Zheng, X. & Zhu, P. 2021. Green synthesis of copper nanoparticles using green coffee bean and their applications for efficient reduction of organic dyes. *Journal of Environmental Chemical Engineering*, 9(4): 105331.

Wang, M., Zhang, W., Zheng, X. & Zhu, P. 2017. Antibacterial and catalytic activities of biosynthesized silver nanoparticles prepared by using an aqueous extract of green coffee bean as a reducing agent. *RSC Advances*, 7(20): 12144–12149.

Wang, Z., Fang, C. & Mallavarapu, M. 2015. Characterization of iron-polyphenol complex nanoparticles synthesized by Sage (Salvia officinalis) leaves. *Environmental Technology and Innovation*, 4: 92–97. http://dx.doi.org/10.1016/j.eti.2015.05.004.

Whatmore, R.W. 2006. Nanotechnology - What is it? Should we be worried? *Occupational medicine (Oxford, England)*, 56: 295–299.

Wianowska, D. & Gil, M. 2019. Recent advances in extraction and analysis procedures of natural chlorogenic acids. *Phytochemistry Reviews*, 18(1): 273–302. https://doi.org/10.1007/s11101-018-9592-y.

Wu, H., Gu, J., BK, A., Nawaz, M.A., Barrow, C.J., Dunshea, F.R. & Suleria, H.A.R. 2022. Effect of processing on bioaccessibility and bioavailability of bioactive compounds in coffee beans. *Food Bioscience*, 46: 101373. https://www.sciencedirect.com/science/article/pii/S2212429221004983.

Xiao, R., Luo, Z., Wei, Z., Luo, S., Spinney, R., Yang, W. & Dionysiou, D.D. 2018. Activation of peroxymonosulfate/persulfate by nanomaterials for sulfate radical-based advanced oxidation technologies. *Current Opinion in Chemical Engineering*, 19: 51–58. https://www.sciencedirect.com/science/article/pii/S2211339817300849.

Yang, J., Chen, C., Ji, H., Ma, W. & Zhao, J. 2005. Mechanism of TiO2-Assisted Photocatalytic Degradation of Dyes under Visible Irradiation: Photoelectrocatalytic Study by TiO2-Film Electrodes. *The Journal of Physical Chemistry B*, 109(46): 21900–21907. https://doi.org/10.1021/jp0540914.

Yang, M.H., Chandra, S., Khan, S., ElSohly, M.A., Avula, B., Lata, H. & Khan, I.A. 2014. Assessment of Total Phenolic and Flavonoid Content, Antioxidant Properties, and Yield of Aeroponically and Conventionally Grown Leafy Vegetables and Fruit Crops: A Comparative Study. *Evidence-Based Complementary and Alternative Medicine*, 2014: 1–9.

Yang, Q., Choi, H. & Dionysiou, D.D. 2007. Nanocrystalline cobalt oxide immobilized on titanium dioxide nanoparticles for the heterogeneous activation of peroxymonosulfate. *Applied Catalysis B: Environmental*, 74(1–2): 170–178. https://www.sciencedirect.com/science/article/pii/S0926337307000422 1 July 2019.

Yao, W.-T., Yu, S.-H., Zhou, Y., Jiang, Jun, Wu, Q.-S., Zhang, L. & Jiang, Jie. 2005. Formation of Uniform CuO Nanorods by Spontaneous Aggregation: Selective Synthesis of CuO, Cu2O, and Cu Nanoparticles by a Solid−Liquid Phase Arc Discharge Process. *The Journal of Physical Chemistry B*, 109(29): 14011–14016. https://doi.org/10.1021/jp0517605.

Yao, Y., Yang, Z., Sun, H. & Wang, S. 2012. Hydrothermal Synthesis of Co3O4–Graphene for Heterogeneous Activation of Peroxymonosulfate for Decomposition of Phenol. *Industrial & Engineering Chemistry Research*, 51(46): 14958–14965. https://doi.org/10.1021/ie301642g.

Yarestani, M., Khalaji, A., Rohani, A. & Das, D. 2014. Hydrothermal synthesis of cobalt oxide nanoparticles: Its optical and magnetic properties. *Journal of Sciences, Islamic Republic of Iran*, 25: 339–343.

Yaseen, D.A. & Scholz, M. 2019. Textile dye wastewater characteristics and constituents of synthetic effluents: a critical review. *International Journal of Environmental Science and Technology*, 16(2): 1193–1226. https://doi.org/10.1007/s13762-018-2130-z.

Zapesochnaya, G.G. & Ban'kovskii, A.I. 2004. Plant polyphenols. *Chemistry of Natural Compounds*, 1(4): 224–227.

Zazouli, M.A., Ghanbari, F., Yousefi, M. & Madihi-Bidgoli, S. 2017. Photocatalytic degradation of food dye by Fe3O4–TiO2 nanoparticles in presence of peroxymonosulfate: The effect of UV sources. *Journal of Environmental Chemical Engineering*, 5(3): 2459–2468. https://www.sciencedirect.com/science/article/pii/S2213343717301744.

Zhan, G., Huang, J., Lin, L., Lin, W., Emmanuel, K. & Li, Q. 2011. Synthesis of gold nanoparticles by Cacumen Platycladi leaf extract and its simulated solution: toward the plant-mediated biosynthetic mechanism. *Journal of Nanoparticle Research*, 13(10): 4957. https://doi.org/10.1007/s11051-011-0476-y.

Zhang, B., Zhang, Y., Xiang, W., Teng, Y. & Wang, Y. 2017. Comparison of the catalytic performances of different commercial cobalt oxides for peroxymonosulfate activation during dye degradation. *Chemical Research in Chinese Universities*, 33(5): 822–827. https://doi.org/10.1007/s40242-017-6413-6.

Zhang, J., Chen, M. & Zhu, L. 2016. Activation of persulfate by Co3O4 nanoparticles for orange G degradation. *RSC Advances*, 6(1): 758–768. http://dx.doi.org/10.1039/C5RA22457H.

Zhang, M., Chen, X., Zhou, H., Murugananthan, M. & Zhang, Y. 2015. Degradation of p-nitrophenol by heat and metal ions co-activated persulfate. *Chemical Engineering Journal*, 264: 39–47. https://www.sciencedirect.com/science/article/pii/S1385894714015198.

Zhang, Q., Chen, J., Dai, C., Zhang, Y. & Zhou, X. 2015. Degradation of carbamazepine and toxicity evaluation using the UV/persulfate process in aqueous solution. *Journal of Chemical Technology and Biotechnology*, 90(4): 701–708.

Zhang, Q., Kano, J. & Saito, F. 2007. Chapter 11 Fine Grinding of Materials in Dry Systems and Mechanochemistry. *Handbook of Powder Technology*, 12: 509–528. https://www.sciencedirect.com/science/article/pii/S0167378507120145 5 August 2019.

Zhang, T., Zhou, T., He, L., Xu, D. & Bai, L. 2020. Oxidative degradation of Rhodamine B by Ag@CuO nanocomposite activated persulfate. *Synthetic Metals*, 267: 116479. https://www.sciencedirect.com/science/article/pii/S0379677920302101.

Zhang, X. & Chan, K.-Y. 2003. Water-in-Oil Microemulsion Synthesis of Platinum−Ruthenium Nanoparticles, Their Characterization and Electrocatalytic Properties. *Chemistry of Materials*, 15(2): 451–459. https://doi.org/10.1021/cm0203868.

Zhao, Y., Dai, X., Wang, F., Zhang, X., Fan, C. & Liu, X. 2019. Nanofabrication based on DNA nanotechnology. *Nano Today*, 26: 123–148.

Zheng, B., Kong, T., Jing, X., Odoom-Wubah, T., Li, X., Sun, D., Lu, F., Zheng, Y., Huang, J.

& Li, Q. 2013. Plant-mediated synthesis of platinum nanoparticles and its bioreductive mechanism. *Journal of Colloid and Interface Science*, 396: 138–145. https://www.sciencedirect.com/science/article/pii/S0021979713000441.

Zhou, L., Song, W., Chen, Z. & Yin, G. 2013. Degradation of Organic Pollutants in Wastewater by Bicarbonate-Activated Hydrogen Peroxide with a Supported Cobalt Catalyst. *Environmental Science & Technology*, 47(8): 3833–3839. https://doi.org/10.1021/es400101f.

Zhu, K., Wang, J., Wang, Y., Jin, C. & Ganeshraja, A.S. 2016. Visible-light-induced photocatalysis and peroxymonosulfate activation over ZnFe2O4 fine nanoparticles for degradation of Orange II. *Catalysis Science & Technology*, 6(7): 2296–2304. http://dx.doi.org/10.1039/C5CY01735A.

Zuorro, A., Maffei, G., Iannone, A. & Lavecchia, R. 2017. Production of silver nanoparticles by spent coffee grounds extracts. *Trends in Green Chemistry*, 03(02): 9889–9889.

Appendix

Western Cape Coffee Data

Page 1

This short electronic survey aims to assist in the retrieval of data regarding the daily consumption of coffee in the Western Cape and the disposal of the coffee waste in order to gain new insight on the industry.

Please complete the following fields *

Name & Surname	_Caiau Nodi_
Company/Franchise	████████████
Employment Position	_Manager_
Suburb	_Milnerton_

Giving an average estimation, how many bags of coffee does your store use each month *

Please provide the mass of each coffee bag below *

~1 kg PH

80 kg / month

Do you donate your daily coffee waste to landfill? *

○ yes
○ no

If you answered no to the previous question, please state how your store handles its daily coffee waste

Western Cape Coffee Data

Page 1

This short electronic survey aims to assist in the retrieval of data regarding the daily consumption of coffee in the Western Cape and the disposal of the coffee waste in order to gain new insight on the industry.

Please complete the following fields *

Name & Surname	Georgina Farrell
Company/Franchise	██████████
Employment Position	Manager
Suburb	Milnetton

Giving an average estimation, how many bags of coffee does your store use each month *

[ ]

Please provide the mass of each coffee bag below *

40 Kg /PM grams

40 Kg / month

Do you discard your daily coffee waste to landfills? *

(✓) yes

( ) no

If you selected no to the previous question, please state how your store handles its daily coffee waste

133

Western Cape Coffee Data

Page 1

This short electronic survey aims to assist in the retrieval of data regarding the daily consumption of coffee in the Western Cape and the disposal of the coffee waste in order to gain new insight on the industry.

Please complete the following fields *

Name & Surname	Willan Harelun
Company/Franchise	████████████████
Employment Position	General Manager -
Suburb	Milneton

Giving an average estimation, how many bags of coffee does your store use each month *

Please provide the mass of each coffee bag below *

18 - 24 kg   grams ✗ 24 kg / W

192 Kg / month

Do you discard your daily coffee waste to landfills? *

⊘ yes

◯ no

If you selected no to the previous question, please state how your store handles its daily coffee waste

Landfill

134

Western Cape Coffee Data

Page 1

This short electronic survey aims to assist in the retrieval of data regarding the daily consumption of coffee in the Western Cape and the disposal of the coffee waste in order to gain new insight on the industry.

Please complete the following fields *

Name & Surname	Andrew Evans
Company/Franchise	███████████
Employment Position	Manager
Suburb	CBD

Giving an average estimation, how many bags of coffee does your store use each month *

Please provide the mass of each coffee bag below *

23 Kg / d grams

713 Kg / month

Do you discard your daily coffee waste to landfills? *

○ yes

✓ no

If you selected no to the previous question, please state how your store handles its daily coffee waste

Reuse coffee to make iced coffees.

135

Western Cape Coffee Data

Page 1

This short electronic survey aims to assist in the retrieval of data regarding the daily consumption of coffee in the Western Cape and the disposal of the coffee waste in order to gain new insight on the industry.

Please complete the following fields *

Name & Surname	Debbie
Company/Franchise	███████
Employment Position	Manager
Suburb	Tygervalley

Giving an average estimation, how many bags of coffee does your store use each month *

Please provide the mass of each coffee bag below *

5 Kg /10 kg   grams   1 2

(180 Kg 1 month)

Do you discard your daily coffee waste to landfills? *

☑ yes

◯ no

If you selected no to the previous question, please state how your store handles its daily coffee waste

Western Cape Coffee Data

Page 1

This short electronic survey aims to assist in the retrieval of data regarding the daily consumption of coffee in the Western Cape and the disposal of the coffee waste in order to gain new insight on the industry.

Please complete the following fields *

Name & Surname	Ray GUTSA
Company/Franchise	████████████
Employment Position	Manager
Suburb	Tygervalley Mall

Giving an average estimation, how many bags of coffee does your store use each month *

Please provide the mass of each coffee bag below *

6 Kg/d   grams   6 kg

186 Kg / month

Do you discard your daily coffee waste to landfills? *

◉ yes

◯ no

If you selected no to the previous question, please state how your store handles its daily coffee waste

Western Cape Coffee Data

Page 1

This short electronic survey aims to assist in the retrieval of data regarding the daily consumption of coffee in the Western Cape and the disposal of the coffee waste in order to gain new insight on the industry.

Please complete the following fields *

Name & Surname	Max Neube
Company/Franchise	███████████
Employment Position	Manager
Suburb	Conference Hotel

Giving an average estimation, how many bags of coffee does your store use each month *

Please provide the mass of each coffee bag below *

14 Kg/W   grams

56 Kgs/month

Do you discard your daily coffee waste to landfills? *

(⦿) yes

( ) no

If you selected no to the previous question, please state how your store handles its daily coffee waste

Western Cape Coffee Data

Page 1

This short electronic survey aims to assist in the retrieval of data regarding the daily consumption of coffee in the Western Cape and the disposal of the coffee waste in order to gain new insight on the industry.

Please complete the following fields *

Name & Surname	ONeday Hokwe
Company/Franchise	███████████
Employment Position	Banista
Suburb	Durbonville.

Giving an average estimation, how many bags of coffee does your store use each month *

[ ]

Please provide the mass of each coffee bag below *

100 cups /d | grams (4 Kg / d)

(12.4 Kg / month)

Do you discard your daily coffee waste to landfills? *

☑ yes

◯ no

If you selected no to the previous question, please state how your store handles its daily coffee waste

Western Cape Coffee Data

Page 1

This short electronic survey aims to assist in the retrieval of data regarding the daily consumption of coffee in the Western Cape and the disposal of the coffee waste in order to gain new insight on the industry.

Please complete the following fields *

Name & Surname	Mandisi
Company/Franchise	███████████
Employment Position	Barista
Suburb	Durbanville.

Giving an average estimation, how many bags of coffee does your store use each month *

Please provide the mass of each coffee bag below *

2-5kg   grams

124 kg / month

Do you discard your daily coffee waste to landfills? *

☑ yes

◯ no

If you selected no to the previous question, please state how your store handles its daily coffee waste